University of Wisconsin Milwaukee

UWM Digital Commons

August 2019

Flavobacterium Gliding Motility: From Protein Secretion to Cell Surface Adhesin Movements

Joseph Johnston
University of Wisconsin-Milwaukee

Follow this and additional works at: https://dc.uwm.edu/etd

Part of the Biology Commons, Microbiology Commons, and the Molecular Biology Commons

FLAVOBACTERIUM GLIDING MOTILITY: FROM PROTEIN SECRETION TO CELL

SURFACE ADHESIN MOVEMENTS

by

Joseph J. Johnston

A Dissertation Submitted in

Partial Fulfillment of the

Requirements for the Degree of

Doctor of Philosophy

in Biological Sciences

at

The University of Wisconsin-Milwaukee

August 2019

ABSTRACT

FLAVOBACTERIUM GLIDING MOTILITY: FROM PROTEIN SECRETION TO CELL
SURFACE ADHESIN MOVEMENTS

by

Joseph J. Johnston

The University of Wisconsin-Milwaukee, 2019
Under the Supervision of Dr. Mark J. McBride

Flavobacterium johnsoniae exhibits rapid gliding motility over surfaces. At least twenty genes are

involved in this process. Seven of these, *gldK*, *gldL*, *gldM*, *gldN*, *sprA*, *sprE,* and *sprT* encode proteins of

the type IX protein secretion system (T9SS). The T9SS is required for surface localization of the motility

adhesins SprB and RemA, and for secretion of the soluble chitinase ChiA. This thesis demonstrates that

the gliding motility proteins GldA, GldB, GldD, GldF, GldH, GldI and GldJ are also essential for

secretion. Cells with mutations in the genes encoding any of these seven proteins had normal levels of

gldK mRNA but dramatically reduced levels of GldK protein, which may explain the secretion defects of

the motility mutants. GldJ is necessary for stable accumulation of GldK and each mutant lacked GldJ

protein. *F. johnsoniae* cells that produced truncated GldJ, lacking eight to thirteen amino acids from the

C-terminus, accumulated GldK but were deficient in gliding motility. SprB was secreted by these cells

but was not propelled along their surfaces. This C-terminal region of GldJ is thus required for gliding

motility but not for secretion. The identification of mutants that are defective for motility but competent

for secretion begins to untangle the *F. johnsoniae* gliding motility machinery from the T9SS.Proteins

secreted by the T9SS typically have conserved C-terminal domains (CTDs) belonging to the type A CTD

or type B CTD families. Attachment of 70 to 100 amino acid type A CTDs to a foreign protein allow its

secretion. Type B CTDs are common but have received little attention. Secretion of the foreign protein

sfGFP fused to regions spanning the SprB type B CTD (sfGFP-CTD$_{SprB}$) was analyzed. CTDs of 218

amino acids or longer resulted in secretion of sfGFP whereas a 149 amino acid region did not. Some

sfGFP was secreted in soluble form whereas the rest was attached on the cell surface. Surface-attached sfGFP was rapidly propelled along the cell, suggesting productive interaction with the motility machinery. This did not result in rapid cell movement, which apparently requires additional regions of SprB. Secretion of sfGFP-CTD$_{SprB}$ required coexpression with *sprF*, which lies downstream of *sprB*. SprF is similar in sequence to *Porphyromonas gingivalis* PorP. Most *F. johnsoniae* genes encoding proteins with type B CTDs lie immediately upstream of *porP*/*sprF*-like genes. sfGFP was fused to the type B CTD from one such protein (Fjoh_3952). This resulted in secretion of sfGFP only when it was coexpressed with its cognate PorP/SprF-like protein. These results highlight the need for extended regions of type B CTDs and for coexpression with the appropriate PorP/SprF-like protein for efficient secretion and cell-surface localization of cargo proteins.

TABLE OF CONTENTS

LIST OF FIGURES

Chapter 1

Chapter 2

Chapter 3

Chapter 4

Appendix

LIST OF TABLES

Chapter 1: Introduction

   The phylum *Bacteroidetes* consists of a wide variety of Gram-negative, rod shaped

bacteria that occupy many ecological niches (1). *Flavobacterium johnsoniae* is a member of this

phylum that is commonly found in freshwater and soil. *F. johnsoniae* is not known to be

pathogenic; however, the related bacteria *Flavobacterium columnare* and *Flavobacterium*

psychrophilum are known to infect economically important fish such as catfish and trout (2, 3).

F. johnsoniae and other members of the phylum *Bacteroidetes* possess a novel form of gliding

motility and a protein secretion system, the type IX secretion system (T9SS); both of which are

apparently confined to the phylum. Genes associated with these systems are named *gld* or *spr* as

many were identified because mutations in these genes cause defects in gliding motility and

colony spreading as shown in Figure 1 (4-14). The T9SS and gliding machinery appear to be

interconnected, and some evidence suggests that the motor responsible for cell gliding may

consist of two of the core proteins of the T9SS, GldL and GldM (15, 16). In addition to this

proposed role in motility, the T9SS is responsible for secretion of the cell surface motility

adhesin SprB to the cell surface (17). It also secretes many other soluble and cell surface proteins

that are unrelated to gliding (18, 19).
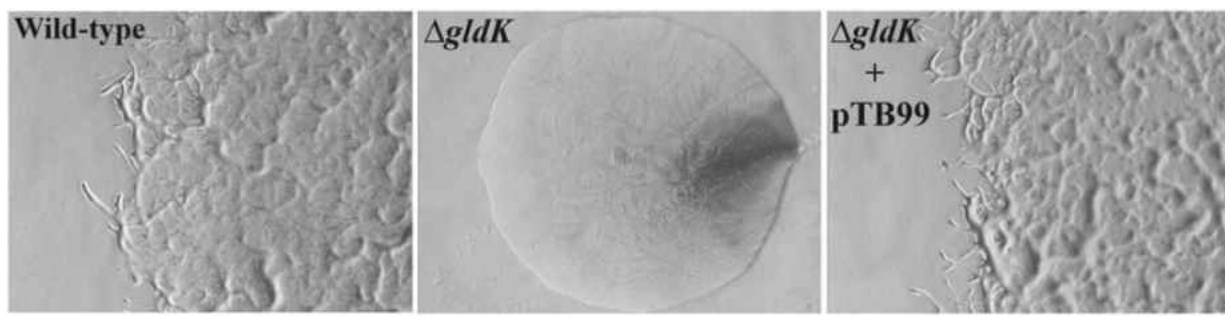
Figure 1. Photomicrographs of spreading and non-spreading *F. johnsoniae* colonies on agar. Wild-type colony on left shows spreading film of growth at colony edge which contrasts with well defined margins of *gldK* deletion mutant shown in center. Right panel shows restoration of spreading phenotype when *gldK* deletion mutant is complemented with pTB99 which carries *gldK*. Scale bar = 1.0 mm and applies to all panels. (14)

Gliding Motility

Rather than using flagella or type IV pili, the *Bacteroidetes* gliding motility machinery propels surface adhesins around the exterior of the cell in a manner similar to conveyor belts or tank tracks (12, 20, 21). Gliding motility is dispersed widely throughout the phylum (22). Bacteria capable of gliding can move across a variety of organic and inorganic substrates in aquatic and terrestrial environments. Gliding motility is a distinct form of cellular movement that relies on the translocation of cell surface adhesins such as SprB over long distances on a helical track (12, 21, 23, 24). When these translocating proteins "grab" the substratum, the result is propulsion of the cell in the opposite direction of the protein translocation and rotation of the cell about its long axis (Fig 2B). The T9SS is responsible for secretion of SprB and other adhesins to the cell surface (17).

Other forms of bacterial gliding motility have been well studied in *Myxococcus xanthus* and *Mycoplasma mobile*. While motility in these species also fits the definition of gliding motility as movement along surfaces without the aid of flagella or type IV pili, the motility mechanisms are not all similar, and the components of the *F. johnsoniae, M. xanthus,* and *M. mobile* motility machineries are very different at the genetic and protein levels (25).

The δ proteobacteria *M. xanthus* is capable of two types of motility for "crawling" along surfaces, these are termed Adventurous 'A-motility' and Social 'S-motility' (26). Social motility is not gliding motility, but actually twitching motility as it uses extension and retraction of type IV pili to move over surfaces (26). Adventurous motility is true gliding motility, though the mechanics are not fully understood. Two models, the focal adhesion model and the helical rotor model, have been proposed to explain the transmission of motive force from the proton channel AglRQS motor to the substratum (27-29). The focal adhesion model relies on propulsion of

focal adhesion complexes in direct interaction with the substratum (28). The helical rotor model

requires transmission of pressure waves generated by cell surface distortion and force

transmission to the substratum by adhesive slime (29). Both models require the presence of a

helical track that is likely constructed of the cytoskeletal protein MreB (27, 30). Though

mechanistically similar to proposed *F. johnsoniae* gliding motility models, there is no protein

similarity and *M. xanthus* gliding is much slower (4 μm/min) than *F. johnsoniae* (2-4 μm/sec)

(31, 32).

M. mobile* cells and gliding motility are vastly different from *F. johnsoniae*. The *M.

mobile* cells are flask or bowling pin shaped with the motility machinery localized to the edge of

the neck region where the cell tapers in size. The machinery consists of many 'legs' that protrude

from the cell in a ring concentric with the long axis of the cell. These legs function similar to

those on a centipede as they extend, grip the surface, then contract to pull the cell along (25).

Rather than PMF driven motors, like those used by *F. johnsoniae* and *M. xanthus*, the legs are

driven by ATP hydrolysis (33).

Genetic analyses identified 19 genes involved in *F. johnsoniae* gliding motility. These

include the *gld* genes (*gldA, B, D, F, G, H, I, J, K, L, M, N*) that are essential for gliding, and the

spr genes (*sprA, B, C, D, E, F, T*) that are important for gliding but not completely essential.

Disruption of any of the *gld* or *spr* genes described above results in the formation of

nonspreading colonies on agar as a result of the motility defects. Whereas individual cells of *gld*

mutants exhibit no motility on glass, cells of the *spr* mutants may exhibit slight movements,

indicating partially functional motility machinery (4-14, 17, 34). SprB is a major motility adhesin

that is propelled rapidly along the cell surface, resulting in gliding movement. Deletion of *sprB*

results in dramatic but incomplete loss of motility (12). The residual cell movement is explained

by the presence of genes encoding semi-redundant cell surface motility adhesins that can

partially replace SprB. One of these redundant motility (*rem*) genes is *remA*. Deletion of *remA*

only results in noticeable defects in motility when it is combined with an *sprB* mutation. Like

SprB, RemA moves rapidly along the cell surface. RemA binds to a polysaccharide produced by

F. johnsoniae and is thought to facilitate gliding on surfaces coated with this polymer (21).
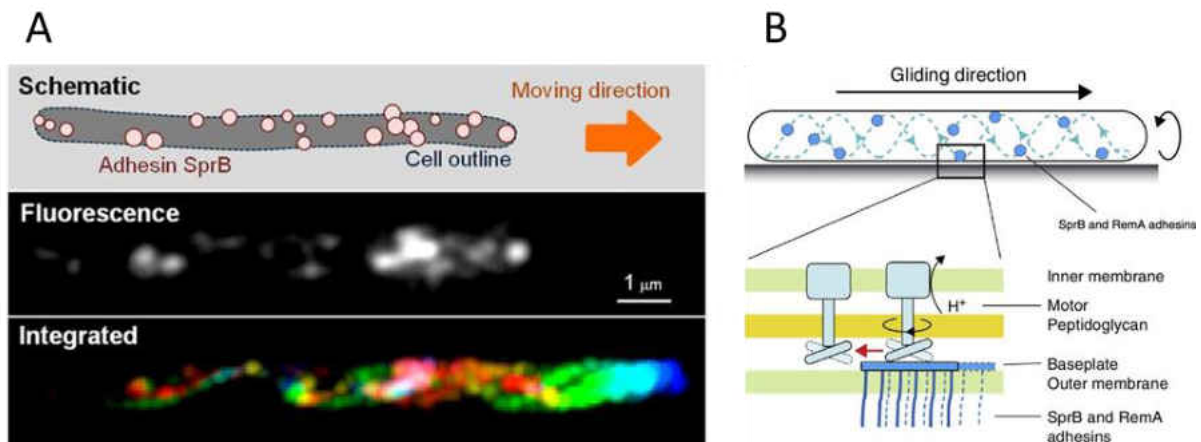
Figure 2. Helical motion of *F. johnsoniae* cell surface adhesins. In panel A, the path of SprB
is visualized by coloring the signal of fluorescent labelling from red (time= 0 s) to blue (time= 2
s) as the cell translocates along a glass surface (20). Panel B illustrates a proposed model for the
movement of cell surface adhesins, resulting in cell movement (24).

Study of surface adhesin motion in *F. johnsoniae* shows that the cell surface adhesins

SprB and RemA appear to travel in helical "tracks" around the cell (Fig. 2). The underlying

structure of a track system or how the adhesins are guided around the cell is not well understood.

However, disruption of the cell division gene *ftsX* causes defects in gliding and cell division (35).

In addition, *F. johnsoniae* cells undergoing division have been observed to stop moving until

completion of division. This could be related to rearrangement of a track system during division,

or possible participation of track related proteins in the division process. The components of the

tracks themselves are not known, however there is circumstantial evidence that GldJ may be a

component since electron micrographs show helical arrangement of GldJ (Fig. 3).
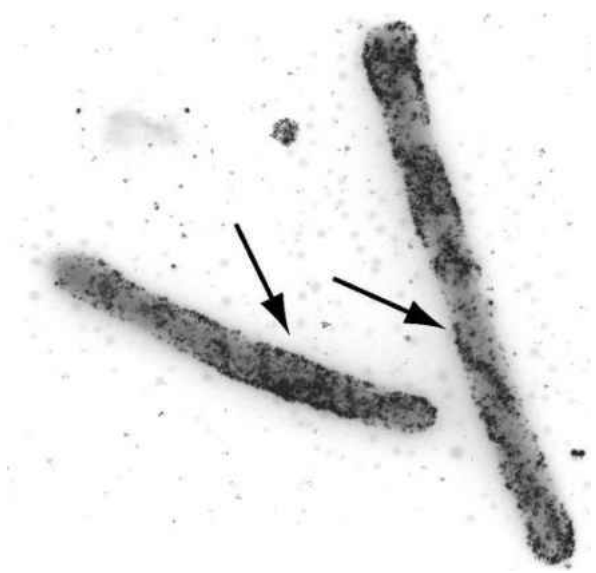
Figure 3. Helical arrangement of GldJ protein in the cell. Electron micrograph of permeabilized *F. johnsoniae* cells treated with GldJ primary antiserum and labelled with secondary antibodies conjugated to 1.4 nm gold particles (6).

The Type IX Secretion System

Comparative genome analyses revealed that some of the Gld and Spr proteins are found not only in gliding members of the phylum *Bacteroidetes*, but also in some non-gliding members such as the human oral pathogen *Porphyromonas gingivalis*. In 2007 researchers independently published papers describing *F. johnsoniae* SprA and *P. gingivalis* sov, which are similar in sequence (13, 36). SprA was recognized as being involved in gliding motility, and sov was identified as being required for secretion of gingipain protease virulence factors. Additional studies quickly revealed that these proteins, and others, comprise the core of the secretion system that came to be called the T9SS (37). Discovery of the T9SS solved a longstanding mystery regarding the pleiotropic phenotypes of many *F. johnsoniae* motility mutants. These mutants were deficient in motility, but many were also deficient in chitin utilization, attachment to surfaces, and sensitivity to bacteriophages (14, 17, 19, 34). Each of these phenotypes can now be explained by inability to secrete proteins (chitinase, adhesins, phage receptors) to the cell surface

or beyond. The T9SS is restricted to the phylum *Bacteroidetes*, but is found in most genera and species of this large phylum. Recent bioinformatic analysis of published genomes revealed that members of 60 of 65 genera, and nearly all species and strains within these genera, have the core T9SS genes (18). Members of the well-studied genus *Bacteroides* and closely related bacteria are the major exceptions since they lack T9SS genes.

The *F. johnsoniae* T9SS consists of the core group of cell envelope proteins GldK, GldL, GldM, GldN, SprA, SprE, and SprT (Fig. 4). All other *Bacteroidetes* that use T9SSs have homologs of these core proteins. In addition, all *Bacteroidetes* that exhibit gliding have genes encoding these core components of the T9SS. Mutations in these genes cause a disruption in both gliding and secretion, thus motility and secretion systems appear to be linked. However, not all organisms that use T9SSs are capable of gliding motility (18, 22). Those that glide have additional *gld* and *spr* genes. All of these motile *Bacteroidetes* have *gldB*, *gldD*, *gldH*, and *gldJ*, and many also have *gldA*, *gldF*, *gldG*, and *gldI*. GldA, GldF, and GldG comprise an ATP-binding cassette (ABC) transporter (4, 7). In *F. johnsoniae*, each of the *gld* genes mentioned above are required for gliding. Many of the motility and T9SS proteins (GldB, GldD, GldH, GldI, GldJ, GldK, SprE) are lipoproteins. As mentioned above, gliding cells also require cell-surface motility adhesins (SprB, RemA, and/or others) and proteins that support the secretion or function of these adhesins (SprC, SprD, SprF). The adhesins, such as SprB, are propelled rapidly along the cell surface by the gliding machinery. This gliding machinery is thought to be comprised of some of the Gld and Spr proteins listed above, but the exact functions of most individual proteins are not known. Evidence suggests that the gliding motor and/or secretion apparatus is powered by the transmembrane proton gradient (38, 39).

The core T9SS proteins are required for gliding, and may be central components of the gliding motility machinery. Recently, a proton gradient driven rotary motor that co-localized with GldL, and may power motility, was identified in *F. johnsoniae* (15, 16). It has been suggested that the cytoplasmic membrane proteins GldL and GldM may comprise this motor. GldL and GldM are the only identified proteins that span the cytoplasmic membrane and are also required for gliding in all motile *Bacteroidetes*. Such transmembrane proteins are needed to harvest the proton gradient to propel surface adhesins such as SprB. Perhaps a rotary motor comprised of GldL and GldM interacts with other components of the motility machinery to drive SprB along the cell surface. An alternative possibility is that GldL and GldM only power secretion of T9SS targeted proteins, and some other yet-to-be-identified proteins perform the motor functions that drive cell movement.

A comparison of the T9SS and associated proteins from *F. johnsoniae* and from the nonmotile human pathogen *P. gingivalis* is shown in Figure 4. Those proteins in the blue barrel are identified as core components of the T9SS. Loss of any of these proteins in either species results in secretion defects of proteins transported by the T9SS (14, 37, 40, 41). In *F. johnsoniae*, the loss of T9SS core components also results in loss of motility. This motility defect may be the result of mis-localization of cell surface adhesins such as SprB and RemA that are secreted by the T9SS, or the T9SS may also have a more direct role in cell movement, as indicated above.
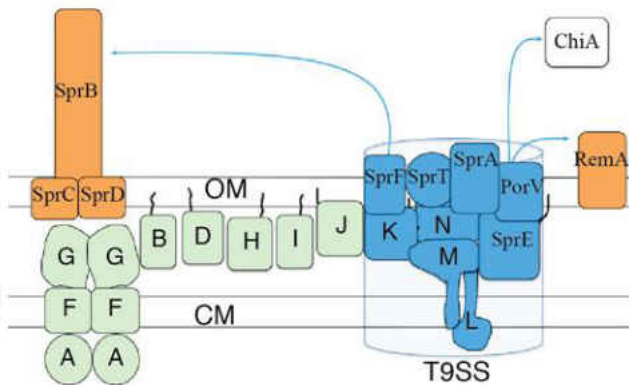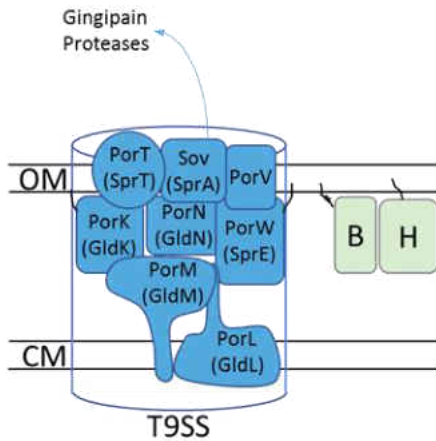
Figure 4. Model of T9SS and motility associated proteins in *F. johnsoniae* (A) and of T9SS proteins in *P. gingivalis* (B). Proteins in orange are cell surface adhesins and associated proteins needed for motility. Proteins in blue make up the core components of the T9SS and are required for secretion indicated by blue arrows in both species. Light green proteins are motility associated proteins of *F. johnsoniae* and are not thought to be components of the T9SS. Homologous proteins (GldB, GldH) are also shown for *P. gingivalis*, where their functions are unknown. Single letter labels of proteins are all prefixed by "Gld" in protein names. Black lines indicate lipid tails of lipoproteins. Cartoon representation is not indicative of stoichiometry or protein scale. It is not certain in all cases that the pictured lipoproteins localize to the outer membrane (OM) as shown. CM indicates cytoplasmic membrane.

The roles of the green colored Gld proteins outside the blue barrel in Fig. 4A are not well understood. However, mutations in the genes encoding these proteins results in phenotypes (inability to digest chitin, resistance to phages) that suggest possible secretion defects (4, 6-11). The proteins GldA, GldF, and GldG are thought to be components of an ABC transporter; however, homologs of this cluster are notably absent in a few *Bacteroidetes* capable of gliding motility (22). The remaining proteins GldB, GldD, GldH, GldI, and GldJ are lipoproteins. Of these, GldB and GldH have homologs in the nonmotile *P. gingivalis* as well as in other *Bacteroidetes* that are incapable of gliding or that lack T9SS core proteins. This implies that the functions of GldB and GldH may not be related specifically to gliding motility or protein secretion. GldI has sequence similarity to peptidyl-prolyl isomerases involved in protein folding, but many gliding *Bacteroidetes* lack obvious GldI orthologs. However, each of these bacteria have other periplasmic peptidyl-prolyl isomerases that may perform the same function. The functions of the remaining proteins, GldD and GldJ, are unknown. However, GldD and GldJ are present in all known gliding *Bacteroidetes* with published genome sequences, and are absent from all, or nearly all, nonmotile members of the phylum that have been examined. The roles of GldJ in gliding and secretion will be explored further in chapter 2 of this thesis. A survey of the presence of T9SS orthologs and related motility proteins in species with completed genome sequences as of 2012 is shown in Figure 5.

Class | **Organism** | **Genes** | **PorSS genes**

Genes columns: gldA, gldB, gldD, gldF, gldG, gldH, gldI, gldJ, gldK, gldL, gldM, gldN, sprA, sprE, sprT

Flavobacteriia
- * *Capnocytophaga canimorsus* Cc5
- * *Capnocytophaga ochracea* DSM 7271^T
- * *Cellulophaga algicola* DSM 14237^T
- * *Cellulophaga lytica* DSM 7489^T
- * *Croceibacter atlanticus* HTCC2559^T
- * *Flavobacteriaceae* bacterium 3519-10
- * *Flavobacterium johnsoniae* ATCC 17061^T
- * *Flavobacterium psychrophilum* J1P02/86
- * 'Gramella forsetii' KT0803
- * *Maribacter* sp. HTCC2170
- * *Riemerella anatipestifer* DSM 15868^T
- * *Robiginitalea biformata* HTCC2501^T
- *Weeksella virosa* DSM 16922^T
- *Zunongwangia profunda* SM-A87^T

Cytophagia
- * *Cytophaga hutchinsonii* ATCC 33406^T
- *Dyadobacter fermentans* DSM 18053^T
- *Leadbetterella byssophila* DSM 17132^T
- * *Marivirga tractuosa* DSM 4126^T
- *Spirosoma linguale* DSM 74^T

Sphingobacteriia
- * *Chitinophaga pinensis* DSM 2588^T
- * *Pedobacter heparinus* DSM 2366^T
- * *Pedobacter saltans* DSM 12145^T

Bacteroidia
- *Alistipes shahii* WAL 8301^T
- *Bacteroides fragilis* NCTC 9343^T
- *Bacteroides helcogenes* P 36-108^T
- *Bacteroides salanitronis* DSM 18170^T
- *Bacteroides thetaiotaomicron* VPI-5482^T
- *Bacteroides vulgatus* ATCC 8482^T
- *Bacteroides xylanisolvens* XB1A^T
- *Odoribacter splanchnicus* DSM 20712^T
- * *Paludibacter propionicigenes* WB4^T
- *Parabacteroides distasonis* ATCC 8503^T
- *Porphyromonas gingivalis* ATCC 33277^T
- *Prevotella melaninogenica* ATCC25845^T
- *Prevotella ruminicola* 23

Figure 5. Distribution of T9SS and gliding motility orthologs identified by reciprocal BLASTP analysis in *Bacteroidetes* genomes. A colored square indicates the presence of an ortholog, and a white square indicates the absence of an ortholog. Colors of squares correspond to predicted or verified functional groups: red, ABC transporter components; yellow, peptidyl-prolyl isomerase; blue, T9SS components; green, gliding motility associated proteins. Green and blue squares correspond to core gliding motility proteins. Asterisks indicate species with verified gliding motility. Adapted from (22).

The outer membrane proteins SprC and SprD may provide a platform supporting SprB attachment (34). Non-polar mutations in the genes encoding these proteins result in motility defects and the formation of nonspreading colonies on agar (Fig. 6). No defects in secretion were observed for these mutants. Although partially defective for motility, cells of these non-polar *sprC* and *sprD* mutants can bind latex spheres coated with anti-SprB antibody and propel them along the cell. This suggests there may also be some redundancy in the function of these proteins.
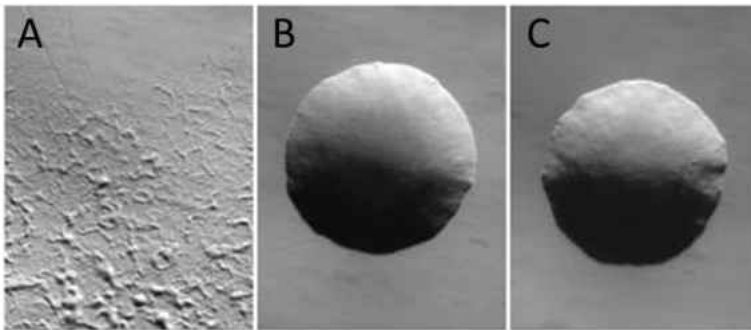
Figure 6. Colony morphology of wild-type *F. johnsoniae* (A) and mutants of SprC (B) and SprD (C). Phase contrast images of colony morphology show that SprC and SprD mutants form nonspreading colonies on agar (34)**.**
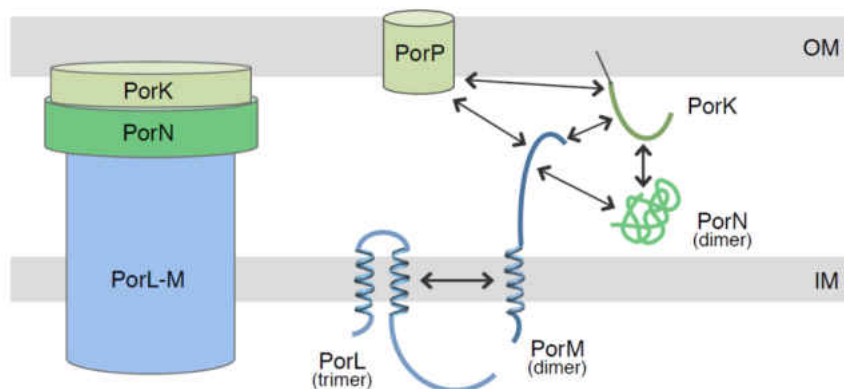
Figure 7. Model of T9SS architecture in *P. gingivalis*. Depiction shows the arrangement of the core T9SS complex consisting of PorKLMN. Arrows on the diagram indicate interactions between proteins of the complex as observed by co-immunoprecipitation and bacterial two-hybrid analyses. Terms in parentheses indicate oligomeric state as determined by size exclusion chromatography (42).

The molecular arrangement of the core T9SS proteins in *F. johnsoniae* and how they are linked to the motility machinery is uncharacterized. However, recent characterization of the arrangement of *P. gingivalis* PorK (GldK), PorL (GldL), PorM (GldM), PorN (GldN), and PorP (SprF) may be broadly applicable to T9SSs in general (Fig. 7) (42, 43). Interaction between proteins of the *Porphyromonas* T9SS were determined by bacterial 2-hybrid assays and verified by co-immunoprecipitation. Oligomeric states were determined by expression of the cytoplasmic domain of PorL, the periplasmic domain of PorM, and the PorN protein. These proteins were then subjected to size exclusion chromatography leading to determination of mass of the peak and thus the oligomeric state. Additionally, PorK and PorN complexes were isolated in a manner similar to that used in isolating type 3 secretion system membrane components (43, 44). After isolation, the PorK/PorN complexes were stained and visualized by TEM leading to the identification of ring structures. Native polyacrylamide gel electrophoresis approximated the molecular weight of these structures to be ≥4500 kDa.

The suggested architecture of PorKLMN shows a complex that spans from the cytoplasm to the periplasmic face of the outer membrane. In *F. johnsoniae, sprF* is co-transcribed with *sprB* and SprF is required for the secretion of SprB, but not for the secretion of other proteins targeted to the T9SS (18, 34). Multiple other similar arrangements of genes encoding secreted proteins and their own SprF-like proteins are found in the *F. johnsoniae* genome. This implies that some proteins secreted by the T9SS are accompanied by their own adapter (SprF-like protein) that interfaces with common components of the T9SS. Other secreted *F. johnsoniae* proteins do not have a co-transcribed adapter but may share a common adapter. PorV appears to be one such adapter, necessary for the secretion of RemA and the soluble extracellular chitinase

ChiA (45).   An adapter could form at least part of the final span across the outer membrane or allow linkage to cell surface components, such as the motility machinery.

In addition to the PorV's potential role as an adapter, structural studies of an outer membrane pore complex indicate that it functions as the outer 'gate' of the complex (46). The transmembrane pore itself is formed by the 267-kDa protein SprA. Through cryo-electron microscopy and docking of known domain structures from the Protein Data Bank (PDB: https://www.rcsb.org), the structure of SprA is revealed as a 36 strand β-barrel. The internal pore measuring approximately 70Å in diameter is alternately blocked by either SprA on the exterior or the Plug protein (Fjoh_1759) on the interior, possibly to prevent uncontrolled transit. The proposed mechanism of action has PorV blocking the pore until presented from the inside with a recognized protein. When PorV interacts with a T9SS substrate it may then release from the SprA complex and allow passage of the secreted protein. During this time when PorV is not bound, the Plug protein interacts with the periplasmic face of the pore to function as the inner gate. The plug would remain bound until a PorV molecule interacts with SprA at the outer opening. This process is shown in Figure 8. Since the plug is bound only when PorV is not present, the channel may always be occluded in the Δ*porV* strain and explain why a subset of T9SS proteins are not secreted (45).

Proteins secreted by the T9SS proceed first across the cytoplasmic membrane through the Sec system and then traverse the outer membrane through the T9SS (45, 47). These proteins utilize an amino-terminal (N-terminal) signal peptide for recognition by the Sec machinery which is cleaved during secretion through the cytoplasmic membrane (48). Two TIGRFAM families of carboxy-terminal domains (CTDs), TIGR04183 and TIGR04131, are known to target proteins for secretion through the T9SS (18, 45, 47). Cleavage of the CTD occurs during

secretion by peptidases, such as PorU in *P. gingivalis* (49), after which the secreted protein is either released or attached to the cell surface (48, 50).

Secretion and processing of proteins with TIGR04183 CTDs ('type A CTDs') is better understood than those with TIGR04131 CTDs ('type B CTDs'). It has been shown that fusing 70-90 amino acids from the carboxy terminus of a type A CTD protein and the N-terminal signal peptide to the respective ends of a foreign protein, such as GFP or mCherry, is sufficient for export from the cytoplasm to the extracellular milieu (18, 19, 48). Previous research showed that disruption of the type B CTD of SprB caused a defect in SprB secretion and attachment to the cell surface (12). However, attempts to perform the CTD fusion experiment with a type B CTD did not result in secretion of the foreign protein (18). It appears that type B CTDs have different requirements for secretion and cell surface attachments, as will be explored further in chapter 3.

The focus of this thesis is the dissection of the T9SS to better understand if certain associated proteins have roles in just secretion, motility, or both. Additionally, this work examines the large cell surface adhesin SprB and other type B CTD proteins to characterize the requirements for secretion through the T9SS and attachment to the cell surface. Chapter 2 examines the motility associated proteins GldA, B, D, F, G, H, I, and J to better understand their functions in secretion and motility. A modified version of Chapter 2 was published in the Journal of Bacteriology (51). Chapter 3 characterizes the secretion, cell surface attachment, and interactions of type B CTDs with the gliding motility machinery. A modified version of Chapter 3 was published in the Journal of Bacteriology (52). The appendix that follows the main text examines motility and secretion defects of strains generated by transposon mutagenesis.
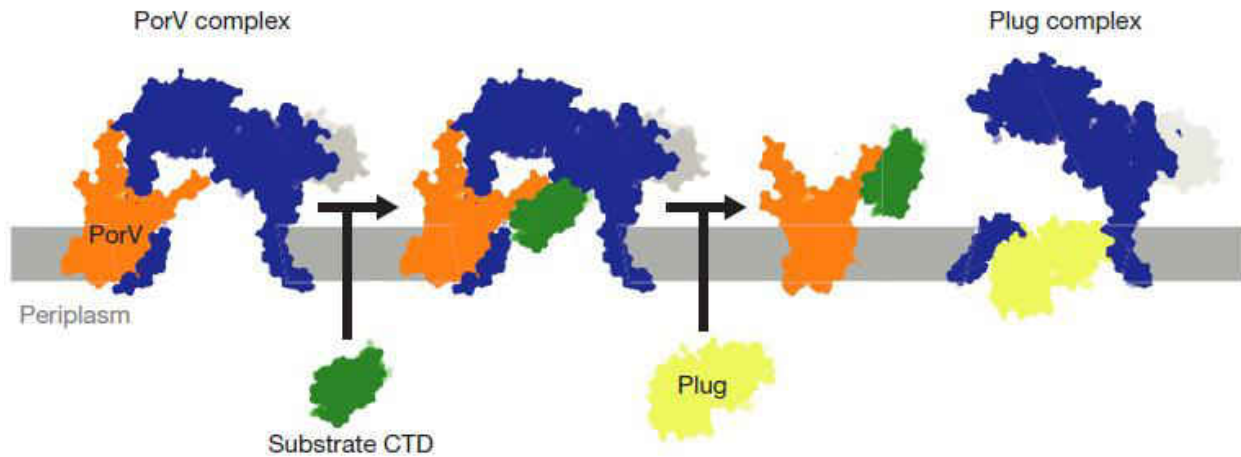
Figure 8. Proposed operation of PorV-SprA-Plug complex. From left to right: In the absence of a substrate, PorV (orange) blocks the outer opening of SprA (blue). Upon recognition of a substrate or substrate CTD, PorV retracts from the opening to allow passage. During this conformation of SprA, the Plug protein binds the periplasmic face of SprA to prevent leakage (46).

References

1. Parte A, Krieg NR, Ludwig W, Whitman WB, Hedlund BP, Paster BJ, Staley JT, Ward N, Brown D. 2010. Bergey's Manual of Systematic Bacteriology : Volume 4: The Bacteroidetes, Spirochaetes, Tenericutes (Mollicutes), Acidobacteria, Fibrobacteres, Fusobacteria, Dictyoglomi, Gemmatimonadetes, Lentisphaerae, Verrucomicrobia, Chlamydiae, and Planctomyc. Springer New York, New York, NY, United States.

2. Li N, Zhu Y, LaFrentz BR, Evenhuis JP, Hunnicutt DW, Conrad RA, Barbier P, Gullstrand CW, Roets JE, Powers JL, Kulkarni SS, Erbes DH, Garcia JC, Nie P, McBride MJ. 2017. The type IX secretion system is required for virulence of the fish pathogen *Flavobacterium columnare*. Appl Environ Microbiol 83:e01769-17.

3. Nematollahi A, Decostere A, Pasmans F, Haesebrouck F. 2003. Flavobacterium psychrophilum infections in salmonid fish. J Fish Dis 26:563-74.

4. Agarwal S, Hunnicutt DW, McBride MJ. 1997. Cloning and characterization of the *Flavobacterium johnsoniae* (*Cytophaga johnsonae*) gliding motility gene, gldA. Proc Natl Acad Sci U S A 94:12139-44.

5. Braun TF, Khubbar MK, Saffarini DA, McBride MJ. 2005. *Flavobacterium johnsoniae* gliding motility genes identified by mariner mutagenesis. J Bacteriol 187:6943-52.

6. Braun TF, McBride MJ. 2005. *Flavobacterium johnsoniae* GldJ is a lipoprotein that is required for gliding motility. J Bacteriol 187:2628-37.

7. Hunnicutt DW, Kempf MJ, McBride MJ. 2002. Mutations in *Flavobacterium johnsoniae gldF* and *gldG* disrupt gliding motility and interfere with membrane localization of GldA. J Bacteriol 184:2370-8.

8. Hunnicutt DW, McBride MJ. 2000. Cloning and characterization of the *Flavobacterium johnsoniae* gliding-motility genes *gldB* and *gldC*. J Bacteriol 182:911-8.

9. Hunnicutt DW, McBride MJ. 2001. Cloning and characterization of the *Flavobacterium johnsoniae* gliding motility genes *gldD* and *gldE*. J Bacteriol 183:4167-75.

10. McBride MJ, Braun TF. 2004. GldI is a lipoprotein that is required for *Flavobacterium johnsoniae* gliding motility and chitin utilization. J Bacteriol 186:2295-302.

11. McBride MJ, Braun TF, Brust JL. 2003. *Flavobacterium johnsoniae* GldH is a lipoprotein that is required for gliding motility and chitin utilization. J Bacteriol 185:6648-57.

12. Nelson SS, Bollampalli S, McBride MJ. 2008. SprB is a cell surface component of the *Flavobacterium johnsoniae* gliding motility machinery. J Bacteriol 190:2851-7.

13. Nelson SS, Glocka PP, Agarwal S, Grimm DP, McBride MJ. 2007. *Flavobacterium johnsoniae* SprA is a cell surface protein involved in gliding motility. J Bacteriol 189:7145-50.

14. Shrivastava A, Johnston JJ, van Baaren JM, McBride MJ. 2013. *Flavobacterium johnsoniae* GldK, GldL, GldM, and SprA are required for secretion of the cell surface gliding motility adhesins SprB and RemA. J Bacteriol 195:3201-12.

15. Shrivastava A, Berg HC. 2015. Towards a model for *Flavobacterium* gliding. Curr Opin Microbiol 28:93-7.

16. Shrivastava A, Lele PP, Berg HC. 2015. A rotary motor drives *Flavobacterium* gliding. Curr Biol 25:338-41.

17. Rhodes RG, Samarasam MN, Shrivastava A, van Baaren JM, Pochiraju S, Bollampalli S, McBride MJ. 2010. *Flavobacterium johnsoniae gldN* and *gldO* are partially redundant genes required for gliding motility and surface localization of SprB. J Bacteriol 192:1201-11.
18. Kulkarni SS, Zhu Y, Brendel CJ, McBride MJ. 2017. Diverse C-Terminal Sequences Involved in *Flavobacterium johnsoniae* Protein Secretion. J Bacteriol 199.
19. Kharade SS, McBride MJ. 2014. *Flavobacterium johnsoniae* chitinase ChiA is required for chitin utilization and is secreted by the type IX secretion system. J Bacteriol 196:961-70.
20. Nakane D, Sato K, Wada H, McBride MJ, Nakayama K. 2013. Helical flow of surface protein required for bacterial gliding motility. Proc Natl Acad Sci U S A 110:11145-50.
21. Shrivastava A, Rhodes RG, Pochiraju S, Nakane D, McBride MJ. 2012. *Flavobacterium johnsoniae* RemA is a mobile cell surface lectin involved in gliding. J Bacteriol 194:3678-88.
22. McBride MJ, Zhu Y. 2013. Gliding motility and Por secretion system genes are widespread among members of the phylum *Bacteroidetes*. J Bacteriol 195:270-8.
23. Jarrell KF, McBride MJ. 2008. The surprisingly diverse ways that prokaryotes move. Nat Rev Microbiol 6:466-76.
24. Nan B, McBride MJ, Chen J, Zusman DR, Oster G. 2014. Bacteria that glide with helical tracks. Curr Biol 24:R169-73.
25. Nan B, Zusman DR. 2016. Novel mechanisms power bacterial gliding motility. Mol Microbiol 101:186-93.
26. Munoz-Dorado J, Marcos-Torres FJ, Garcia-Bravo E, Moraleda-Munoz A, Perez J. 2016. *Myxobacteria*: Moving, Killing, Feeding, and Surviving Together. Front Microbiol 7:781.
27. Mignot T, Shaevitz JW, Hartzell PL, Zusman DR. 2007. Evidence that focal adhesion complexes power bacterial gliding motility. Science 315:853-856.
28. Sun M, Wartel M, Cascales E, Shaevitz JW, Mignot T. 2011. Motor-driven intracellular transport powers bacterial gliding motility. Proc Natl Acad Sci USA 108:7559-7564.
29. Nan B, Chen J, Neu JC, Berry RM, Oster G, Zusman DR. 2011. *Myxobacteria* gliding motility requires cytoskeleton rotation powered by proton motive force. Proceedings of the National Academy of Sciences of the United States of America 108:2498-503.
30. Mauriello EM, Mouhamar F, Nan B, Ducret A, Dai D, Zusman DR, Mignot T. 2010. Bacterial motility complexes require the actin-like protein, MreB and the Ras homologue, MglA. The EMBO journal 29:315-26.
31. Liu J, McBride MJ, Subramaniam S. 2007. Cell-surface filaments of the gliding bacterium *Flavobacterium johnsoniae* revealed by cryo-electron tomography. J Bacteriol 189:7503-7506.
32. Nan B, Zusman DR. 2011. Uncovering the mystery of gliding motility in the *Myxobacteria*. Annu Rev Genet 45:21-39.
33. Miyata M. 2010. Unique centipede mechanism of *Mycoplasma* gliding. Annu Rev Microbiol 64:519-537.
34. Rhodes RG, Samarasam MN, Van Groll EJ, McBride MJ. 2011. Mutations in *Flavobacterium johnsoniae sprE* result in defects in gliding motility and protein secretion. J Bacteriol 193:5322-7.
35. Kempf MJ, McBride MJ. 2000. Transposon insertions in the *Flavobacterium johnsoniae ftsX* gene disrupt gliding motility and cell division. J Bacteriol 182:1671-9.

36. Saiki K, Konishi K. 2007. Identification of a *Porphyromonas gingivalis* novel protein sov required for the secretion of gingipains. Microbiol Immunol 51:483-91.

37. Sato K, Naito M, Yukitake H, Hirakawa H, Shoji M, McBride MJ, Rhodes RG, Nakayama K. 2010. A protein secretion system linked to *Bacteroidete* gliding motility and pathogenesis. Proc Natl Acad Sci U S A 107:276-81.

38. Dzink-Fox JL, Leadbetter ER, Godchaux W, 3rd. 1997. Acetate acts as a protonophore and differentially affects bead movement and cell migration of the gliding bacterium *Cytophaga johnsonae* (*Flavobacterium johnsoniae*). Microbiology 143 (Pt 12):3693-701.

39. Pate JL, Chang L-YE. 1979. Evidence that gliding motility in prokaryotic cells is driven by rotary assemblies in the cell envelopes. Curr Microbiol 2:59-64.

40. Chen YY, Peng B, Yang Q, Glew MD, Veith PD, Cross KJ, Goldie KN, Chen D, O'Brien-Simpson N, Dashper SG, Reynolds EC. 2011. The outer membrane protein LptO is essential for the O-deacylation of LPS and the co-ordinated secretion and attachment of A-LPS and CTD proteins in *Porphyromonas gingivalis*. Mol Microbiol 79:1380-401.

41. Glew MD, Veith PD, Peng B, Chen YY, Gorasia DG, Yang Q, Slakeski N, Chen D, Moore C, Crawford S, Reynolds EC. 2012. PG0026 is the C-terminal signal peptidase of a novel secretion system of *Porphyromonas gingivalis*. J Biol Chem 287:24605-17.

42. Vincent MS, Canestrari MJ, Leone P, Stathopulos J, Ize B, Zoued A, Cambillau C, Kellenberger C, Roussel A, Cascales E. 2017. Characterization of the *Porphyromonas gingivalis* Type IX Secretion Trans-envelope PorKLMNP Core Complex. J Biol Chem 292:3252-3261.

43. Gorasia DG, Veith PD, Hanssen EG, Glew MD, Sato K, Yukitake H, Nakayama K, Reynolds EC. 2016. Structural Insights into the PorK and PorN Components of the *Porphyromonas gingivalis* Type IX Secretion System. PLoS Pathog 12:e1005820.

44. Marlovits TC, Kubori T, Sukhan A, Thomas DR, Galán JE, Unger VM. 2004. Structural Insights into the Assembly of the Type III Secretion Needle Complex. Science 306:1040-1042.

45. Kharade SS, McBride MJ. 2015. *Flavobacterium johnsoniae* PorV is required for secretion of a subset of proteins targeted to the type IX secretion system. J Bacteriol 197:147-58.

46. Lauber F, Deme JC, Lea SM, Berks BC. 2018. Type 9 secretion system structures reveal a new protein transport mechanism. Nature 564:77-82.

47. Sato K, Yukitake H, Narita Y, Shoji M, Naito M, Nakayama K. 2013. Identification of *Porphyromonas gingivalis* proteins secreted by the Por secretion system. FEMS Microbiol Lett 338:68-76.

48. Veith PD, Nor Muhammad NA, Dashper SG, Likic VA, Gorasia DG, Chen D, Byrne SJ, Catmull DV, Reynolds EC. 2013. Protein substrates of a novel secretion system are numerous in the *Bacteroidetes* phylum and have in common a cleavable C-terminal secretion signal, extensive post-translational modification and cell surface attachment. J Proteome Res 12:4449-4461.

49. Glew MD, Veith PD, Peng B, Chen YY, Gorasia DG, Yang Q, Slakeski N, Chen D, Moore C, Crawford S, Reynolds E. 2012. PG0026 is the C-terminal signal peptidase of a novel secretion system of *Porphyromonas gingivalis*. J Biol Chem 287:24605-24617.

50.   Gorasia DG, Veith PD, Chen D, Seers CA, Mitchell HA, Chen YY, Glew MD, Dashper SG, Reynolds EC. 2015. *Porphyromonas gingivalis* type IX secretion substrates are cleaved and modified by a sortase-like mechanism. PLoS Pathog 11:e1005152.
51.   Johnston JJ, Shrivastava A, McBride MJ. 2017. Untangling Flavobacterium johnsoniae gliding motility and protein secretion. J Bacteriol doi:10.1128/JB.00362-17.
52.   Kulkarni SS, Johnston JJ, Zhu Y, Hying ZT, McBride MJ. 2019. The carboxy-terminal region of *Flavobacterium johnsoniae* SprB facilitates its secretion by the type IX secretion system and propulsion by the gliding motility machinery. J Bacteriol doi:10.1128/JB.00218-19.

Chapter 2. Untangling *Flavobacterium johnsoniae* gliding motility and protein secretion.

This chapter is a modified version of a paper of the same title published in the Journal of

Bacteriology:

Johnston JJ[#], Shrivastava A[#], McBride MJ. Untangling *Flavobacterium johnsoniae* Gliding

Motility and Protein Secretion. J Bacteriol. 2017 Dec 20;200(2). pii:

e00362-17. doi: 10.1128/JB.00362-17. Print 2018 Jan 15. PubMed PMID: 29109184;

PubMed Central PMCID: PMC5738736.

[#]These authors contributed equally to this work

This chapter includes some of the online supplemental materials of the J. Bacteriol. Paper listed

above integrated into the body of the text. Dr. Abhishek Shrivastava is responsible for

preliminary observations leading to the experimental design of the portion of this work

concerned with the stability of GldK in *gldA-gldJ* mutants. Dr. Shrivastava also generated the

plasmid pAB31. Dr. Mark McBride is responsible for generating plasmids named as

"pMMxxx". pMM318 was critical in identifying regions of GldJ that allow accumulation of

GldK. Dr. McBride also prepared figures of protein alignments and provided overall guidance

for this study. Johnston was responsible for generation of strains with chromosomal truncation

or deletion of *gldJ*. Johnston performed the western blots, qPCR, flow cytometry, chitinase

assays, light or immunofluorescence microscopy and motility studies presented in the figures and

tables presented in this chapter.

Abstract

Flavobacterium johnsoniae exhibits rapid gliding motility over surfaces. At least twenty genes are involved in this process. Seven of these, *gldK*, *gldL*, *gldM*, *gldN*, *sprA*, *sprE,* and *sprT* encode proteins of the type IX protein secretion system (T9SS). The T9SS is required for surface localization of the motility adhesins SprB and RemA, and for secretion of the soluble chitinase ChiA. Here we demonstrate that the gliding motility proteins GldA, GldB, GldD, GldF, GldH, GldI and GldJ are also essential for secretion. Cells with mutations in the genes encoding any of these seven proteins had normal levels of *gldK* mRNA but dramatically reduced levels of GldK protein, which may explain the secretion defects of the motility mutants. GldJ is necessary for stable accumulation of GldK and each mutant lacked GldJ protein. *F. johnsoniae* cells that produced truncated GldJ, lacking eight to thirteen amino acids from the C-terminus, accumulated GldK but were deficient in gliding motility. SprB was secreted by these cells but was not propelled along their surfaces. This C-terminal region of GldJ is thus required for gliding motility but not for secretion. The identification of mutants that are defective for motility but competent for secretion begins to untangle the *F. johnsoniae* gliding motility machinery from the T9SS.

Introduction

Cells of *Flavobacterium johnsoniae* crawl rapidly over surfaces in a process known as gliding motility. This form of movement is common throughout the phylum *Bacteroidetes*, of which *F. johnsoniae* is a member (1). Gliding motility is also found in bacteria belonging to other phyla, but these appear to rely on motility machines that are unrelated to those of the *Bacteroidetes* (2-5). At least twenty Gld, Spr, and Rem proteins (Fig. 1) are involved in *Flavobacterium* gliding (6-11). Gliding involves the rapid movement of adhesins such as SprB and RemA along the cell surface (11-13). These are propelled along an apparently helical track by other components of the motility machinery that comprise the gliding 'motor'. The exact nature of this motor is uncertain but a proton gradient across the cytoplasmic membrane appears to be required for gliding, and recent results suggest that the motor may have a rotary component (14).

Seven proteins (GldK, GldL, GldM, GldN, SprA, SprE and SprT) are required for secretion of SprB and RemA to the cell surface (7, 9, 10, 15). These proteins are thought to be the core components of the *F. johnsoniae* type IX secretion system (T9SS) that secretes these adhesins. The *F. johnsoniae* T9SS is also involved in secretion of the soluble extracellular chitinase ChiA and many other proteins (16, 17). Other T9SS components that are not essential for its function include SprF (needed for secretion of SprB, but not for secretion of RemA and ChiA) and PorV (needed for secretion of RemA and ChiA, but not for secretion of SprB) (8, 11, 17). Mutations in the genes encoding any of the core components of the T9SS result in defects in gliding motility. These motility defects may be entirely the result of failure to secrete the motility adhesins. Alternatively, some T9SS components may have functions in motility in addition to their roles in protein secretion.

22
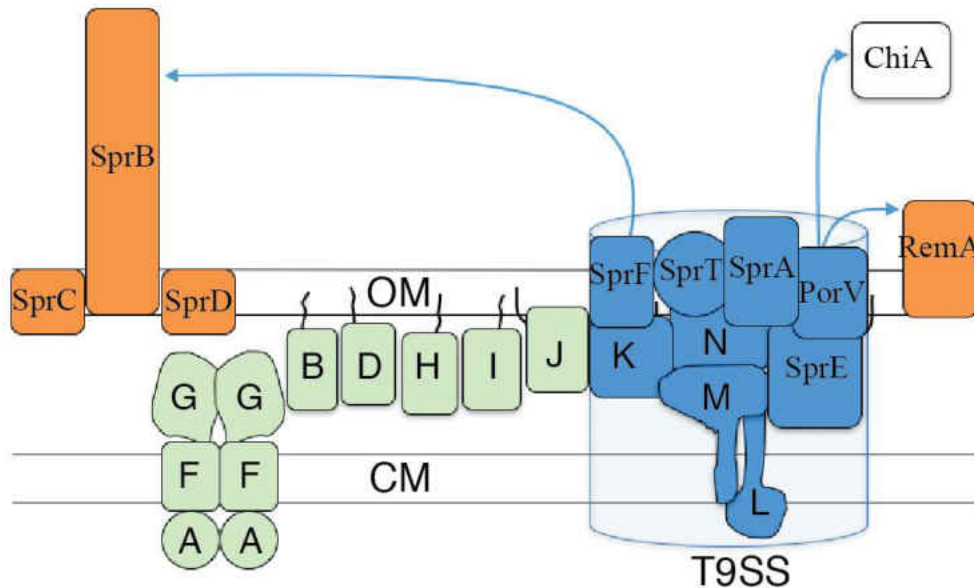
Figure 1. Proteins involved in *F. johnsoniae* gliding motility and protein secretion. SprB and RemA (orange) are motility adhesins that are propelled along the cell surface. SprC and SprD support SprB function. GldK, GldL, GldM, GldN, SprA, SprE, SprT (blue) are components of the T9SS that are required for secretion of SprB and RemA, and for motility. The T9SS also secretes the chitinase ChiA (white), which is not involved in motility. PorV is needed for secretion of RemA and ChiA but not SprB. SprF is needed for secretion of SprB but not RemA or ChiA. Proteins in green (GldA, GldB, GldD, GldF, GldG, GldH, GldI, and GldJ) are also required for gliding motility. Black lines indicate lipid tails on lipoproteins. Proteins are not drawn to scale, stoichiometry of components is not known, and it is not known whether any of the lipoproteins localize to the cytoplasmic membrane (CM) instead of the outer membrane (OM) as shown.

T9SSs were originally discovered in the nonmotile periodontal pathogen *Porphyromonas gingivalis* and in *F. johnsoniae* (1, 15, 18). They are common in but apparently confined to the phylum *Bacteroidetes* (1, 19). Proteins secreted by the T9SS have N-terminal signal peptides that target them for export across the cytoplasmic membrane by the Sec system, and conserved C-terminal domains (CTDs) that are required for secretion across the outer membrane by the T9SS (17-21). In most cases the CTDs are thought to be removed after secretion by the activity of the protease PorU (22). Some proteins secreted by the T9SS, such as SprB, are attached to the cell

surface and thus remain cell associated, whereas others, such as ChiA, are secreted in soluble

form (10, 16). The mechanism by which SprB attaches to the cell surface is not yet known, but

some *P. gingivalis* proteins secreted by the T9SS are covalently linked to outer membrane lipids

(23, 24). In *P. gingivalis* a complex comprised of PorK, PorL, PorM, and PorN (orthologs of *F.

johnsoniae* GldK, GldL, GldM, and GldN, respectively) has been characterized (15, 25, 26). This

complex appears to span the cell envelope. It has been suggested that the cytoplasmic membrane

spanning proteins GldL and GldM (PorL and PorM in *P. gingivalis*) may harvest the proton

gradient to energize secretion (10, 26). The *P. gingivalis* orthologs of GldN and of the

lipoprotein GldK appear to form ring-like structures on the inside of the outer membrane (25,

26). The outer membrane proteins SprA, SprE, and SprT (orthologs of the *P. gingivalis* T9SS

proteins Sov, PorW, and PorT respectively) are also required for secretion and may assist transit

of the outer membrane, although the exact functions of these proteins are not known. Genome

analyses revealed the co-occurrence of SprA with proteins carrying T9SS CTDs suggesting the

possibility that they may interact (19).

P. gingivalis has orthologs of each of the *F. johnsoniae* T9SS genes but it lacks orthologs

of other *F. johnsoniae* genes involved in gliding including *gldA*, *gldD*, *gldF*, *gldG*, *gldH*, *gldI*,

gldJ, *sprB*, *sprC*, *sprD* and *remA*. These *F. johnsoniae* genes were proposed to have roles in

motility rather than in secretion, a suggestion that was supported by comparative analysis of the

genomes of motile and nonmotile members of the phylum *Bacteroidetes* (1). However, indirect

evidence suggests that mutations in some of these *F. johnsoniae* motility genes may cause T9SS

defects. Cells with mutations in *gldA*, *gldD*, *gldF*, *gldG*, *gldH*, *gldI*, or *gldJ* are defective in

chitin utilization and exhibit resistance to bacteriophages that are thought to use SprB and RemA

as receptors (27-33). Here we directly demonstrate that cells of these mutants exhibit T9SS

defects, and that they fail to accumulate the T9SS protein GldK, which may explain the secretion defects. Specific *gldJ* mutants that were deficient in gliding but competent for secretion of SprB were identified indicating that GldJ is required for gliding motility independent of its role in secretion. The *F. johnsoniae* gliding motility apparatus and T9SS appear to be intertwined. The identification of mutants with defects in motility but not secretion begins to untangle these two processes.

Results

       Mutations in *gldA*, *gldB*, *gldD*, *gldF*, *gldH*, *gldI* or *gldJ* result in defects in secretion of ChiA and SprB. GldK, GldL, GldM, GldN, SprA, SprE, and SprT are components of the T9SS and are required for efficient secretion of SprB and ChiA (9-11, 15, 16, 34). The demonstrated motility defects of cells with mutations in the genes encoding these T9SS proteins (6, 7, 9, 15) may be explained by the absence of SprB and other motility adhesins on the cell surface. The roles of the other proteins that are required for gliding motility (GldA, GldB, GldD, GldF, GldG, GldH, GldI and GldJ) are less clear. Cells with mutations in the genes encoding any of these proteins exhibit phenotypes such as phage resistance and inability to digest chitin that suggest T9SS defects (27-33). To directly test the effect of these genes on secretion we examined wild-type and mutant cells for the presence of intracellular and secreted forms of ChiA and SprB. ChiA was found in the spent culture fluid of wild-type cells, but not in the spent culture fluid of cells with mutations in *gldA*, *gldB*, *gldD*, *gldH*, *gldI* and *gldJ* (Fig. 2). Instead ChiA accumulated in cells of the mutants, as has previously been demonstrated for T9SS mutants (10, 11, 16). In each case complementation with the appropriate *gld* gene restored secretion of ChiA. Similar results were obtained for the *gldF* mutant CJ787, which has a Tn*4351* insertion in *gldF* that is

polar on the downstream gene *gldG* (Fig. 2). CJ787 fails to produce both GldF and GldG (29). *gldK* mutant cells also failed to secrete ChiA, as expected given the demonstrated requirement of GldK for secretion (10). Previous results indicate that SprB is found on the surface of wild-type cells, whereas T9SS mutants accumulate SprB inside of cells (9, 10, 13, 15, 34). This was confirmed here since cells of the ΔgldK mutant failed to secrete SprB to the cell surface (Fig. 3). Cells with mutations in *gldA*, *gldB*, *gldD*, *gldF, gldH*, *gldI* and *gldJ* behaved like the ΔgldK mutant. They produced SprB but failed to secrete it to the cell surface (Fig. 3). These results demonstrate that mutations in *F. johnsoniae gldA*, *gldB*, *gldD*, *gldF, gldH*, *gldI* and *gldJ* result in T9SS defects. However, some other motility genes are not required for secretion. Cells with mutations in *sprB*, *sprC*, and *sprD* have severe but incomplete motility defects but retain the ability to digest chitin and to secrete chitinase (8).
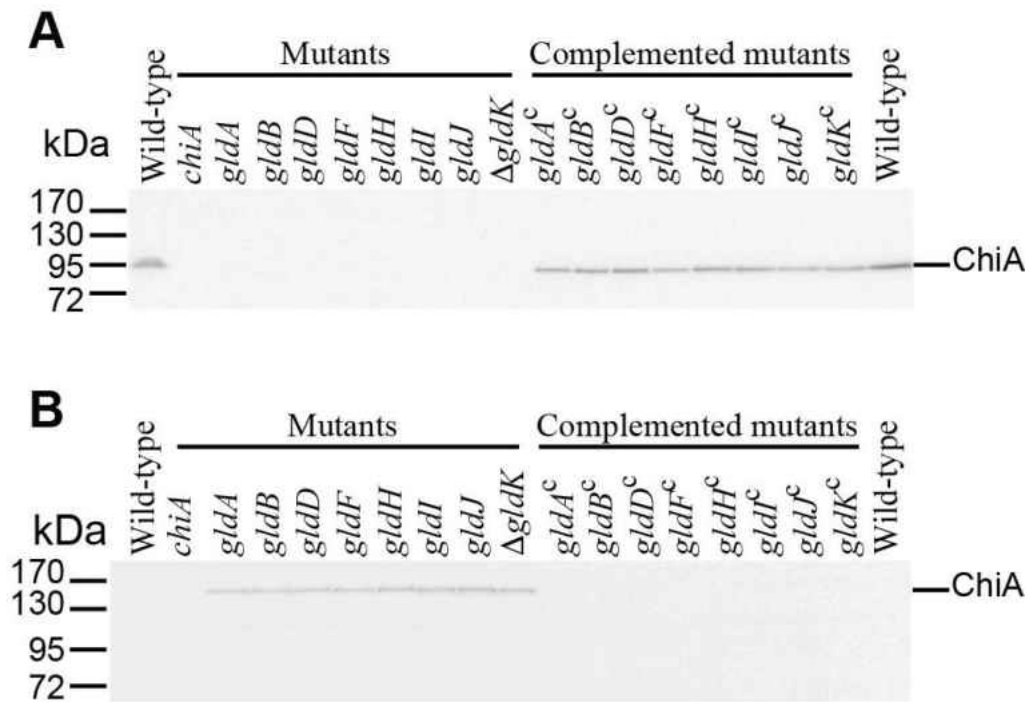
Figure 2. Mutations in *gldA*, *gldB*, *gldD*, *gldF*, *gldH*, *gldI*, and *gldJ* result in defects in secretion of the soluble extracellular chitinase ChiA. Cell-free spent media (A) and cells (B) were examined for ChiA by SDS-PAGE followed by western blot analysis using antiserum against recombinant ChiA. ChiA is proteolytically processed during or after secretion as previously reported (16), accounting for the smaller size in (A). Cells analyzed were wild-type *F. johnsoniae* UW101, *chiA* mutant CJ1808, *gldA* mutant UW101-288, *gldB* mutant CJ569, *gldD* mutant CJ282, *gldF* mutant CJ787, *gldH* mutant CJ1043, *gldI* mutant UW102-41, *gldJ* mutant UW102-80, and Δ*gldK* mutant CJ2122. *gldA*^c, *gldB*^c, *gldD*^c, *gldF*^c, *gldH*^c, *gldI*^c, *gldJ*^c, and Δ*gldK*^c, are complemented versions of the mutants that carry pSA21, pDH223, pMM209, pMK314, pMM293, pMM291, pMM313, and pTB99 respectively. Samples loaded in (B) corresponded to 15 µg protein per lane, and samples loaded in (A) corresponded to the volume of spent medium that contained 15 µg cell protein before the cells were removed.
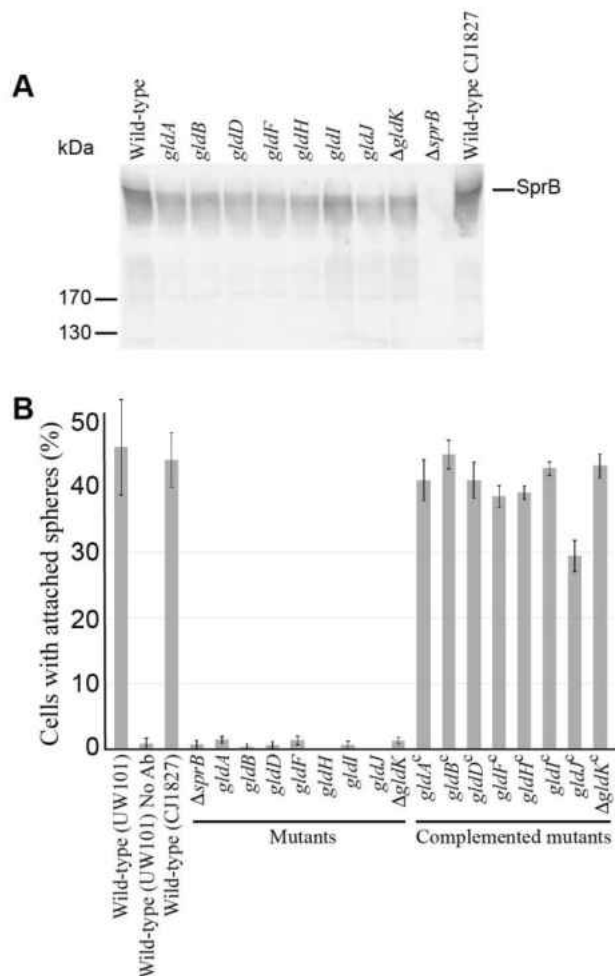
Figure 3. Cells with mutations in *gldA*, *gldB*, *gldD*, *gldF*, *gldH*, *gldI*, and *gldJ* produce the motility adhesin SprB but fail to secrete it to the cell surface. (A) Immunodetection of SprB in cells of wild-type or mutant *F. johnsoniae* strains. Whole cells were analyzed from cultures of wild-type *F. johnsoniae* UW101, streptomycin resistant 'wild-type' CJ1827, *gldA* mutant UW101-288, *gldB* mutant CJ569, *gldD* mutant CJ282, *gldF* mutant CJ787, *gldH* mutant CJ1043, *gldI* mutant UW102-41, *gldJ* mutant UW102-80, Δ*gldK* mutant CJ2122, and Δ*sprB* mutant CJ1922. Cell samples corresponded to 15 μg protein per lane. Samples were separated by SDS-PAGE and SprB was detected using antiserum against SprB. SprB is predicted to be 669 kDa after removal of its N-terminal signal peptide, and has previously been shown to migrate as a diffuse band (13). (B) Detection of SprB on the surface of wild-type or mutant cells. Anti-SprB antiserum and 0.5-μm-diameter protein G-coated polystyrene spheres were added to cells and examined using a phase contrast microscope as described in Materials and Methods. Images were recorded for 30s, and 100 randomly selected cells were examined for the presence of spheres that remained attached to the cells during this time. Wild-type and mutant strains were as described in (A). 'No Ab' indicates no antisera added to this sample. Complemented mutants (indicated by superscript 'c') carried the appropriate plasmids to express GldA (pSA21), GldB (pDH223), GldD (pMM209), GldF and GldG (pMK314), GldH (pMM293), GldI (pMM291), GldJ (pMM313), and GldK (pTB99). Error bars indicate standard deviations from three measurements.

28

Mutations in *gldA*, *gldB*, *gldD*, *gldF*, *gldH*, *gldI* or *gldJ* result in dramatically reduced levels of the T9SS protein GldK. *gldK*, *gldL*, *gldM*, and *gldN* comprise an operon with each gene being required for T9SS function (10). Levels of GldK, GldL, GldM, and GldN were examined in wild-type and mutant cells. GldK was absent or present at greatly reduced levels in cells with mutations in *gldA*, *gldB*, *gldD*, *gldF*, *gldH*, *gldI* or *gldJ* (Fig. 4). Since none of these genes reside near the *gldKLMN* operon the absence of GldK was not the result of polarity. Further, the genes downstream of *gldK* were expressed since GldL, GldM, and GldN were present in each of the seven mutants (Fig. 4). The level of *gldK* mRNA in wild-type and mutant cells was examined by quantitative RT-PCR. The nearly identical cycle thresholds for detection of *gldK* mRNA in wild-type cells and in cells with mutations in *gldA*, *gldB*, *gldD*, *gldF*, *gldH*, *gldI* and *gldJ* indicates that similar levels of *gldK* mRNA were present in each. (Fig. 5). A likely explanation for the absence of GldK protein in these mutants is instability of GldK in the absence of the proteins encoded by these *gld* genes. *gldA*, *gldB*, *gldD*, *gldF*, *gldH*, and *gldI* are also each needed for the accumulation of stable GldJ protein although they are not needed for transcription of *gldJ* (28). Loss of GldJ in cells of the mutants may thus account for the absence of GldK protein. Although GldJ is required for the accumulation of stable GldK, GldK is not required for accumulation of GldJ protein (6) (Fig. 6).
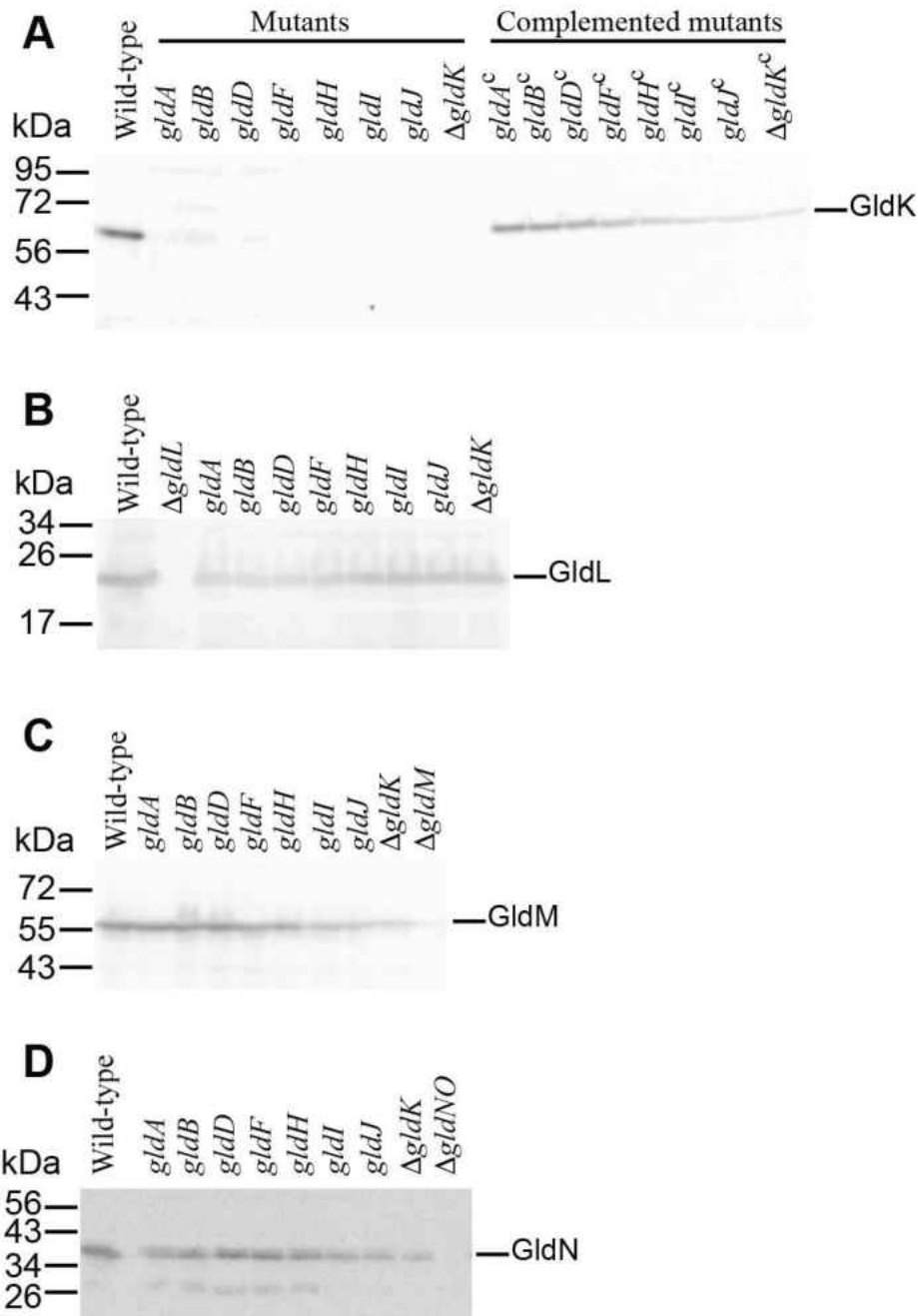
Figure 4. Immunodetection of GldK (A), GldL (B), GldM (C) and GldN (D) in cells of wild-type and mutant *F. johnsoniae* strains. Cell extracts (15 μg of protein) of wild-type (UW101), *gldA* mutant (CJ101-288), *gldB* mutant (CJ569), *gldD* mutant (CJ282), *gldF* mutant (CJ787), *gldH* mutant (CJ1043), *gldI* mutant (UW102-41) and *gldJ* mutant (UW102-80) were separated by SDS-PAGE and GldK, GldL, GldM, and GldN were detected by western blot using the appropriate antisera (10, 34). Complemented mutants (indicated by superscript 'c') carried the plasmids indicated in Fig. 3. ΔgldK mutant (CJ2122), ΔgldL mutant (CJ2157), ΔgldM mutant (CJ2262) and ΔgldNO mutant (CJ2090) were used as controls in panel A, B, C and D respectively.
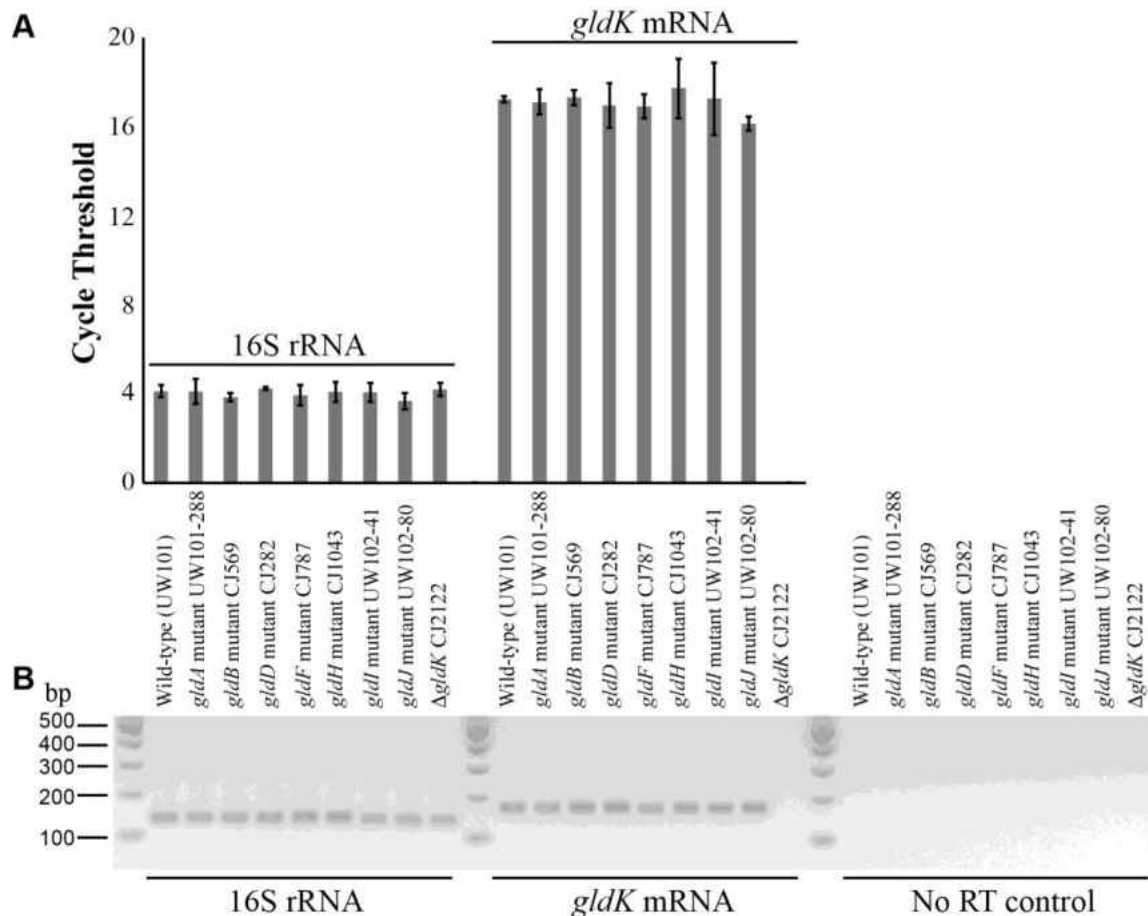
Figure 5. *gldK* **mRNA levels in wild-type and mutant *F. johnsoniae*.** cDNA was generated and real-time quantitative PCR (qPCR) was performed as described in Materials and Methods. (A) RNA levels as indicated by the cycle number at which fluorescence exceeded the predetermined threshold for qPCR for 16s rRNA (using primers 1508 and 1509) and *gldK* mRNA (using primers 1506 and 1507), respectively. Error bars indicate 1 standard deviation of 6 runs (3 procedural replicates of 2 biological replicates). The Δ*gldK* CJ2122 sample probed for *gldK* mRNA never crossed the fluorescence threshold indicating absence of *gldK* mRNA. No RT controls were samples prepared without reverse transcriptase that were amplified using primers 1508 and 1509. The predetermined thresholds were placed above the background fluorescence observed for these no RT controls. (B) Agarose gel of pooled samples of the qPCR products. Strain labels apply to both panels.
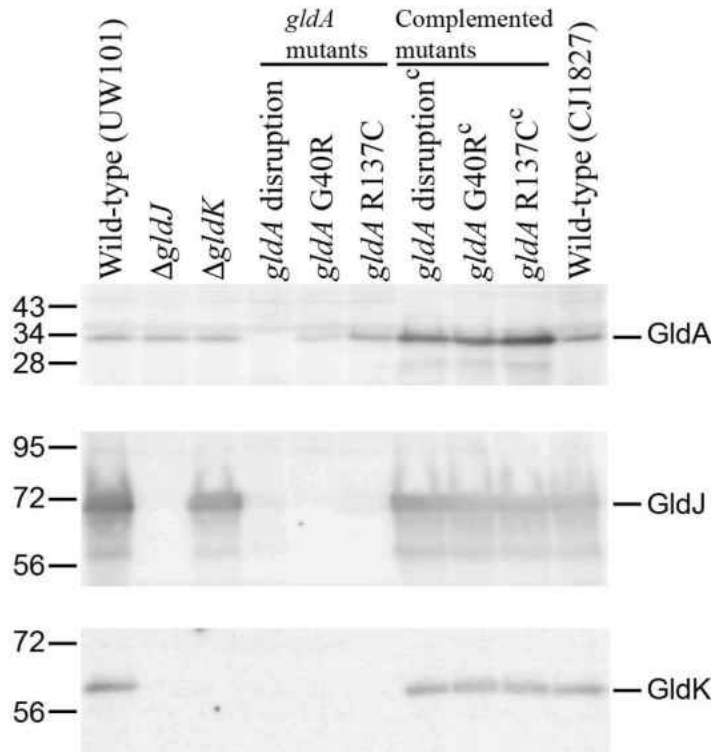
Figure 6. Immunodetection of GldA, GldJ and GldK in wild-type cells and in cells of strains with mutations in *gldA*, *gldJ*, and *gldK*. UW101 is the *F. johnsoniae* type strain. CJ1827 is a streptomycin resistant *rpsl* mutant of strain UW101 and is wild-type for motility and secretion. The deletion mutants Δ*gldJ* and Δ*gldK* are CJ2360 and CJ2122 respectively. '*gldA* disruption' refers to mutant CJ101-288. '*gldA* G40R' and '*gldA* R137C' refer to mutants UW102-9 and UW102-168 respectively, which produce GldA with the indicated amino acid changes. Strains listed with superscript 'c' denote complementation with pSA21 which carries wild-type *gldA*.

Mutations in the T9SS genes *sprA*, *sprE*, and *sprT* did not dramatically effect GldJ or GldK levels. Cells with mutations in *sprA*, *sprE*, and *sprT* also exhibit defects in gliding motility and protein secretion (9, 10, 15). To determine if these defects are the result of instability of GldJ and/or GldK, cells of the mutants were examined by western blot analysis. Each of the mutants accumulated GldJ and GldK proteins, indicating that SprA, SprE, and SprT are not needed to stabilize GldJ and GldK (Fig. 7). SprA, SprE, and SprT are required for normal T9SS function (9, 10, 15) but the exact roles of these outer membrane proteins in secretion are not known.

32
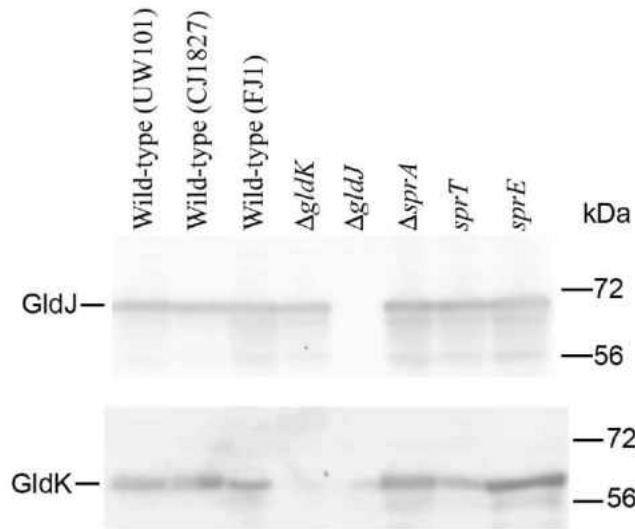
Figure 7. Mutations in *sprA, E, T* had no effect on levels of GldJ and GldK. GldJ and GldK in cells of wild-type or mutant *F. johnsoniae* strains were detected by western blot analyses. Whole cells were analyzed for cultures of wild type *F. johnsoniae* UW101, streptomycin resistant 'wild type' CJ1827, wild type strain FJ1, Δ*gldK* mutant CJ2122, Δ*gldJ* mutant CJ2360, Δ*sprA* mutant CJ2302, *sprT* mutant KDF001, and *sprE* mutant FJ149. Cell samples corresponded to 15 μg protein per lane. Samples were separated by SDS-PAGE and GldJ and GldK were detected using the appropriate antisera (10, 28).

Point mutations that alter the predicted active site of GldA lead to loss of GldJ and GldK proteins, and defects in secretion. Most of the Gld proteins are not similar to proteins of known function, complicating predictions of exact biochemical activities. GldA however is an exception. GldA is predicted to be the ATP binding component of an ATP-binding-cassette (ABC) transporter (27). The membrane proteins GldF and GldG are also components of this putative transporter (29). Disruption of *F. johnsoniae gldA, gldF*, or *gldG* results in complete loss of motility (27, 29). The results presented above suggest that the proteins encoded by these genes are also needed for T9SS-mediated secretion.

 F. johnsoniae strains with spontaneous and chemically induced point mutations in *gldA* were examined to determine whether GldA has a central role in motility, in protein secretion, or both. Two nonmotile mutants (UW102-9 and UW102-168) that had point mutations in *gldA* produced GldA protein as detected by western blot analyses (Fig. 6). Sequence analyses revealed

that UW102-9 has a single nucleotide change (G118A numbered from the 'A' of the *gldA* start codon) resulting in a G40R amino acid substitution in the predicted ATP-binding site of GldA whereas UW102-168 has a C409T nucleotide change resulting in a R137C amino acid substitution in the ABC transporter signature sequence LSKGYRQR (site of change underlined). GldJ and GldK levels were dramatically reduced in both mutants, and complementation with wild-type *gldA* on pSA21 restored GldJ and GldK to wild-type levels (Fig. 6). These results suggest that stable accumulation of GldJ and GldK requires not only GldA protein, but also GldA function. We do not know the function of GldA but it presumably binds to and hydrolyzes ATP, and mutations predicted to disrupt this activity resulted in loss of GldJ and GldK proteins.

GldK accumulates in cells expressing C-terminal truncated versions of GldJ.

If GldJ interacts with and stabilizes GldK it is possible that some GldJ fragments would be sufficient to stabilize GldK resulting in T9SS function, but would be insufficient to support motility, thus separating gliding motility from secretion. To identify such fragments, strains producing truncated forms of GldJ were generated. Plasmids encoding truncated forms of GldJ were introduced into the *gldJ* null mutant UW102-55 (28). pMM317, pAB31, and pMM318 encode the first 337 ($GldJ_{337}$), 542 ($GldJ_{542}$), and 547 ($GldJ_{547}$) amino acids of GldJ, whereas pMM313 encodes full length GldJ (561 amino acids). These strains with plasmid-encoded truncated versions of GldJ were examined for the presence of GldJ and GldK proteins. Immunoblot analysis showed that GldJ and GldK were absent in cells of the *gldJ* mutant UW102-55 (Fig. 8A), which has a frame-shift mutation (G inserted after position 88 numbered from the A of the *gldJ* start codon) (28). Cells of UW102-55 carrying pMM317 (produces $GldJ_{337}$) also accumulated no detectable GldJ and GldK proteins. In contrast, cells of UW102-55 carrying pAB31 accumulated a small amount of truncated $GldJ_{542}$ but failed to accumulate GldK,

and cells of UW102-55 carrying pMM318 accumulated GldJ$_{547}$ and a small amount of GldK (Fig. 8A). Complementation of UW102-55 with pMM313 (expresses full length GldJ$_{561}$) resulted in large amounts of GldJ and wild-type levels of GldK.

The plasmid expression experiments above suggested that a short region near the C-terminus of GldJ may be dispensable for accumulation of GldK. To explore this region in greater detail and to avoid issues of overexpression of GldJ from plasmid, we identified and constructed strains with truncated versions of *gldJ* on the chromosome. UW102-81 has a point mutation (A to T at position 1627 numbered from the A of the *gldJ* start codon) that results in a premature stop codon and termination of GldJ after amino acid 542 (Fig. 9) (28). CJ2386 and CJ2443 have in-frame deletions that terminate GldJ after amino acids 548 and 553 respectively. UW102-81 accumulated no detectable GldJ$_{542}$, suggesting that the C-terminal 19 amino acids of GldJ may be required for its stability (Fig. 8B). In contrast CJ2386 and CJ2443 produced GldJ$_{548}$ and GldJ$_{553}$ respectively. Each strain was also examined for levels of GldK protein. As expected, UW102-81, which accumulated no GldJ, had no detectable GldK (Fig. 8B). In contrast CJ2386 (produces GldJ$_{548}$) and CJ2443 (produces GldJ$_{553}$) each accumulated GldK protein.
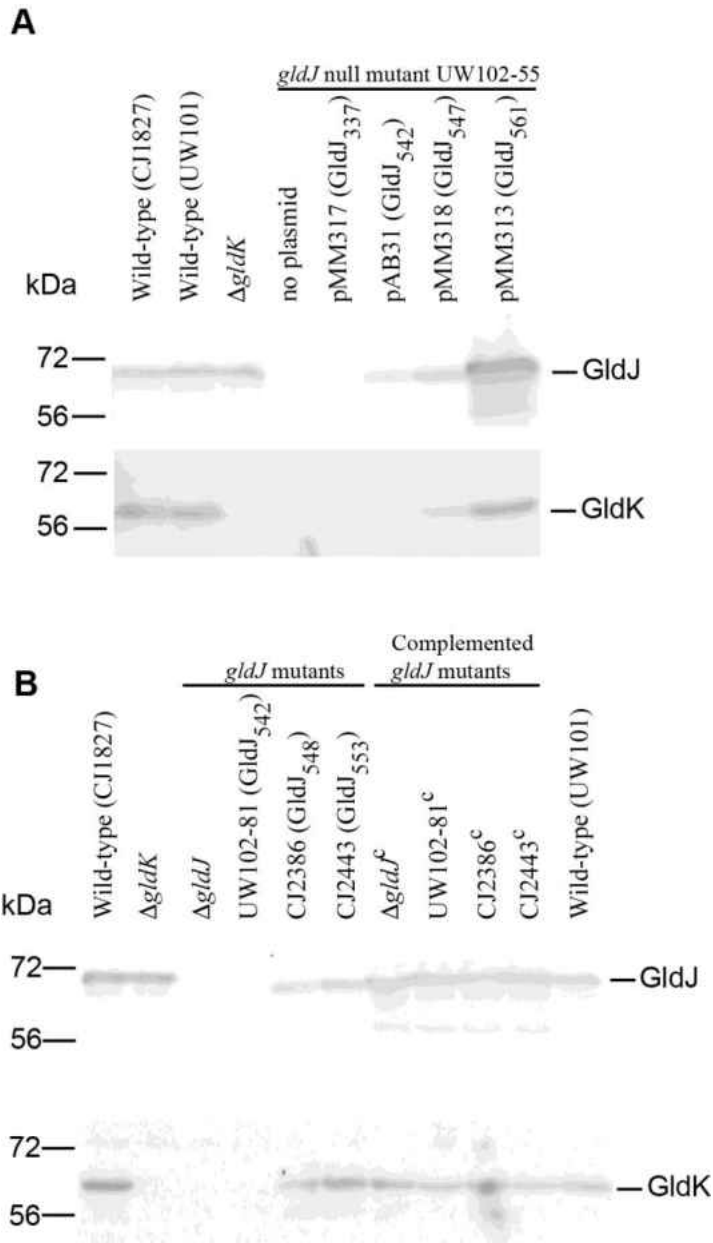
Figure 8. Immunodetection of GldJ and GldK in cells that produce truncated forms of GldJ. (A) Truncated forms of GldJ expressed from plasmids. Cells of wild-type, Δ*gldK* mutant, *gldJ* null mutant UW102-55 (expresses the first 29 AAs of GldJ), and UW102-55 carrying pMM317 that expresses the first 337 AAs of GldJ (GldJ$_{337}$), pAB31 that expresses the first 542 AAs of GldJ (GldJ$_{542}$), pMM318 that expresses the first 547 AAs of GldJ (GldJ$_{547}$), and pMM313 that expresses full length GldJ (GldJ$_{561}$) were examined for GldJ and GldK protein by western blot analyses. (B) Truncated forms of GldJ expressed from the chromosome. Cells of wild-type, Δ*gldK* mutant, Δ*gldJ* mutant, and of chromosomal *gldJ* mutants that express the first 542, 548, and 553 AAs of GldJ were examined for GldJ and GldK protein by western blot analyses. Strains listed with superscript 'c' denote complementation with pMM313 which carries wild-type *gldJ*. For both panels samples (15 µg protein per lane) were separated by SDS-PAGE and GldJ and GldK were detected using the appropriate antisera (10, 28).

36
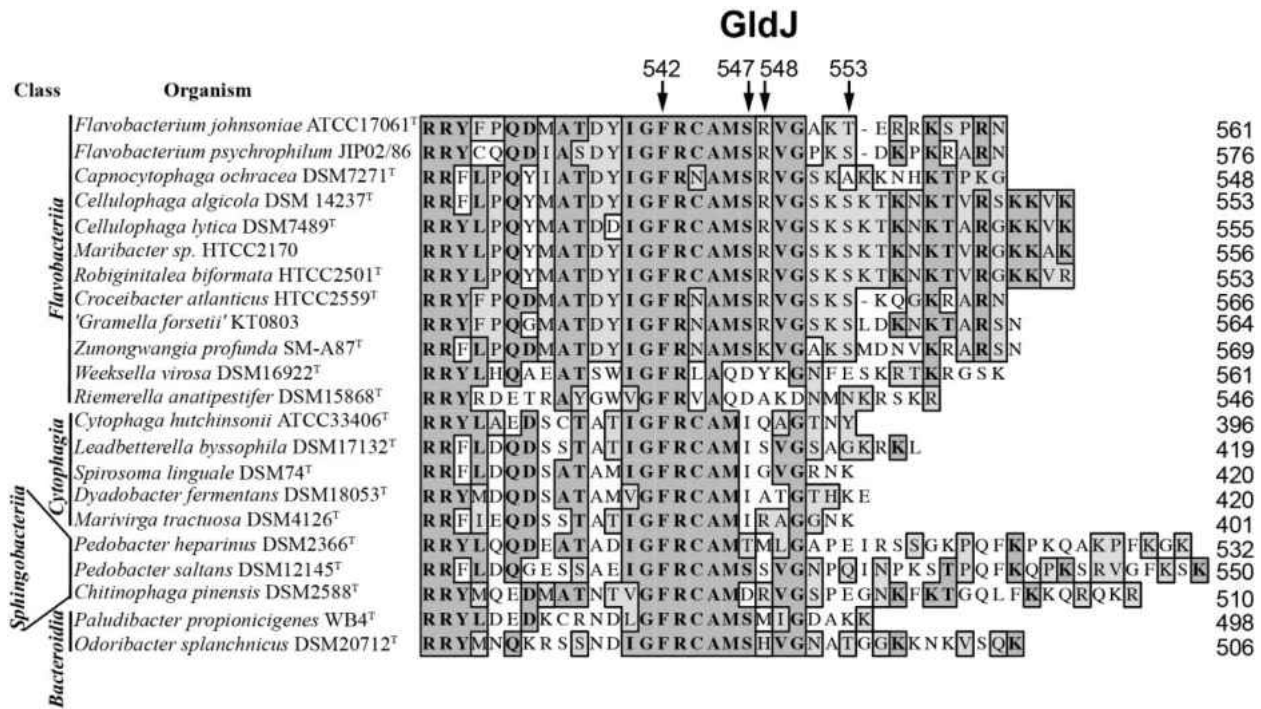
Figure 9. Alignment of C-terminal regions of GldJ proteins. GldJ sequences from 22 members of the phylum *Bacteroidetes* were aligned using MUSCLE. Dark shading indicates identical amino acids and light shading indicates similar amino acids. Numbers at the right correspond to the length of each wild-type GldJ protein including signal peptide. Arrows indicate the C-terminal amino acids of mutant *F. johnsoniae* GldJ proteins truncated at 542, 547, 548, and 553 AAs. Sequences were organized with those most similar to *F. johnsoniae* GldJ at the top and those least similar at the bottom, with Class of organisms within the phylum *Bacteroidetes* indicated on the left. See Fig. S2 in supplemental material of (35) for alignment of full-length GldJ sequences.

The C-terminal thirteen amino acids of GldJ are required for motility but not for T9SS-mediated secretion of ChiA and SprB. The ability of some truncated versions of GldJ to support accumulation of the T9SS protein GldK suggested that secretion might be functional in strains expressing these truncated forms of GldJ. Cells expressing GldJ$_{542}$ failed to utilize chitin and failed to secrete ChiA into the culture fluid (Fig. 10A, B). Instead, these cells accumulated ChiA in the cells (Fig. 10C). This secretion defect was not surprising since as mentioned above cells expressing GldJ$_{542}$ failed to accumulate the T9SS protein GldK. In contrast cells expressing GldJ$_{547}$, GldJ$_{548}$, and GldJ$_{553}$, digested chitin and secreted ChiA, although cells expressing

37

GldJ$_{547}$ and GldJ$_{548}$ did not accumulate as much extracellular ChiA as did wild-type cells. Similar results were observed for secretion of the motility adhesin SprB, except that cells expressing GldJ$_{548}$ appeared to secrete SprB as well as did cells expressing full length GldJ. CJ2360 ($\Delta gldJ$) produced SprB (Fig. 11A) but failed to secrete it to the cell surface as determined by lack of attachment of anti-SprB-coated polystyrene spheres to these cells (Fig. 11B). In contrast, CJ2386 (expresses GldJ$_{548}$) and CJ2443 (expresses GldJ$_{553}$), secreted SprB, indicating the presence of functional T9SSs in these strains (Fig. 11B). The experiments described above used limiting amounts of anti-SprB to avoid large aggregates of cells and polyvalent spheres. In order to more accurately determine what % of cells harbored SprB on the cell surface we examined cells by immunofluorescence microscopy using anti-SprB and F(ab') fragment of goat anti-rabbit IgG conjugated to Alexa-488 (Fig. 12). The results indicate that nearly all wild-type cells carried SprB on their surfaces, whereas cells of the T9SS mutant $\Delta gldK$, and of the $\Delta gldJ$ mutant that fails to accumulate GldK protein, lacked surface exposed SprB. In contrast, nearly all cells of the $gldJ$ truncation mutants expressing GldJ$_{548}$ and GldJ$_{553}$ had cell-surface SprB. The results of flow cytometry analyses (Fig. 13) confirm the presence of SprB on over 90% of the cells of the $gldJ$ truncation mutants expressing GldJ$_{548}$ and GldJ$_{553}$. They also indicate that the levels of SprB on the surface of cells of these two $gldJ$ truncation mutants and of the wild-type were similar.

38
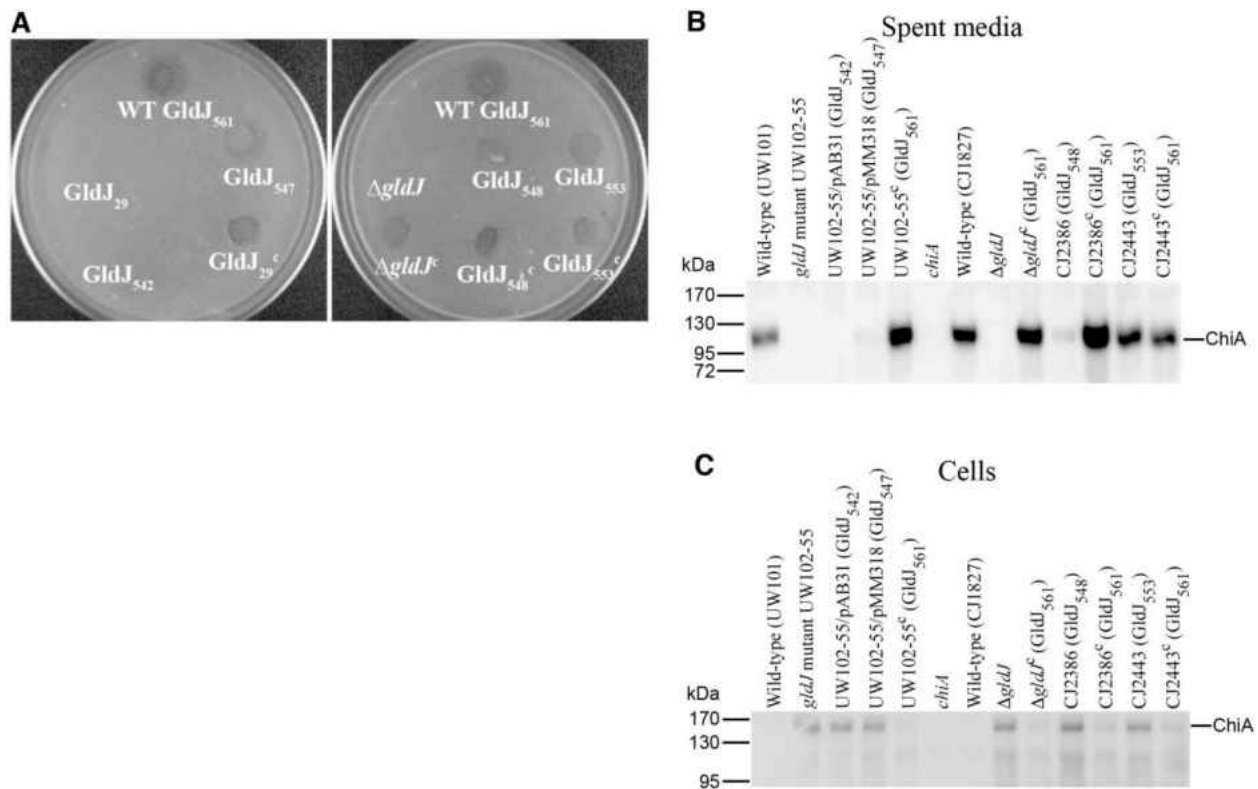
Figure 10. Effect of truncated GldJ on chitin utilization and secretion of ChiA. (A) Chitin utilization. Approximately 10^6 cells of wild-type or mutant *F. johnsoniae* were spotted on MYA-chitin medium and incubated at $25^\circ C$ for 48 h. The plate on the left shows wild-type *F. johnsoniae* (WT, top) which expresses full length GldJ (GldJ$_{561}$), *gldJ* null mutant UW102-55 which expresses the first 29 AAs of GldJ (GldJ$_{29}$), UW102-55 carrying pAB31 that expresses the first 542 AAs of GldJ (GldJ$_{542}$), UW102-55 carrying pMM318 that expresses the first 547 AAs of GldJ (GldJ$_{547}$), and UW102-55 complemented with pMM313 that expresses full length GldJ (GldJ$_{29}^c$). The plate on the right shows wild-type *F. johnsoniae* (expresses GldJ$_{561}$), $\Delta gldJ$ mutant, and the chromosomal *gldJ* mutants CJ2386 and CJ2443 that express the first 548 (GldJ$_{548}$), and 553 (GldJ$_{553}$) AAs of GldJ respectively. $\Delta gldJ^c$, GldJ$_{548}^c$, and GldJ$_{553}^c$ denote the indicated mutants complemented with pMM313 which carries wild-type *gldJ*. (B) and (C) Secretion of ChiA. Cell-free spent media (B) and cells (C) were examined for ChiA by SDS-PAGE followed by western blotting using antiserum against ChiA. Strains wild-type for *gldJ* included UW101, the *chiA* disruption mutant CJ1808 (*chiA*) and the *rpsl* mutant of UW101, CJ1827. Plasmids pAB31 that expresses GldJ$_{542}$, pMM318 that expresses GldJ$_{547}$, and pMM313 that expresses full length GldJ (GldJ$_{561}$) were expressed in the *gldJ* null mutant UW102-55. Plasmids encoding truncated GldJ are indicated by '/pAB31 (GldJ$_{542}$)' and '/pMM318 (GldJ$_{547}$)'. CJ2386 and CJ2443 are chromosomal *gldJ* mutants that express the first 548 and 553 AAs of GldJ respectively. Samples loaded in (C) correspond to 15 μg protein per lane, and samples loaded in (B) correspond to the volume of spent medium that contained 15 μg cell protein before the cells were removed.
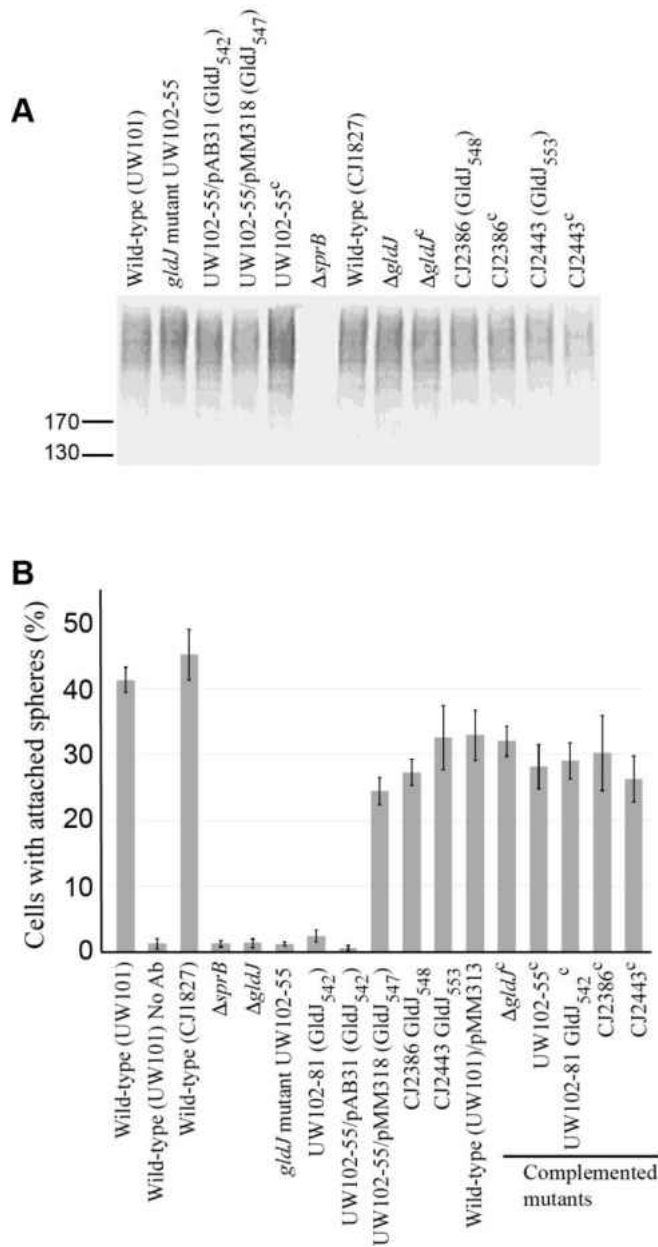
Figure 11. Secretion of SprB by cells with truncated GldJ. (A) Cell-associated SprB levels were examined by western blot. Cells of wild-type strains (UW101 and CJ1827), of *gldJ* null mutants (UW102-55 and Δ*gldJ*), and of strains expressing truncated forms of GldJ (indicated by 'GldJ' followed by length in amino acids in subscript) were lysed in SDS-PAGE loading buffer and proteins (15 µg per lane) were separated by SDS–PAGE and detected using antisera against SprB. Superscript 'c' indicates complementation with pMM313 that carries wild-type *gldJ* (applies to panels A and B). CJ1922 (Δ*sprB*) was used as a negative control. (B) SprB on the cell-surface was detected by adding anti-SprB antiserum and 0.5-µm-diameter protein G-coated polystyrene spheres to cells. 100 randomly selected cells were examined for the presence of spheres that remained attached to the cells during 30 s of microscopic observation. Error bars indicate standard deviations from three measurements. 'No Ab' indicates no antisera added to this sample.

	DIC	Fluorescence	Merge

Wild-type CJ1827

Wild-type CJ1827 No α-SprB

Δ*sprB* CJ1922

Δ*gldK* CJ2122

Δ*gldJ* CJ2360

CJ2386 (GldJ$_{548}$)

CJ2443 (GldJ$_{553}$)
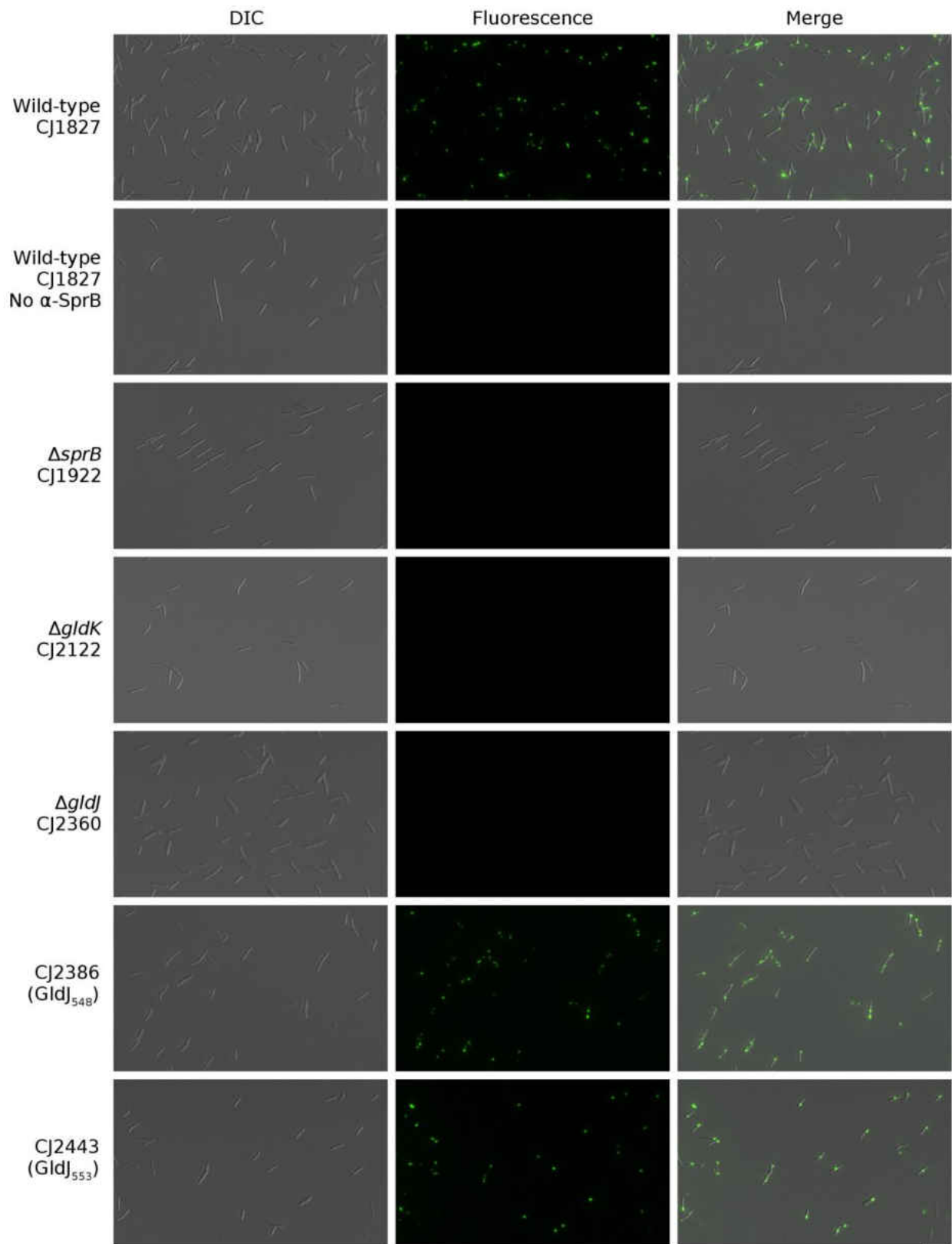
Figure 12. Detection of surface-localized SprB by immunofluorescence labeling. (A) Cells of wild-type and mutant *F. johnsoniae* were exposed to anti-SprB antiserum followed by F(ab') fragment of goat anti-rabbit IgG conjugated to Alexa-488. Cells of mutants CJ2386 and CJ2443 produce truncated versions of GldJ (548 and 553 AA respectively). Images of cells were recorded by differential interference contrast microscopy (DIC; left column) and by immunofluorescence microscopy (center column) and then overlaid (right column). The same exposure time was used for all DIC images, and the same exposure time was used for all fluorescence images. 'No α-SprB' indicates no primary antiserum added to this sample. Bar (lower right) indicates 10 μm and applies to all images.
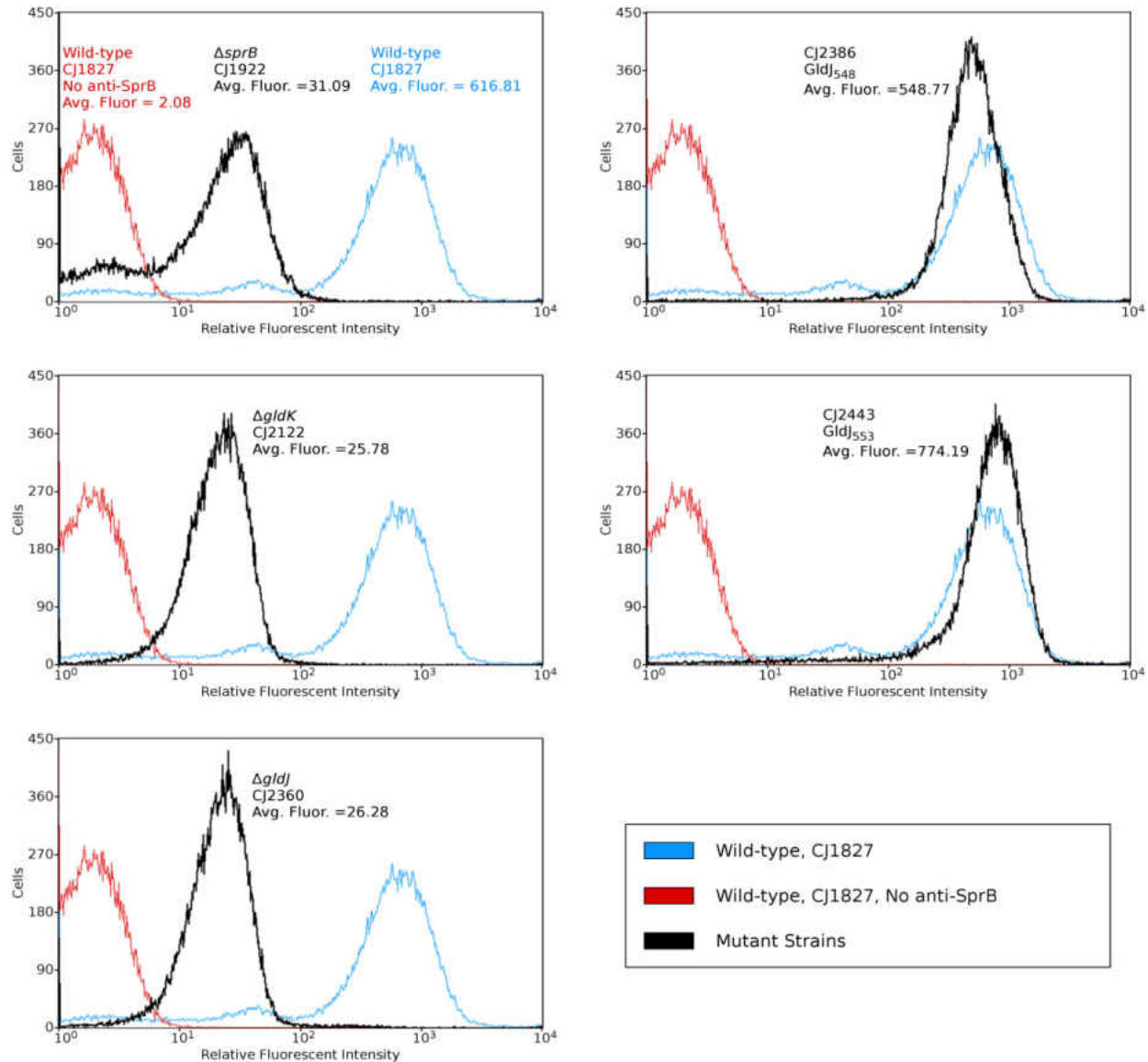
Figure 13. Cell-surface SprB as measured by immuno-labeling and flow cytometry. Cells were exposed to anti-SprB antiserum and F(ab') fragment of goat anti-rabbit IgG conjugated to Alexa-488 and detected by flow cytometry as described in the main text. The relative fluorescence intensities of individual cells (minimum of 49,877 cells per strain) are plotted for each strain and average fluorescence intensities of cells are indicated. Red indicates wild-type cells without anti-SprB antiserum (negative control). Blue indicates wild-type cells with anti-SprB antiserum (positive control). Black indicates individual mutants with anti-SprB antiserum as listed in each panel. The positive and negative controls are repeated in each panel to facilitate comparisons. The Δ*sprB* strain (fails to make SprB) and Δ*gldJ* and Δ*gldK* strains (fail to secrete SprB) each had low levels of background fluorescence presumably because the rabbit anti-SprB antiserum detected other cell-surface antigens besides SprB. Less than 0.6% of cells of strains Δ*sprB*, Δ*gldJ*, and Δ*gldK* exhibited fluorescence above a background cutoff of 10^2 indicating absence of cell-surface SprB for these strains. Greater than 91% of cells of strains CJ2386 makes truncated GldJ548) and CJ2443 (makes truncated GldJ553) exhibited fluorescence above this background cutoff indicating that nearly all cells of these mutants had SprB on their surfaces.

Motility of strains expressing truncated versions of GldJ was also examined. Strains expressing GldJ$_{542}$, GldJ$_{548}$, and GldJ$_{553}$, all produced nonspreading colonies (Fig. 14) indicating motility defects. Examination of cells in tunnel slides revealed dramatic defects in gliding for each of these strains (Fig. 15, and Movies S1, S2, and S3 in supplemental material of (35)). Cells expressing GldJ$_{542}$ and GldJ$_{548}$ were completely nonmotile, whereas cells expressing GldJ$_{553}$ exhibited limited but detectable cell movement. Cells expressing GldJ$_{542}$ failed to even bind to the glass slide presumably as a result of a defect in secretion of cell-surface adhesins, whereas cells expressing GldJ$_{548}$ attached to glass but failed to glide. Introduction of pMM313 carrying wild-type *gldJ* restored gliding motility to each of the mutants. Although the complemented cells exhibited obvious movement on glass (Fig. 15, and Movies S1, S2, and S3 in supplemental material of (35)) they formed colonies that spread less well than those of the wild type, indicating a partial motility defect (Fig. 14, right hand side). This appears to be a result of overexpression of wild-type GldJ since as previously reported (28), and as confirmed here, expression of *gldJ* from pMM313 (copy number approximately 10) in wild-type cells also results in decreased spreading (Fig. 14).

The ability of strains expressing wild-type GldJ, GldJ$_{548}$, and GldJ$_{553}$ to propel SprB along the cell surface was examined. Wild-type cells expressing full length GldJ$_{561}$ bound and propelled anti-SprB coated latex spheres, indicating the rapid movement of SprB (Movies S4, S5 and S6 in supplemental material of (35)). In contrast, cells expressing GldJ$_{542}$ failed to bind the spheres (Fig. 11, and Movie S4 in supplemental material of (35)), and cells expressing GldJ$_{548}$ bound the spheres but failed to propel them (Fig. 11, and Movie S5 in supplemental material of (35)). Cells expressing GldJ$_{553}$ bound the anti-SprB-coated spheres and exhibited some slight movements of the spheres. Although many spheres failed to move, a few moved short distances,

44

suggesting a severe but incomplete defect in motility. Introduction of pMM313 carrying wild-type *gldJ* restored the ability to propel SprB to each of the mutants (Movies S3, S4 and S5 in supplemental material of (35)). To explore the impact of truncation of GldJ on SprB movement in more detail, spheres that were attached to different cells expressing full length GldJ, GldJ$_{548}$, and GldJ$_{553}$ were examined quantitatively for movement (Table 1). Of the spheres attached to cells expressing full length GldJ, 84% moved greater than 3 µm within 10 s, whereas 0% and 6% of the spheres attached to cells expressing GldJ$_{548}$, and GldJ$_{553}$ did. The few spheres that were propelled on cells expressing GldJ$_{553}$ moved intermittently and more slowly than those on wild-type cells. As a result, when the window used to examine these cells was reduced to 5 s none of the spheres attached to cells expressing GldJ$_{553}$ moved 3 µm, whereas 76% of spheres on wild-type cells moved this distance. These results suggest that the C-terminal 13 amino acids of GldJ, while not required for accumulation of GldK or for secretion of SprB by the T9SS, are important for movement of SprB on the cell surface and for gliding motility.
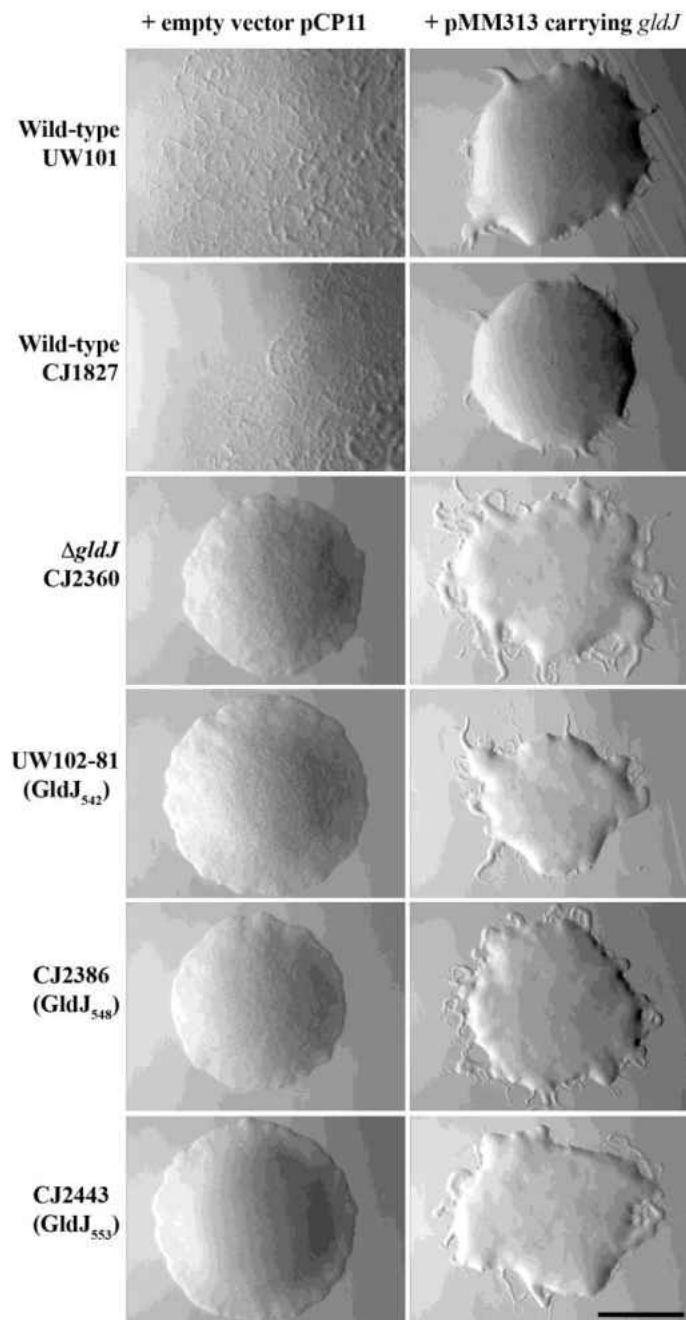
Figure 14. Photomicrographs of *F. johnsoniae* colonies. Colonies were incubated at 25°C on PY2 agar for 36 h. Photomicrographs were taken with a Photometrics Cool-SNAP$_{cf}^{2}$ camera mounted on an Olympus IMT-2 phase-contrast microscope. Wild-type strains used were *F. johnsoniae* UW101 and CJ1827 (*rpsl* mutant of UW101) and the Δ*gldJ* mutant was CJ2360. Truncated *gldJ* chromosomal mutants expressing GldJ proteins of 542 amino acids (GldJ$_{542}$), 548 amino acids (GldJ$_{548}$) and 553 amino acids (GldJ$_{553}$) are also shown. Full length wild-type GldJ is 561 amino acids in length. In each case the colony on the left has the empty vector pCP11 and the colony on the right has pMM313 which expresses wild-type GldJ. Bar indicates 1 mm, and applies to all panels.
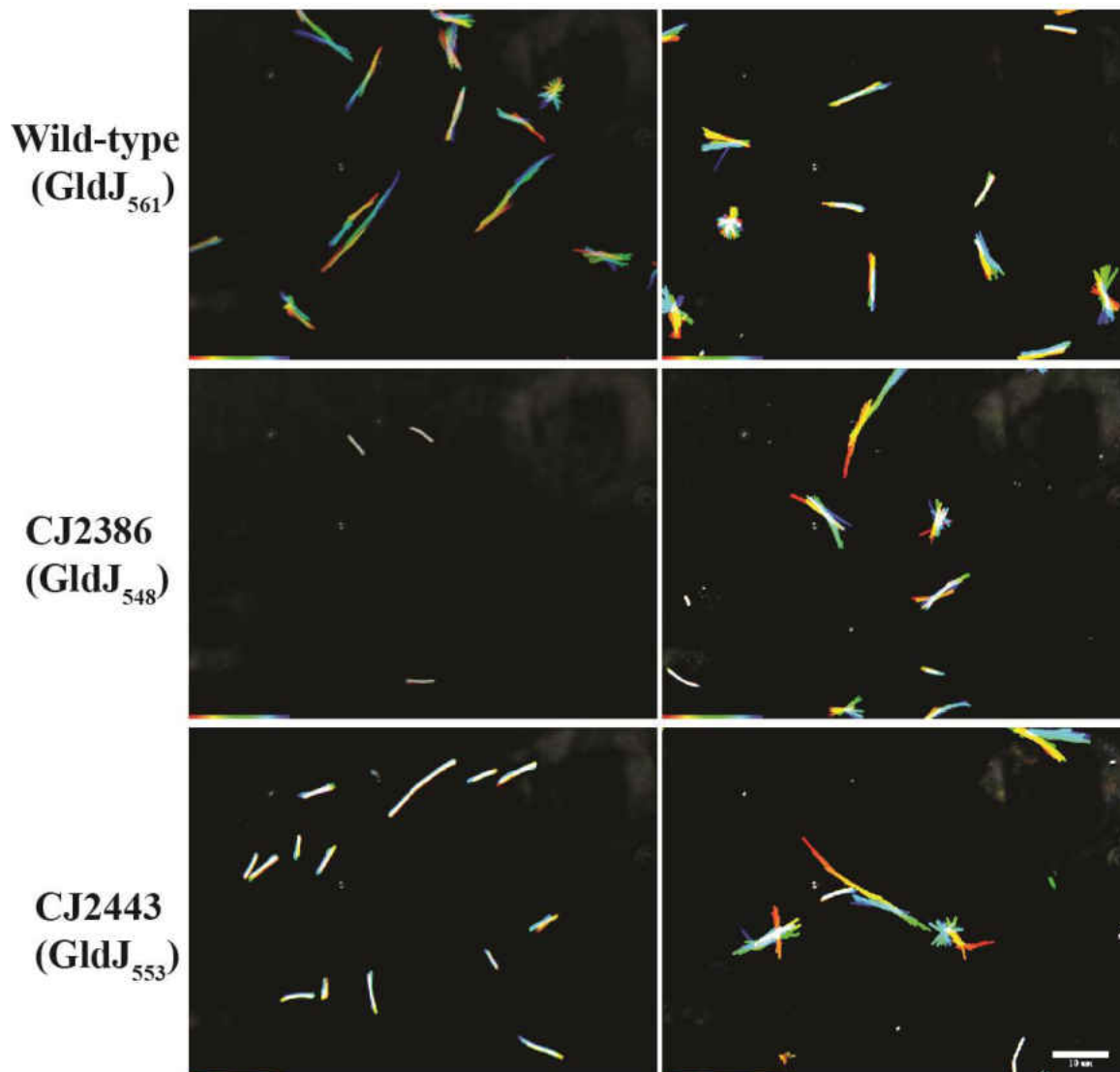
Figure 15. Gliding of wild-type cells and of cells of mutants that express truncated forms of GldJ. Cells were grown in MM medium overnight without shaking at 25°C, introduced into glass tunnel slides, and observed for motility at 25°C using a phase contrast microscope. A series of images were taken for 30 s. Individual frames were colored from red (time zero) to yellow, green, cyan, and finally blue (30 s) and integrated into one image, resulting in rainbow traces of gliding cells. White cells correspond to cells that exhibited little or no net movement. Multicolored "stars" indicate cells attached to the glass by one pole that rotated or flipped. The rainbow traces correspond to the sequences shown in Movies S2 and S3 in supplemental material of (35). Cells in the top row are wild-type *F. johnsoniae* CJ1827 and express full-length (561 AA) GldJ, cells in the middle row are the *gldJ* mutant CJ2386 which expresses the first 548 AAs of GldJ, and cells in the bottom row are the *gldJ* mutant CJ2443 which expresses the first 553 AAs of GldJ. Cells in the right column carry pMM313 which expresses full-length GldJ. The scale bar indicates 10 μm and applies to all panels.

47

Discussion

Many members of the phylum *Bacteroidetes* have gliding motility and T9SS machineries that are apparently not shared with bacteria outside of this phylum (1). *F. johnsoniae* is a model organism for understanding gliding motility and T9SS-mediated protein secretion (9, 10, 15-17, 36). *F. johnsoniae* gliding motility and T9SS-mediated secretion both require the function of many novel proteins and the two processes appear to be intertwined. More than twenty proteins involved in *F. johnsoniae* gliding motility have been identified (Fig. 1). Mutations in the genes encoding many of these proteins result in defects not only in gliding, but also in chitin utilization and in susceptibility to bacteriophages (9, 10, 28, 32-34). Comparative analysis of *F. johnsoniae* with the nonmotile oral pathogen *P. gingivalis* provided an explanation for this pleiotropy and linked some of the gliding motility genes (*gldK*, *gldL*, *gldM*, *gldN*, *sprA*, *sprE*, *sprT*) to protein secretion (9, 10, 15, 34). The proteins encoded by these genes are thought to form the core of the T9SS that secretes the motility adhesin SprB to the cell surface. This may explain the motility defects exhibited by T9SS mutants since gliding involves the movement of SprB along the cell surface (12, 13). Circumstantial evidence suggested that mutations in some of the other motility genes (*gldA*, *gldB*, *gldD*, *gldF*, *gldG*, *gldH*, *gldI*, and *gldJ*) might also disrupt T9SS function. Mutations in these genes resulted not only in loss of motility but also inability to digest chitin and resistance to bacteriophages (27-33). Since secretion of the extracellular chitinase ChiA requires the T9SS (16), and the T9SS is required for infection by bacteriophages (10), it was hypothesized that mutations in these 8 *gld* genes disrupted T9SS function. In this paper, we directly demonstrate that mutations in *F. johnsoniae gldA*, *gldB*, *gldD*, *gldF*, *gldH*, *gldI*, and *gldJ* result in T9SS defects as shown by inability of the mutants to secrete ChiA and SprB. We also present an explanation for the secretion defects since the T9SS protein GldK was absent in each

of the mutants. The mutants had normal levels of *gldK* mRNA, so lack of transcription was not responsible for the lack of GldK protein. Instead we suggest that stability of GldK protein may have been compromised in the mutants.

It was previously reported that strains with mutations in *gldA*, *gldB*, *gldD*, *gldF*, *gldH*, and *gldI* expressed *gldJ* mRNA but failed to accumulate GldJ protein (28). This suggested that the proteins encoded by these genes were required for stability of GldJ. Since GldJ is required for stable accumulation of the T9SS protein GldK, the other proteins (GldA, GldB, GldD, GldF, GldH, GldI) may exert their effects on GldK levels through GldJ.

Truncated versions of GldJ lacking the C-terminal eight to thirteen amino acids allowed accumulation of GldK protein and thus T9SS-mediated secretion of SprB, but failed to support efficient gliding motility. This observation defines a region of GldJ that is important for motility but not for secretion, and begins to untangle these two processes. Comparative analysis of GldJ across 22 members of the phylum *Bacteroidetes*, most of which are known to exhibit gliding motility, revealed that regions near the C-terminus are highly conserved (Fig. 9). The exact function of the C-terminal region in motility remains to be determined.

The *gldJ* truncation mutant expressing GldJ$_{548}$ appeared to secrete SprB well, but was partially defective for secretion of ChiA (Fig. 10). There are several reasons that might explain this difference. The CTDs of ChiA and SprB that target them to the T9SS are not similar in sequence (16, 19). Further, ChiA requires PorV for its secretion, as do other proteins with type A CTDs (these typically belong to TIGRFAM family TIGR04183) (17, 19). In contrast SprB has a type B CTD (belonging to family TIGR04131) and does not require PorV for its secretion but instead requires the unrelated protein, SprF (8, 17). Proteins with type A CTDs and proteins with type B CTDs both require the T9SS for secretion, but they appear to interact differently with this

system. Further study is needed to determine if these differences result in the apparently more severe defect of secretion of ChiA by the *gldJ* truncation mutant producing GldJ$_{548}$. At any rate, it is clear that SprB is secreted to the cell surface of truncated *gldJ* mutant cells expressing GldJ$_{548}$ and GldJ$_{553}$, and that these mutants are defective in gliding motility and in movement of SprB along the cell surface. These results begin to separate T9SS function from gliding motility.

The results reported also reveal aspects of the role of the *gld* ABC transporter, comprised of GldA, GldF, and GldG, in gliding. GldA, GldF, and GldG are required for accumulation of GldJ protein (28) which, as shown here, is needed for accumulation of the T9SS component GldK. Not only is GldA protein required for accumulation of GldJ and GldK, but apparently GldA function is also required. Mutations predicted to disrupt the ATP binding site of GldA resulted in lack of accumulation of GldJ and GldK. The function of GldA in motility is not known but it probably does not function as part of the motor because gliding of *F. johnsoniae* and related bacteria is dependent on proton motive force rather than on ATP hydrolysis (12, 37-40). Most gliding members of the phylum *Bacteroidetes* have orthologs of *gldA*, *gldF*, and *gldG*, and the majority of those that fail to glide (including *P. gingivalis*) lack orthologs (1). The co-occurrence of *gldA*, *gldF*, and *gldG* with gliding, although not universal, suggests that the encoded proteins may perform an important function in motility. However, at least two members of the *Bacteroidetes* that exhibit active gliding, *Cellulophaga algicola* and *Maribacter* sp HTCC2170, lack orthologs of *gldA*, *gldF*, and *gldG* (1, 41). Thus, although these genes are required for *F. johnsoniae* gliding they are not required for gliding of all members of the *Bacteroidetes*.

The motility machinery and T9SS of *F. johnsoniae* appear to be intertwined, reminiscent of the relationship between the bacterial flagellum and the type III secretion system associated

with its assembly (42). We have begun to untangle *Flavobacterium* gliding motility from secretion, but the extent to which these processes can be separated remains unclear. The results presented demonstrate that GldJ has a role in motility independent of its role in secretion of SprB, but the exact function of GldJ in motility is not known. GldJ is an outer membrane lipoprotein and appears to localize in a helical manner (28). Given the helical movements of SprB along the cell surface and the helical movements of gliding cells (12, 43) it is possible that GldJ is a component of a structure on the periplasmic surface of the outer membrane on which SprB is propelled by the gliding motor. Further experiments are needed to clarify the exact role of GldJ in motility. Motility appears to be powered by the proton gradient across the cytoplasmic membrane (12, 39) and proteins that span this membrane must be involved in this process. Besides GldF and GldG (part of the ABC transporter described above), the only known motility proteins that span the cytoplasmic membrane are GldL and GldM. These are components of the T9SS and may drive protein secretion across the outer membrane. Recent results suggest that GldL and GldM may also function as the motor that propels SprB along the cell surface resulting in cell movement (14). Alternatively, other proteins (yet to be identified) may perform this motor function. Further study is necessary to determine the exact nature of the *Bacteroidetes* gliding motor and its relationship to protein secretion.

Materials and Methods

Bacterial strains, plasmids, and growth conditions. *F. johnsoniae* ATCC 17061[T] was the wild-type strain used in this study (44). Two versions of this wild-type strain (UW101 and FJ1) that both originated from the ATCC 17061[T] culture but that had slight phenotypic differences (32) were used in different experiments depending on the mutants under study, which

were derived from strain UW101 or FJ1. The streptomycin resistant *rpsL* mutant CJ1827 (derived from UW101) was used in some experiments since this was the parent strain used to construct gene deletion mutants (45). *F. johnsoniae* cells were grown in Casitone-yeast extract (CYE) medium at 30°C, as previously described (46). To observe colony spreading, *F. johnsoniae* was grown at 25°C on PY2 medium supplemented with 10 g of agar per L (27). Motility medium (MM) was used to observe movement of individual cells in wet mounts (47). Strains and plasmids used in this study are listed in Table 2, and primers are listed in Table 3. The plasmids used for complementation were all derived from pCP1 (46, 48) and have copy numbers of approximately 10 in *F. johnsoniae*. Antibiotics were used at the following concentrations when needed unless indicated otherwise: ampicillin, 100 μg/ml; cefoxitin, 100 μg/ml; erythromycin, 100 μg/ml; streptomycin, 100 μg/ml; and tetracycline, 20 μg/ml.

Determination of sites of *gldA* mutations. The region spanning *gldA* was amplified from the *F. johnsoniae gldA* mutants UW102-9 and UW102-168 by PCR using primers 21 and 22. The PCR products were sequenced to identify the individual mutations.

Construction of the *gldJ* deletion mutant CJ2360. An unmarked deletion of *gldJ* was constructed essentially as previously described (45). Briefly, a 2.3-kbp fragment upstream of *gldJ* was amplified by PCR using Phusion DNA polymerase (New England Biolabs, Ipswich, MA) and primers 1329 (introducing BamHI site) and 1330 (introducing a SalI site). The fragment was digested using BamHI and SalI and ligated into pRR51 that had been digested with the same enzymes, generating pJJ06. The 3.0-kbp fragment downstream of *gldJ* was amplified by PCR with primers 1331 (introducing SalI site) and 1332 (introducing SphI site). The fragment was digested with SalI and SphI and ligated into pJJ06 that had been digested with the same enzymes, generating the deletion construct pJJ07. Plasmid pJJ07 was introduced into *F.*

johnsoniae strain CJ2083 by triparental conjugation, and deletion mutants were isolated as previously described (45).

Construction of strains expressing truncated forms of GldJ. pMM317 and pMM318 produce truncated versions of GldJ that are 337 and 547 amino acids long respectively (28). pAB31, which expresses the first 542 amino acids of GldJ, was generated by amplifying and cloning a fragment of *gldJ* into pCP23. Primers 1360 (introducing a BamHI site) and 1361 (introducing a stop codon and an SphI site) were used to amplify a region spanning the first 1626 bp of *gldJ*. The product was digested with BamHI and SphI and inserted into pCP23 that had been digested with the same enzymes to generate pAB31. pMM317, pMM318, and pAB31 were transferred into the *gldJ* mutant UW102-55. UW102-55 has a frameshift mutation near the beginning of *gldJ* that allows only the first 29 amino acids of GldJ to be translated (28).

Strains with chromosomal mutations resulting in the production of truncated forms of GldJ were also identified and constructed. *F. johnsoniae* strain UW102-81, which was previously described, has a base substitution in *gldJ* (A to T at position 1627 numbered from the A of the *gldJ* start codon) resulting in the production of GldJ truncated after amino acid 542 (28, 49). Mutants expressing GldJ truncated after amino acids 548 and 553 were generated by markerless allele replacement essentially as previously described (45). To delete the region encoding the C-terminal 13 amino acids, a 1.9-kbp fragment upstream of *gldJ* nucleotide 1644 (part of the R548 codon) was amplified by PCR using primers 1502 (introducing BamHI site) and 1503 (introducing a stop codon followed by SalI site). The fragment was digested using BamHI and SalI and ligated into pRR51 that was digested with the same enzymes, to generate pJJ09. The 1.9-kbp fragment downstream of *gldJ* was amplified by PCR with primers 1504 (introducing SalI site) and 1505 (introducing SphI site). The fragment was digested with SalI and SphI and

ligated into pJJ09 digested with the same enzymes, to generate the deletion construct pJJ10. Plasmid pJJ10 was introduced into streptomycin-resistant wild-type *F. johnsoniae* strain CJ1827 by triparental conjugation, and deletion mutants were isolated as previously described (45). Deletion of the C-terminal 8 amino acids was performed using pJJ11, which was constructed in the same way as pJJ10 except that primers 1502 and 1555 were used to amplify the 1.9-kbp fragment upstream of *gldJ* nucleotide 1659 (part of the T553 codon). All deletions were confirmed by DNA sequencing.

Measurement of chitin utilization. The ability of *F. johnsoniae* to utilize chitin was assayed as described previously (34). *F. johnsoniae* cells were grown overnight in MM media without shaking at 25°C. 2 μl of cells were spotted on MYA-chitin containing appropriate antibiotics and plates were incubated for 2.5 days and examined for clearing zones.

Western blot analyses. Wild-type and mutant cells of *F. johnsoniae* were grown to late-log phase in CYE at 25°C except for analyses of ChiA, in which case cells were grown in MM at 25°C. Cells were washed twice in phosphate buffered saline (PBS) consisting of 137 mM NaCl, 2.7 mM KCl, 10 mM Na_2PO_4, and 2 mM KH_2PO_4 (pH 7.4) by centrifugation at 4,000 x g, and were lysed by incubation for 5 min at 100°C in SDS-PAGE loading buffer. Proteins (15 μg per lane) were separated by SDS–PAGE and western blotting was performed as described previously (34) except that polyvinylidene difluoride (PVDF) membranes were used instead of nitrocellulose. Affinity purified antisera (10, 13, 16, 28, 29, 34) were used to detect GldA, GldJ, GldK, GldL, GldM, GldN, SprB, and ChiA. Cell associated and soluble secreted ChiA were separated as previously described (16). In brief, cells grown in MM were pelleted by centrifugation and the culture supernatant (spent medium) was filtered using 0.22 μm pore-size PVDF filters (ThermoFisher Scientific, Rockford, IL). For whole-cell samples, the cells were

suspended in the original culture volume of PBS. Equal amounts of spent media and whole cells were boiled in SDS-PAGE loading buffer and proteins were separated by SDS-PAGE, and western blot analyses were performed. Equal amounts of each sample based on the starting material were loaded in each lane. For cell extracts this corresponded to 15 μg protein whereas for spent medium this corresponded to the equivalent volume of spent medium that contained 15 μg cell protein before the cells were removed.

Quantitative reverse transcriptase PCR (qPCR) to characterize *gldK* mRNA levels in *gld* mutants. Total RNA was isolated from *F. johnsoniae* cells grown in CYE at 25°C to late-log phase by using an RNeasy Mini Kit as previously described (Qiagen) (10). Concentration and purity of RNA was assayed with an Eppendorf model 6131 BioPhotometer (Eppendorf, Hamburg, Germany) and normalized to 100 ng/μl by dilution with diethyl pyrocarbonate-treated water. Contaminant DNA was digested with RNase-free DNase. cDNA was generated using the SuperScript III First-Strand Synthesis System (Invitrogen, Carlsbad, CA) using gene-specific primers. Real-time quantitative PCR (qPCR) was performed using the Applied Biosystems SYBR Select Master Mix (ThermoFisher Scientific) in a DNA Engine Opticon 2 system (MJ Research, Waltham, MA) according to the manufacturer's instructions. Gene specific primers for first strand synthesis and for qPCR are listed in Table 3. Running conditions for qPCR were as follows: 50°C for 2 min, 94°C for 2 min, followed by 35 cycles of 94°C for 15s and 64°C for 40s. A SYBR Green fluorescence reading (excitation 470-505 nm; sensing 523-543 nm) was taken following each cycle to monitor dsDNA product accumulation. A dissociation curve was generated to assay for single PCR product formation following the amplification phase by reading fluorescence every 0.2°C increase from 55°C to 98°C. All PCR reactions were carried

out in triplicate with two independent qPCR experiments. The PCR products were also analyzed by agarose gel electrophoresis.

Microscopic observations of cell movement. Wild-type and mutant cells were examined for movement over glass by phase-contrast microscopy. Cells were grown overnight in MM at 25°C without shaking as previously described (47). Tunnel slides were constructed using double stick tape, glass microscope slides, and glass cover slips, as previously described (11). Cells in growth medium were introduced into the tunnel slides, incubated for 5 min, and observed for motility using an Olympus BH2 phase-contrast microscope with a heated stage at 25°C. Images were recorded with a Photometrics CoolSNAP$_{cf}$^{2} camera and analyzed using MetaMorph software (Molecular Devices, Downingtown, PA).

Analysis of wild-type and mutant cells for surface localization and movement of SprB. Secretion of SprB was examined using anti-SprB antiserum and Protein G-coated polystyrene spheres, essentially as previously described (10). Briefly, cells were grown to late exponential phase in MM medium at 25°C. Purified anti-SprB (1 μl of a 1:10 dilution of a 300-mg/l stock), 0.5-μm-diameter Protein G-coated polystyrene spheres (1 μl of a 0.1% stock preparation; Spherotech Inc., Libertyville, IL), and bovine serum albumin (BSA) (1 μl of a 1% solution) were added to 7 μl of cells (approximately 5 x 10^8 cells per ml) in MM. The cells were introduced into a tunnel slide and examined by phase-contrast microscopy at 25°C. Samples (in triplicate) were observed 3 min after spotting, images were recorded for 30 s, and 100 randomly selected cells were examined for the presence of spheres that remained attached to the cells during this time to determine the % of cells that had surface-associated SprB. Sequences of images were also examined to determine the % of attached spheres that moved greater than 3 μm during 5 to 20 s of observation.

56

Surface localization of SprB was also examined by immunofluorescence microscopy. Cells were grown in MM at 25°C without shaking until late exponential phase. 1 ml of cell culture was centrifuged at 1000 × g for 8 min and the cell pellet was suspended in 1 ml of PBS. The cells were pelleted by centrifugation, suspended in fresh PBS, centrifuged again, and suspended in 50 μl of PBS + 2% BSA. Cells were exposed to 50 μl of polyclonal anti-SprB final bleed (13) for 30 minutes at room temperature and cells were pelleted (1000 × g for 8 min), washed 3 times with 500 μl PBS, suspended in 50 μl PBS + 2% BSA, and exposed to 5 μl of F(ab') fragment of goat anti-rabbit IgG conjugated to Alexa-488 (2 mg/ml; Invitrogen, Carlsbad, CA). Cells were incubated 30 min in the dark and collected by centrifugation. Cells were washed once, suspended in 500 μl of PBS, and kept in the dark until analysis (no more than 1 hour after labeling). Samples were spotted on glass slides previously coated with a thin layer of 0.7% agarose and allowed to sit 30 seconds before applying coverslips. Samples were observed using a Nikon Eclipse 80i microscope with a LH-M100CB-1 mercury lamp and B-2E/C filter (Nikon Instruments, Inc., Melville, NY). Epifluorescence and DIC images were recorded with a QImaging Retiga 2000R camera through a Nikon Plan Apo 40x/0.95 DIC M/N2 objective using QCapture Pro software (QImaging, Surrey, BC, CA).

Fluorescent labeling of cells was quantified by flow cytometry. Cells were cultured as described above, collected by centrifugation, washed with PBS and suspended in PBS at approximately 2×10^6 CFU/ml. Cells were labeled with anti-SprB and F(ab') fragment of goat anti-rabbit IgG conjugated to Alexa-488 as described above. The fluorescence intensities were measured using a FACSCalibur flow cytometer (BD Biosciences, San Jose, CA, U.S.A.) with a 488-nm laser. A minimum of 49,877 cells having the light scattering properties of bacteria were analyzed for each sample and fluorescence data were displayed using a four-decade log scale.

Growth media and buffers used for immunofluorescence microscopy and flow cytometry were filtered (0.22 μm) before use.

Table 1. Movement of latex spheres attached to SprB on wild-type and mutant cells.

Strain	GldJ protein expressed	% of spheres that moved > 3 μm in 5 to 20 s observation period[a]			
		5 s	10 s	15 s	20 s
CJ1827, Wild type	Full length GldJ (561 AA)	76	84	84	84
CJ2386	Truncated GldJ (548 AA)	0	0	0	0
CJ2443	Truncated GldJ (553 AA)	0	6	10	21

[a]Movement of SprB was determined using anti-SprB antiserum and Protein G-coated polystyrene spheres. The movement of 106, 89, and 103 spheres attached to different cells of strains CJ1827, CJ2386, and CJ2443 respectively were examined. Spheres that moved along the cell surface a distance of greater than 3 μm were recorded at 5 s, 10 s, 15 s, and 20 s after the beginning of observation.

Table 2. Strains and plasmids used in this study.

Strain	Genotype and Description[a]	Reference
E. coli **strains**		
DH5αmcr	Strain used for general cloning	Life Technologies (Grand Island, NY, USA)
S17-1 λ *pir*	Strain used for conjugation	(50)
HB101	Strain used with pRK2013 for triparental conjugation	(51, 52)
F. johnsoniae **strains**		
ATCC 17061[T] (UW101)	Wild type	(6, 32, 44)
ATCC 17061[T] (FJ1)	Wild type	(6, 32)
UW102-9	*gldA* mutant encoding GldA$_{G40R}$	(27)
UW102-41	*gldI* null mutant	(32)
UW102-55	*gldJ* null mutant	(28)
UW102-80	*gldJ* null mutant	(28)
UW102-81	*gldJ* mutant encoding truncated GldJ of 542 amino acids	(28)
UW102-168	*gldA* mutant encoding GldA$_{R137C}$	(34)
CJ101-288	*gldA* insertion mutant; (Em^r)	(27)
CJ282	*gldD* Tn*4351* mutant; (Em^r)	(31)
CJ569	*gldB* Tn*4351* mutant; (Em^r)	(30)
CJ787	*gldF* Tn*4351* mutant; (Em^r)	(29)
CJ1043	*gldH* Tn*4351* mutant; (Em^r)	(33)
CJ1808	*chiA* insertion mutant; (Em^r)	(16)
CJ1827	*rpsL2*; 'wild-type' strain derived from ATCC 17061[T] (UW101) and used in construction of deletion mutants described below; (Sm^r)	(45)
CJ1922	Δ*sprB rpsL2*; (Sm^r)	(45)
CJ2083	*remA::myc-tag-1 rpsL2*; (Sm^r)	(11)
CJ2090	Δ*gldNO rpsL2*; (Sm^r)	(11)
CJ2122	Δ*gldK rpsL2*; (Sm^r)	(10)
CJ2157	Δ*gldL rpsL2*; (Sm^r)	(10)
CJ2262	Δ*gldM rpsL2*; (Sm^r)	(10)
CJ2302	Δ*sprA rpsL2*; (Sm^r)	(10)
CJ2360	Δ*gldJ remA::myc-tag-1 rpsL2*; (Sm^r)	This study
CJ2386	*gldJ$_{548}$ rpsL2*; *gldJ* deletion mutation that results in production of GldJ protein truncated after the 548th amino acid; (Sm^r)	This study

CJ2443	*gldJ*$_{553}$ *rpsL2*; *gldJ* deletion mutation that results in production of GldJ protein truncated after the 553rd amino acid; (Sm^r)	This study
FJ149	*sprE HimarEm2* mutant; (Em^r)	(9)
KDF001	*sprT* insertion mutant; (Em^r)	(15)
Plasmid	**Description**	**Reference**
pCP11	*E. coli-F. johnsoniae* shuttle plasmid; Ap^r (Em^r)	(46)
pCP23	*E. coli-F. johnsoniae* shuttle plasmid; Ap^r (Tc^r)	(27)
pCP29	*E. coli-F. johnsoniae* shuttle plasmid; Ap^r (Cf^r Em^r)	(53)
pSA21	pCP23 carrying *gldA*; Ap^r (Tc^r)	(27)
pDH223	pCP11 carrying *gldB*; Ap^r (Em^r)	(30)
pMM209	pCP23 carrying *gldD*; Ap^r (Tc^r)	(31)
pMK314	pCP29 carrying *gldF* and *gldG*; Ap^r (Cf^r Em^r)	(29)
pMM293	pCP23 carrying *gldH*; Ap^r (Tc^r)	(33)
pMM291	pCP11 carrying *gldI*; Ap^r (Em^r)	(32)
pMM313	pCP11 carrying *gldJ*; Ap^r (Em^r)	(28)
pTB99	pCP23 carrying *gldK*; Ap^r (Tc^r)	(6)
pRR51	*rpsl*-containing suicide vector used for constructing deletion mutants; Ap^r (Tc^r)	(45)
pMM317	Fragment encoding the first 337 amino acids of GldJ inserted in pCP11; Ap^r (Em^r)	(28)
pMM318	Fragment encoding the first 547 amino acids of GldJ inserted in pCP11; Ap^r (Em^r)	(28)
pAB31	Fragment encoding the first 542 amino acids of GldJ inserted in pCP23; Ap^r (Tc^r)	This study
pJJ07	Construct used to delete *gldJ*; 2.3-kbp upstream and 3.0-kbp downstream of *gldJ* amplified and ligated into pRR51; Ap^r (Em^r)	This study
pJJ09	1.9-kbp region upstream of base 1644 of *gldJ* (numbered from the 'A' of *gldJ* start codon) amplified with primers 1502 and 1503 and ligated into BamHI-, SalI-digested pRR51; Ap^r (Em^r)	This study
pJJ10	Construct used to generate truncated *gldJ* encoding the first 548 amino acids of GldJ (GldJ$_{548}$); 1.9-kbp region downstream of *gldJ* amplified with primers 1504 and 1505 and ligated into SalI-, SphI-digested pJJ09; Ap^r (Em^r)	This study
pJJ11	Construct used to generate truncated *gldJ* encoding the first 553 amino acids of GldJ (GldJ$_{553}$); 1.9-kpb region upstream of base 1659 of *gldJ* (numbered from the 'A' of *gldJ* start codon) amplified with primers 1502 and 1555 and ligated into BamHI-, SalI-digested pJJ10; Ap^r (Em^r)	This study

Table 3. **Primers used in this study.**

Primer	Sequence and Description
21	5' ATTCGAGCTCTTCAGAAGTATAACCGATG 3'; used to amplify *gldA*
22	5' ATTATCTAGATGCTTGGCAAATATAACAC 3'; used to amplify *gldA*
1329	5' GCTAGGGATCCCTGAGCCTGTGTATTGTCTGAAACTAA 3'; used to construct pJJ07; BamHI site underlined
1330	5' GCTAGGTCGACCATTGACATCATTAATTGCAAGACTAC 3'; used to construct pJJ07; SalI site underlined
1331	5' GCTAGGTCGACGCAATGTCTAGAGTAGGTGCTAAAACT 3'; used to construct pJJ07; SalI site underlined
1332	5' GCTAGGCATGCCAGGTAGAAGGTTTTGATGAAACG 3'; used to construct pJJ07; SphI site underlined
1360	5' GCTAGGGATCCGAAGCGGAAACCATCTCCTG 3'; used to construct pAB31; BamHI site underlined
1361	5' GCTAGGCATGCTTAGAAACCTATGTAATCAGTTGCCAT 3'; used to construct pAB31; SphI site underlined
1502	5' GCTAGGGATCCCGTGAAGCTCCCATTTATCTGAG 3'; used to construct pJJ10 and pJJ11; BamHI site underlined
1503	5' TAGGTCGACTTATCTAGACATTGCACATCTGAAACC 3'; used to construct pJJ10; SalI site underlined
1504	5' GCTAGGTCGACCATAAAAAATTCCAAATTCCAAAGCTG 3'; used to construct pJJ10 and pJJ11; SalI site underlined
1505	5' GCTAGGCATGCCCAAAATCAGGTACGAACAGCA 3'; used to construct pJJ10 and pJJ11; SphI site underlined
1506	5' CTAGTAATCGGCTGTGGTAAGTC 3'; *gldK* mRNA probe for qPCR
1507	5' AGTTCTTGTTGGAGCATCTTCTA 3'; *gldK* mRNA probe for qPCR
1508	5' ATGGACGCAAGTCTGAACC 3'; 16s rRNA probe for qPCR
1509	5' CGGAGTTAGCCGATCCTTATTC 3'; 16s rRNA probe for qPCR
1555	5' TAGGTCGACTTAAGTTTTAGCACCTACTCTAGACATTG 3'; used to construct pJJ11; SalI site underlined

References

1.	McBride MJ, Zhu Y. 2013. Gliding motility and Por secretion system genes are widespread among members of the phylum *Bacteroidetes*. J Bacteriol 195:270-278.
2.	Jarrell KF, McBride MJ. 2008. The surprisingly diverse ways that prokaryotes move. Nat Rev Microbiol 6:466-476.
3.	Islam ST, Mignot T. 2015. The mysterious nature of bacterial surface (gliding) motility: A focal adhesion-based mechanism in *Myxococcus xanthus*. Semin Cell Dev Biol 46:143-154.
4.	Miyata M. 2010. Unique centipede mechanism of *Mycoplasma* gliding. Annu Rev Microbiol 64:519-537.
5.	Nan B, Zusman DR. 2016. Novel mechanisms power bacterial gliding motility. Mol Microbiol 101:186-93.
6.	Braun TF, Khubbar MK, Saffarini DA, McBride MJ. 2005. *Flavobacterium johnsoniae* gliding motility genes identified by *mariner* mutagenesis. J Bacteriol 187:6943-6952.
7.	Nelson SS, Glocka PP, Agarwal S, Grimm DP, McBride MJ. 2007. *Flavobacterium johnsoniae* SprA is a cell-surface protein involved in gliding motility. J Bacteriol 189:7145-7150.
8.	Rhodes RG, Nelson SS, Pochiraju S, McBride MJ. 2011. *Flavobacterium johnsoniae sprB* is part of an operon spanning the additional gliding motility genes *sprC*, *sprD*, and *sprF*. J Bacteriol 193:599-610.
9.	Rhodes RG, Samarasam MN, Van Groll EJ, McBride MJ. 2011. Mutations in *Flavobacterium johnsoniae sprE* result in defects in gliding motility and protein secretion. Journal of Bacteriology 193:5322-7.
10.	Shrivastava A, Johnston JJ, van Baaren JM, McBride MJ. 2013. *Flavobacterium johnsoniae* GldK, GldL, GldM, and SprA are required for secretion of the cell-surface gliding motility adhesins SprB and RemA. J Bacteriol 195:3201-3212.
11.	Shrivastava A, Rhodes RG, Pochiraju S, Nakane D, McBride MJ. 2012. *Flavobacterium johnsoniae* RemA is a mobile cell-surface lectin involved in gliding. J Bacteriol 194:3678-3688.
12.	Nakane D, Sato K, Wada H, McBride MJ, Nakayama K. 2013. Helical flow of surface protein required for bacterial gliding motility. Proc Natl Acad Sci USA 110:11145-11150.
13.	Nelson SS, Bollampalli S, McBride MJ. 2008. SprB is a cell surface component of the *Flavobacterium johnsoniae* gliding motility machinery. J Bacteriol 190:2851-2857.
14.	Shrivastava A, Lele PP, Berg HC. 2015. A rotary motor drives *Flavobacterium* gliding. Curr Biol 25:338-341.
15.	Sato K, Naito M, Yukitake H, Hirakawa H, Shoji M, McBride MJ, Rhodes RG, Nakayama K. 2010. A protein secretion system linked to bacteroidete gliding motility and pathogenesis. Proc Natl Acad Sci USA 107:276-281.
16.	Kharade SS, McBride MJ. 2014. The *Flavobacterium johnsoniae* chitinase ChiA is required for chitin utilization and is secreted by the type IX secretion system. J Bacteriol 196:961-970.

17.	Kharade SS, McBride MJ. 2015. *Flavobacterium johnsoniae* PorV is required for secretion of a subset of proteins targeted to the type IX secretion system. J Bacteriol 197:147-158.

18.	Veith PD, Nor Muhammad NA, Dashper SG, Likic VA, Gorasia DG, Chen D, Byrne SJ, Catmull DV, Reynolds EC. 2013. Protein substrates of a novel secretion system are numerous in the *Bacteroidetes* phylum and have in common a cleavable C-terminal secretion signal, extensive post-translational modification and cell surface attachment. J Proteome Res 12:4449-4461.

19.	Kulkarni SS, Zhu Y, Brendel CJ, McBride MJ. 2017. Diverse C-terminal sequences involved in *Flavobacterium johnsoniae* protein secretion. J Bacteriol 199.

20.	Nguyen KA, Travis J, Potempa J. 2007. Does the importance of the C-terminal residues in the maturation of RgpB from *Porphyromonas gingivalis* reveal a novel mechanism for protein export in a subgroup of Gram-Negative bacteria? J Bacteriol 189:833-843.

21.	Sato K, Yukitake H, Narita Y, Shoji M, Naito M, Nakayama K. 2013. Identification of *Porphyromonas gingivalis* proteins secreted by the Por secretion system. FEMS Microbiol Lett 338:68-76.

22.	Glew MD, Veith PD, Peng B, Chen YY, Gorasia DG, Yang Q, Slakeski N, Chen D, Moore C, Crawford S, Reynolds E. 2012. PG0026 is the C-terminal signal peptidase of a novel secretion system of *Porphyromonas gingivalis*. J Biol Chem 287:24605-24617.

23.	Gorasia DG, Veith PD, Chen D, Seers CA, Mitchell HA, Chen YY, Glew MD, Dashper SG, Reynolds EC. 2015. *Porphyromonas gingivalis* type IX secretion substrates are cleaved and modified by a sortase-like mechanism. PLoS Pathog 11:e1005152.

24.	Chen YY, Peng B, Yang Q, Glew MD, Veith PD, Cross KJ, Goldie KN, Chen D, O'Brien-Simpson N, Dashper SG, Reynolds EC. 2011. The outer membrane protein LptO is essential for the O-deacylation of LPS and the co-ordinated secretion and attachment of A-LPS and CTD proteins in *Porphyromonas gingivalis*. Molecular microbiology 79:1380-401.

25.	Gorasia DG, Veith PD, Hanssen EG, Glew MD, Sato K, Yukitake H, Nakayama K, Reynolds EC. 2016. Structural Insights into the PorK and PorN Components of the Porphyromonas gingivalis Type IX Secretion System. PLoS Pathog 12:e1005820.

26.	Vincent MS, Canestrari MJ, Leone P, Stathopulos J, Ize B, Zoued A, Cambillau C, Kellenberger C, Roussel A, Cascales E. 2017. Characterization of the Porphyromonas gingivalis Type IX Secretion Trans-envelope PorKLMNP Core Complex. J Biol Chem 292:3252-3261.

27.	Agarwal S, Hunnicutt DW, McBride MJ. 1997. Cloning and characterization of the *Flavobacterium johnsoniae* (*Cytophaga johnsonae*) gliding motility gene, *gldA*. Proc Natl Acad Sci USA 94:12139-12144.

28.	Braun TF, McBride MJ. 2005. *Flavobacterium johnsoniae* GldJ is a lipoprotein that is required for gliding motility. J Bacteriol 187:2628-2637.

29.	Hunnicutt DW, Kempf MJ, McBride MJ. 2002. Mutations in *Flavobacterium johnsoniae* *gldF* and *gldG* disrupt gliding motility and interfere with membrane localization of GldA. J Bacteriol 184:2370-2378.

30.	Hunnicutt DW, McBride MJ. 2000. Cloning and characterization of the *Flavobacterium johnsoniae* gliding motility genes, *gldB* and *gldC*. J Bacteriol 182:911-918.

31.	Hunnicutt DW, McBride MJ. 2001. Cloning and characterization of the *Flavobacterium johnsoniae* gliding motility genes *gldD* and *gldE*. J Bacteriol 183:4167-4175.

63

32. McBride MJ, Braun TF. 2004. GldI is a lipoprotein that is required for *Flavobacterium johnsoniae* gliding motility and chitin utilization. J Bacteriol 186:2295-2302.

33. McBride MJ, Braun TF, Brust JL. 2003. *Flavobacterium johnsoniae* GldH is a lipoprotein that is required for gliding motility and chitin utilization. J Bacteriol 185:6648-6657.

34. Rhodes RG, Samarasam MN, Shrivastava A, van Baaren JM, Pochiraju S, Bollampalli S, McBride MJ. 2010. *Flavobacterium johnsoniae gldN* and *gldO* are partially redundant genes required for gliding motility and surface localization of SprB. J Bacteriol 192:1201-1211.

35. Johnston JJ, Shrivastava A, McBride MJ. 2017. Untangling Flavobacterium johnsoniae gliding motility and protein secretion. J Bacteriol doi:10.1128/JB.00362-17.

36. McBride MJ. 2001. Bacterial gliding motility: Multiple mechanisms for cell movement over surfaces. Annu Rev Microbiol 55:49-75.

37. Duxbury T, Humphrey BA, Marshall KC. 1980. Continuous observations of bacterial gliding motility in a dialysis microchamber: the effects of inhibitors. Arch Microbiol 124:169-175.

38. Dzink-Fox JL, Leadbetter ER, Godchaux W, III. 1997. Acetate acts as a protonophore and differentially affects bead movement and cell migration of the gliding bacterium *Cytophaga johnsonae* (*Flavobacterium johnsoniae*). Microbiology 143:3693-3701.

39. Pate JL, Chang L-YE. 1979. Evidence that gliding motility in prokaryotic cells is driven by rotary assemblies in the cell envelopes. Curr Microbiol 2:59-64.

40. Ridgway HF. 1977. Source of energy for gliding motility in *Flexibacter polymorphus*: effects of metabolic and respiratory inhibitors on gliding movement. J Bacteriol 131:544-556.

41. Zhu Y, McBride MJ. 2016. Comparative analysis of *Cellulophaga algicola* and *Flavobacterium johnsoniae* gliding motility. J Bacteriol 198:1743-54.

42. Macnab RM. 2004. Type III flagellar protein export and flagellar assembly. Biochim Biophys Acta 1694:207-217.

43. Shrivastava A, Roland T, Berg HC. 2016. The screw-like movement of a gliding bacterium is powered by spiral motion of cell-surface adhesins. Biophys J 111:1008-1013.

44. McBride MJ, Xie G, Martens EC, Lapidus A, Henrissat B, Rhodes RG, Goltsman E, Wang W, Xu J, Hunnicutt DW, Staroscik AM, Hoover TR, Cheng YQ, Stein JL. 2009. Novel features of the polysaccharide-digesting gliding bacterium *Flavobacterium johnsoniae* as revealed by genome sequence analysis. Appl Environ Microbiol 75:6864-6875.

45. Rhodes RG, Pucker HG, McBride MJ. 2011. Development and use of a gene deletion strategy for *Flavobacterium johnsoniae* to identify the redundant motility genes *remF*, *remG*, *remH*, and *remI*. J Bacteriol 193:2418-2428.

46. McBride MJ, Kempf MJ. 1996. Development of techniques for the genetic manipulation of the gliding bacterium *Cytophaga johnsonae*. J Bacteriol 178:583-590.

47. Liu J, McBride MJ, Subramaniam S. 2007. Cell-surface filaments of the gliding bacterium *Flavobacterium johnsoniae* revealed by cryo-electron tomography. J Bacteriol 189:7503-7506.

48. Alvarez B, Secades P, McBride MJ, Guijarro JA. 2004. Development of genetic techniques for the psychrotrophic fish pathogen *Flavobacterium psychrophilum*. Appl Environ Microbiol 70:581-587.
49. Chang LYE, Pate JL, Betzig RJ. 1984. Isolation and characterization of nonspreading mutants of the gliding bacterium *Cytophaga johnsonae*. J Bacteriol 159:26-35.
50. de Lorenzo V, Timmis KN. 1994. Analysis and construction of stable phenotypes in gram-negative bacteria with Tn5- and Tn10-derived minitransposons. Methods Enzymol 235:386-405.
51. Bolivar F, Backman K. 1979. Plasmids of *Escherichia coli* as cloning vectors. Methods Enzymol 68:245-267.
52. Figurski DH, Helinski DR. 1979. Replication of an origin-containing derivative of plasmid RK2 dependent on a plasmid function provided in trans. Proc Natl Acad Sci USA 76:1648-1652.
53. Kempf MJ, McBride MJ. 2000. Transposon insertions in the *Flavobacterium johnsoniae* *ftsX* gene disrupt gliding motility and cell division. J Bacteriol 182:1671-1679.

Chapter 3. The carboxy-terminal region of *Flavobacterium johnsoniae* SprB facilitates its secretion by the type IX secretion system and propulsion by the gliding motility machinery.

This chapter is a modified version of a paper of the same title published in the Journal of Bacteriology:

This chapter includes some of the online supplemental materials of the J. Bacteriol. paper listed above integrated into the body of the text. Dr. Surashree Kulkarni is responsible for the initial experimental design and conception of experiments that analyzed secretion of sfGFP fused to C-terminal domains of *F. johnsoniae* secreted proteins. Dr. Kulkarni generated the series of plasmids for expression GFP-type B CTD fusion proteins named as "pSKxx" and constructed the Δ*sprF* and Δ*sprB* Δ*gldK* strains. Experiments shown in figures 2A, 2B, 2C, 4, 16A, 16B, 18, and 20 were performed by Kulkarni. Dr. Yongtao Zhu generated the *sfGFP*::*sprB* strain and the plasmid pYT179, which served as the backbone for the pSKxx GFP-typeB CTD plasmids. Zhu and Hying performed the SprF localization experiment shown in figure 19. Dr. Mark McBride performed the comparative genomics, protein alignments, bioinformatic analysis of *F. johnsoniae sprF*-like genes and proteins, and of *F. johnsoniae* proteins predicted to be secreted by the T9SS. Dr. McBride's studies are presented in figures 5, 14, 15, 21, and tables 1-3. Johnston generated the Δ*sprB gldJ_{548}* strain and plasmid pJJ21. Johnston performed western

blots, microscopy, and other experiments shown in figures 2D, 3, 6-13, 16C, and 17. Observations by Johnston were instrumental in identifying regions of type B CTDs that when fused to the foreign protein sfGFP resulted in its secretion across the outer membrane, attachment to the cell surface, and propulsion by the motility machinery.

Abstract

Flavobacterium johnsoniae SprB moves rapidly along the cell surface resulting in gliding motility. SprB secretion requires the type IX secretion system (T9SS). Proteins secreted by the T9SS typically have conserved C-terminal domains (CTDs) belonging to the type A CTD or type B CTD families. Attachment of 70 to 100 amino acid type A CTDs to a foreign protein allow its secretion. Type B CTDs are common but have received little attention. Secretion of the foreign protein sfGFP fused to regions spanning the SprB type B CTD (sfGFP-CTD$_{SprB}$) was analyzed. CTDs of 218 amino acids or longer resulted in secretion of sfGFP whereas a 149 amino acid region did not. Some sfGFP was secreted in soluble form whereas the rest was attached on the cell surface. Surface-attached sfGFP was rapidly propelled along the cell, suggesting productive interaction with the motility machinery. This did not result in rapid cell movement, which apparently requires additional regions of SprB. Secretion of sfGFP-CTD$_{SprB}$ required coexpression with *sprF*, which lies downstream of *sprB*. SprF is similar in sequence to *Porphyromonas gingivalis* PorP. Most *F. johnsoniae* genes encoding proteins with type B CTDs lie immediately upstream of *porP/sprF*-like genes. sfGFP was fused to the type B CTD from one such protein (Fjoh_3952). This resulted in secretion of sfGFP only when it was coexpressed with its cognate PorP/SprF-like protein. These results highlight the need for extended regions of type B CTDs and for coexpression with the appropriate PorP/SprF-like protein for efficient secretion and cell-surface localization of cargo proteins.

67

Introduction

The gliding bacterium *Flavobacterium johnsoniae* secretes many proteins across its outer membrane via the type IX secretion system (T9SS) (1). T9SSs are common in but apparently confined to members of the phylum *Bacteroidetes* (2). They were first identified and have been most well studied in the nonmotile oral pathogen *Porphyromonas gingivalis* and in *F. johnsoniae* (3, 4). Many of the T9SS genes were originally discovered as *F. johnsoniae* genes required for cell movement over surfaces by gliding motility (5, 6). Some of the motility defects caused by mutations in these genes can be explained by failure to secrete the large mobile cell surface motility adhesins SprB and RemA (3, 7, 8). These adhesins are propelled rapidly along the surface of wild type cells by other components of the gliding motility machinery. The adhesins follow a helical path along a cell and their interactions with the substratum result in screw-like movement of the cell (9, 10).

The core components of the *F. johnsoniae* T9SS include GldK, GldL, GldM, GldN, SprA, SprE and SprT (Fig. 1) (3, 5, 6, 8, 11), which are orthologs of *P. gingivalis* PorK, PorL, PorM, PorN, Sov, PorW and PorT respectively (3). Other components involved in but not essential for *F. johnsoniae* secretion include PorU and PorV. Mutations in *porU* and *porV* result in defects in secretion of some proteins that are targeted to the T9SS, but not others (1, 12). *P. gingivalis porP*, *porZ*, and PG1058 are also involved in secretion, and *F. johnsoniae* has orthologs of each of these. *F. johnsoniae* has multiple genes that are similar to *P. gingivalis porP*, and requirement of these for secretion may be masked by redundancy. One of these genes, *sprF*, is required for secretion of SprB, but not for secretion of other proteins that are targeted to the T9SS (7, 13). *sprF* lies immediately downstream of, and is cotranscribed with, *sprB* (13). PorP and SprF are predicted outer membrane β-barrel proteins (13), and outer membrane

68

localization was confirmed for PorP (3). *F. johnsoniae porZ* and PG1058-like genes have not yet been examined for their roles in secretion. Most of the components of the T9SS are unique to members of the phylum *Bacteroidetes*, and none are similar in sequence to components of bacterial type I to type VIII secretion systems (3, 8).

Recent results begin to reveal the structure and function of the T9SS. *P. gingivalis* PorK, PorL, PorM, and PorN (GldK, GldL, GldM, and GldN respectively in *F. johnsoniae*) appear to form a complex that spans the cell envelope (3, 14-16). The cytoplasmic membrane proteins PorL and PorM (GldL and GldM in *F. johnsoniae*) have been suggested to harvest the proton gradient and energize both secretion and motility (8, 15, 17). Studies of *F. johnsoniae* SprA (ortholog of *P. gingivalis* Sov) suggest that it forms the outer membrane pore through which secreted proteins pass (18).

The *F. johnsoniae* T9SS is required for secretion of dozens of proteins. In addition to the cell surface motility adhesins described above, it also secretes soluble extracellular enzymes such as the chitinase ChiA and the amylase AmyB (1, 8, 19). The *P. gingivalis* T9SS is involved in secretion of virulence factors such as the cell-surface gingipain proteases (3). In both organisms, the secreted proteins have N-terminal signal peptides that allow export across the cytoplasmic membrane via the Sec machinery, and conserved C-terminal domains (CTDs) that are required for T9SS-mediated secretion. The CTDs are typically cleaved during or after secretion (20-24). Most known T9SS CTDs belong to either protein domain family TIGR04183 (type A CTDs), or family TIGR04131 (type B CTDs). The roles of type A CTDs in secretion of *F. johnsoniae* and *P. gingivalis* proteins have been studied. Type A CTD regions of 70 to 100 amino acids are sufficient to target a foreign protein such as sfGFP for secretion from the periplasm across the outer membrane by the T9SS (12, 22). The structures of two type A CTDs have been determined

(25, 26). Both have an Ig-like fold with seven β-strands, and are thought to interact with components of the T9SS. Some *F. johnsoniae* proteins with type A CTDs are released in soluble form, whereas others remain attached to the cell surface after secretion.

Type B CTDs are not similar in sequence to type A CTDs, and they have not been studied in detail. The 6497-amino acid protein SprB appears to require its type B CTD for secretion (12, 27). However, attachment of C-terminal regions of *F. johnsoniae* SprB to the foreign protein sfGFP failed to result in its secretion across the outer membrane (12).

Here we present evidence that type B CTDs target proteins for secretion by the T9SS, and that specific PorP/SprF-like outer membrane proteins facilitate secretion of proteins carrying different type B CTDs. Moreover, the C-terminal 218 amino acid region of SprB is sufficient to target a foreign protein for secretion and productive interaction (direct or indirect) with the motility machinery, resulting in rapid movement along the cell surface. The results highlight the diversity of proteins secreted by the T9SS, and the roles of their C-terminal regions in secretion, cell-surface localization, and interaction with the motility machinery.
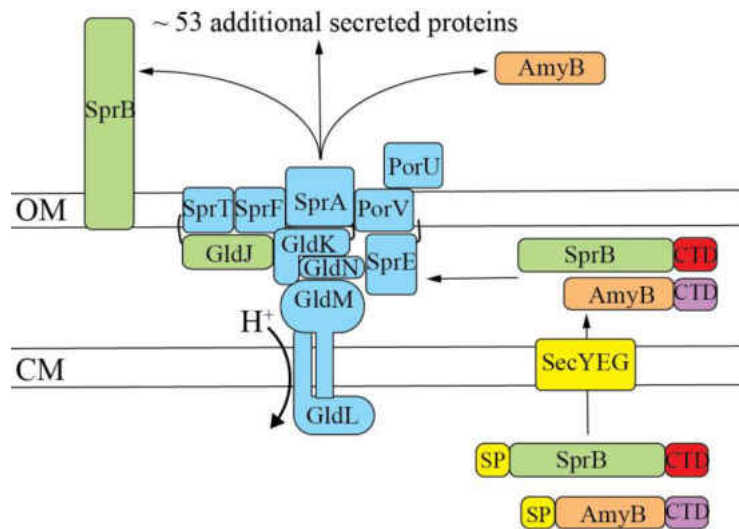
Figure 1. The *F. johnsoniae* type IX protein secretion system. Proteins required for secretion include the cytoplasmic membrane proteins GldL and GldM that have been proposed to energize secretion, and the outer membrane-associated proteins GldK, GldN, SprA, SprE, and SprT. The gliding motility protein GldJ (green) is needed to stabilize the T9SS protein GldK (28). Many of the T9SS proteins may also have roles in motility in addition to their functions in secretion. SprF is required for the secretion of SprB but not for the secretion of other proteins by the T9SS (13). The secreted proteins have N-terminal signal peptides (SP) that target them for export across the cytoplasmic membrane by the Sec system before delivery to the T9SS. Proteins secreted by T9SSs have type A (purple) or type B (red) C-terminal domains (CTDs) required for secretion. PorV appears to be required for the secretion of proteins that have type A CTDs but is not needed for the secretion of SprB or for the secretion of some other proteins that have type B CTDs (1). Black lines on the lipoproteins GldJ, GldK and SprE indicate lipid tails. OM, outer membrane; CM, cytoplasmic membrane.

Results

    Fusion of sfGFP to C-terminal regions of SprB resulted in its secretion. Many

proteins secreted by T9SSs have type A CTDs, and the involvement of these in secretion has

been demonstrated (1, 12, 21, 22, 29). Type B CTDs, such as the carboxy-terminal region of

SprB, have been less well studied. Previous results indicated that sfGFP fused to a signal peptide

at its amino terminus (SP-sfGFP), and to C-terminal regions of SprB of 99, 218, and 1182 amino

acids in length (SP-sfGFP-CTD$_{SprB(99AA)}$, SP-sfGFP-CTD$_{SprB(218AA)}$, and SP-sfGFP-

CTD$_{SprB(1182AA)}$ respectively) were not secreted by wild type cells (12). SprF is required for secretion of SprB, but not for secretion of other proteins that are targeted to the T9SS (13). We previously suggested that SprF may play an adapter or chaperone-like function that facilitates secretion of SprB (13). One possible explanation for the failure of wild type cells to secrete SP-sfGFP-CTD$_{SprB}$ is that the SprF in wild type cells may have been fully engaged with its coexpressed partner, SprB, leaving little available to interact with SP-sfGFP-CTD$_{SprB}$. To relieve this situation, we deleted *sprB*. Δ*sprB* mutants carrying pSK56, which expresses SP-sfGFP-CTD$_{SprB(218AA)}$, exhibited wild-type levels of SprF protein (Fig. 2D) and appeared to secrete a small amount of sfGFP (Fig. 2A, 2B). Co-expression of SP-sfGFP-CTD$_{SprB}$ and SprF from pSK55 resulted in higher levels of SprF (Fig. 2D) and increased secretion of sfGFP (Fig. 2B). Secretion did not occur in cells of the double mutant Δ*sprB* Δ*gldK* carrying the same plasmid (Fig. 2B), indicating that a functional T9SS was required. The presence of sfGFP in the spent medium was not likely the result of cell lysis or leakage because coexpression of SP-sfGFP-CTD$_{SprB}$ (from pSK55) and SP-mCherry (from pJJ21) allowed secretion of sfGFP but not leakage of mCherry (Fig. 3). A shorter region of the C-terminus of SprB (149 amino acids) failed to result in secretion of sfGFP even when coexpressed with SprF (Fig. 2C). Regions of SprB spanning the C-terminal 368, 448, 663, and 1182 amino acids were also fused to SP-sfGFP and examined for their ability to facilitate secretion of sfGFP. *sprF* was co-expressed on the same plasmids. Western immunoblot analyses of the strains expressing the fusion proteins demonstrated the accumulation of sfGFP in the spent medium (Fig. 4). The apparent molecular mass of the soluble secreted sfGFP (approximately 30 kDa) did not change when the length of the C-terminal region of SprB fused to sfGFP was increased beyond 218 amino acids. This suggests processing of the fusion protein during or after secretion, with accumulation of stable

72

sfGFP in the medium. *F. johnsoniae* produces many secreted proteases that could contribute to this partial digestion of the secreted protein (30). The results suggest that a CTD longer than 149 amino acids was required for secretion, and that coexpression of SP-sfGFP-CTD$_{SprB}$ and SprF from the same plasmid resulted in enhanced secretion. Alignment of the C-terminus of SprB with other *F. johnsoniae* proteins with type B CTDs indicates that regions of sequence identity extend only for the C-terminal 85 to 100 amino acids (Fig. 5). Apparently, additional regions outside of this conserved C-terminal region of SprB are required to effectively target SP-sfGFP-CTD$_{SprB}$ for secretion.
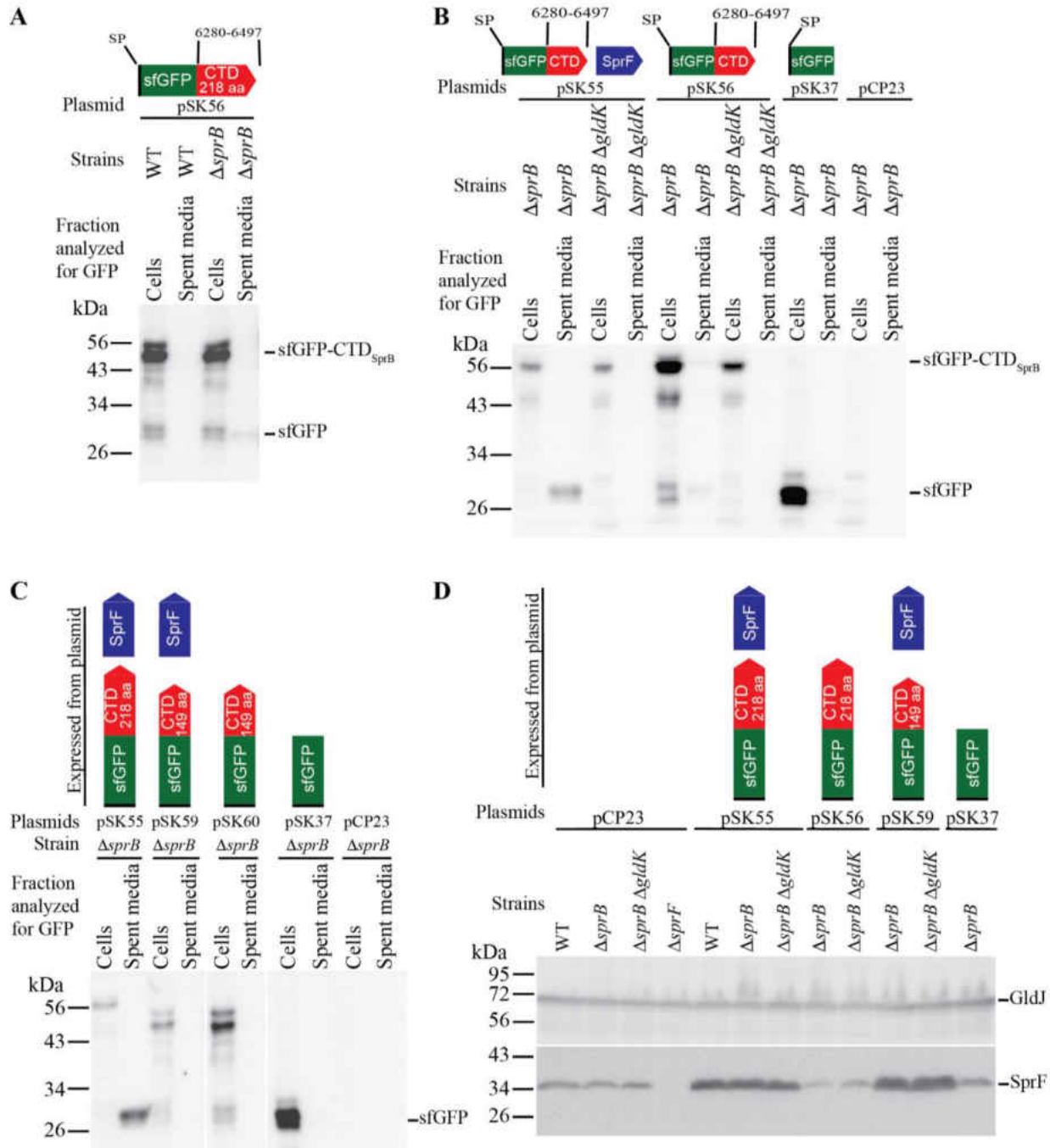
Figure 2. T9SS-mediated secretion of sfGFP fused to the CTD of SprB, with or without co-expression with SprF. Cultures of wild type (WT), Δ*sprB* mutant, Δ*sprB* Δ*gldK* T9SS-defective mutant, and Δ*sprF* mutant, carrying the plasmids indicated, were incubated in CYE at 25°C with shaking and harvested in the late exponential phase of growth. Strains with *gldK* deleted (Δ*gldK*) lack a functional T9SS. All strains except for the Δ*sprF* strain in panel D were wild type for *sprF* on the chromosome, but some expressed additional SprF from plasmid as indicated. For panels A-C cells and spent culture media were separated by centrifugation and analyzed by Western

blot using antiserum against GFP. Cell samples corresponded to 10 μg protein per lane and samples from spent media corresponded to the volume of spent medium that contained 10 μg protein before the cells were removed. For panel D, cells (20 μg protein per lane) were examined by Western blot using antiserum against SprF and antiserum against GldJ (loading control). Plasmids used were pCP23 (Empty vector); pSK37, which expresses sfGFP with N-terminal signal peptide (SP); pSK56, which expresses SP-sfGFP fused to the 218-amino acid CTD of SprB (SP-sfGFP-CTD$_{SprB218AA}$); pSK55, which co-expresses SP-sfGFP- CTD$_{SprB218AA}$ and SprF; pSK60, which expresses SP-sfGFP fused to the 149-amino acid CTD of SprB (SP-sfGFP-CTD$_{SprB149AA}$); or pSK59, which co-expresses SP-sfGFP- CTD$_{SprB149AA}$ and SprF. Cartoons depicting the proteins expressed from the plasmids are indicated above the appropriate lanes.
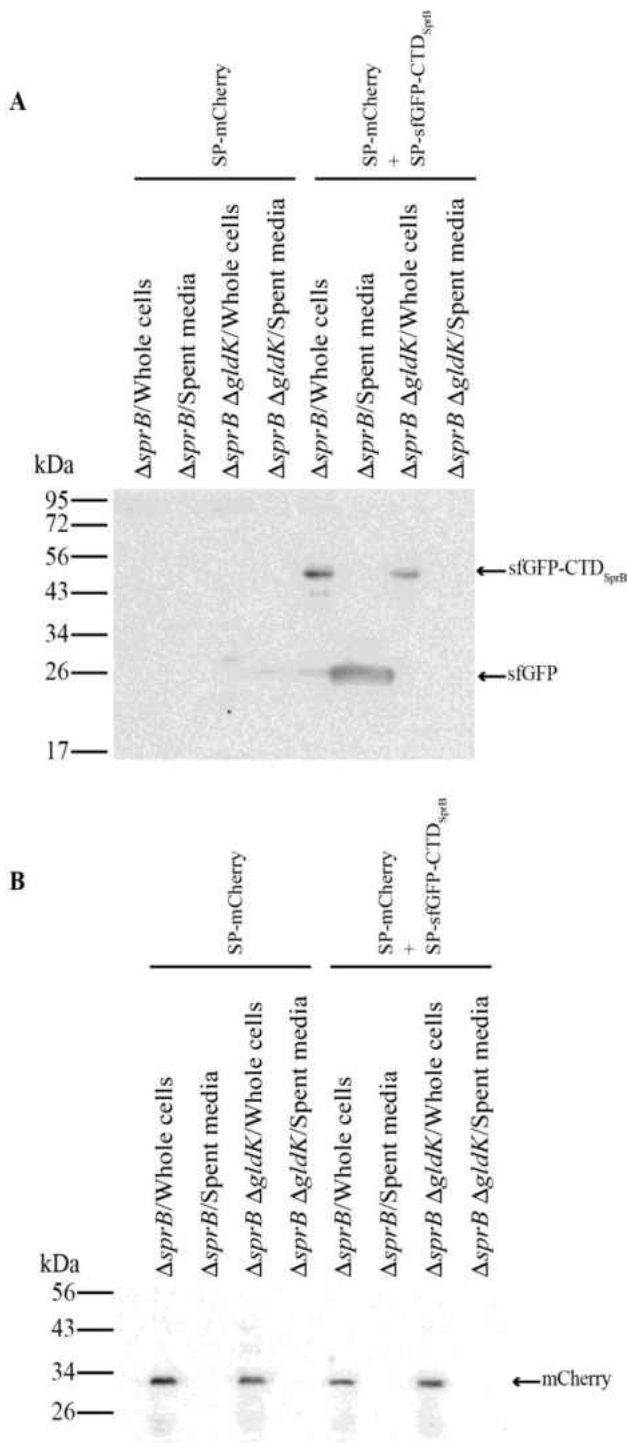
Figure 3. Analysis of cells for leakage of periplasmic mCherry. Cultures of Δ*sprB* mutant or of the T9SS mutant Δ*sprB* Δ*gldK* expressing SP-mCherry (pJJ21), or SP-sfGFP-CTD$_{SprB}$ (pSK55) and SP-mCherry (pJJ21) were incubated in CYE at 25°C with shaking. One ml samples were centrifuged at 22,000 x g for 15 min. The culture supernatant (spent medium) and intact cells were analyzed by SDS-PAGE, followed by western blot using (A) anti-GFP antibodies (to detect secretion of SP-sfGFP-CTD$_{SprB}$) and (B) anti-mCherry antibodies (to detect leakage of periplasmic mCherry). Identical samples were used in panels A and B. Cell samples corresponded to 15 μg protein per lane and samples from spent media corresponded to the volume of spent medium that contained 15 μg protein before the cells were removed. For additional controls regarding specificity of the anti-mCherry antibodies see (1, 12, 19).

76
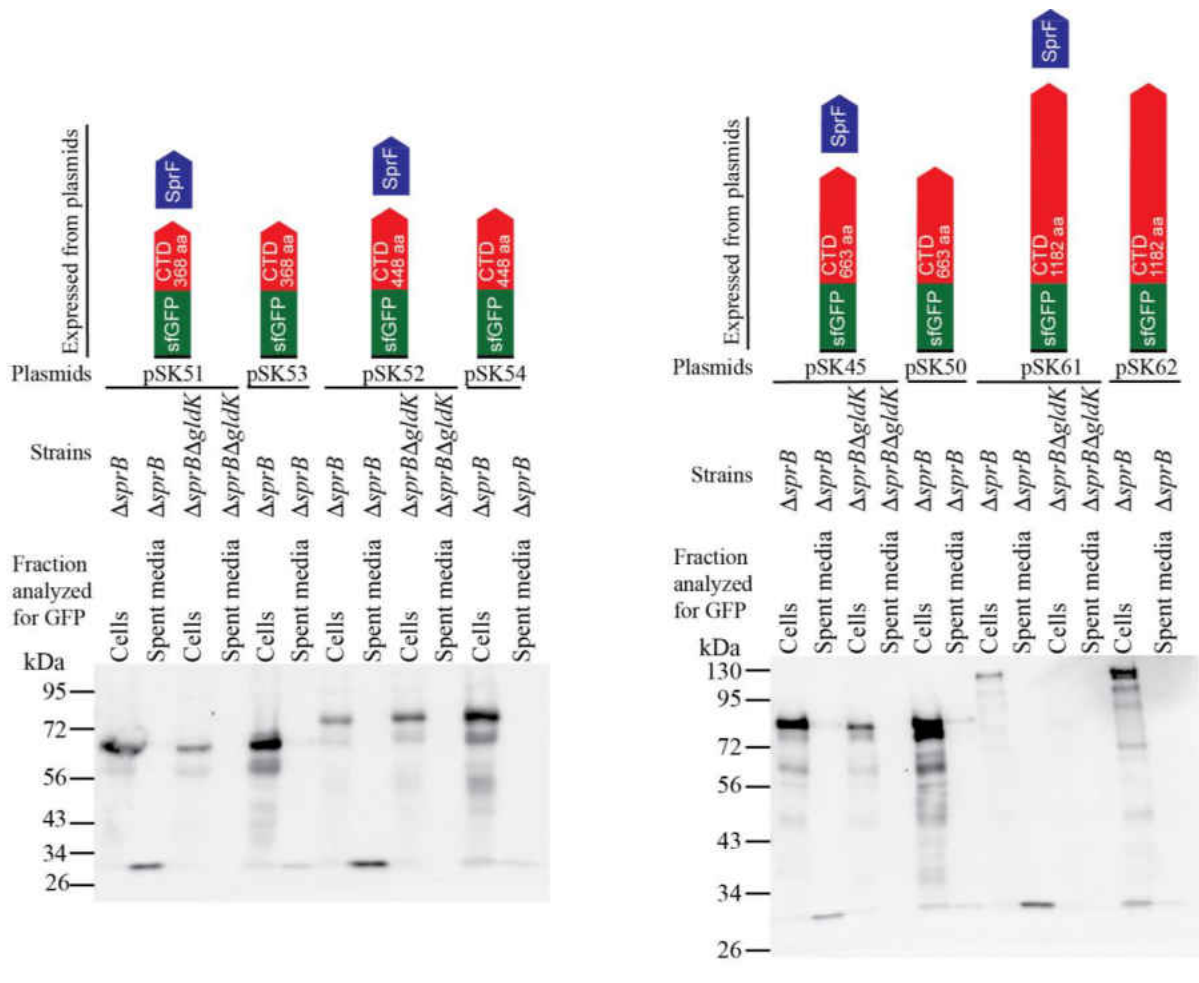
Figure 4. T9SS-mediated secretion of sfGFP fused to long C-terminal regions (CTDs) of SprB, with or without plasmid co-expression of SprF. Cultures carrying the plasmids indicated were incubated in CYE at 25°C with shaking and harvested in the late exponential phase of growth. Cells and spent culture media were separated by centrifugation and analyzed by SDS-PAGE followed by Western blot using antiserum against GFP. Whole cell samples corresponded to 10 μg protein per lane and samples from spent media corresponded to the volume of spent medium that contained 10 μg protein before the cells were removed. All strains carried a deletion of *sprB* to avoid SprF being sequestered by SprB. Some strains carried a *gldK* deletion (Δ*gldK*) to disable the T9SS. All strains were wild type for *sprF* on the chromosome but some expressed additional SprF from plasmid as indicated. Plasmids used were pSK53, which expresses SP-sfGFP fused to the 368-amino acid CTD of SprB (SP-sfGFP-CTD$_{SprB368}$); pSK51, which co-expresses SP-sfGFP-CTD$_{SprB368}$ and SprF; pSK54, which expresses SP-sfGFP fused to the 448 amino acid CTD of SprB (SP-sfGFP-CTD$_{SprB448}$); pSK52, which co-expresses SP-sfGFP-CTD$_{SprB448}$ and SprF; pSK50, which expresses SP-sfGFP fused to the 663 amino acid CTD of SprB (SP-sfGFP-CTD$_{SprB663}$); pSK45 which co-expresses SP-sfGFP-CTD$_{SprB663}$ and SprF; pSK62, which expresses SP-sfGFP fused to the 1182 amino acid CTD of SprB (SP-sfGFP-CTD$_{SprB1182}$); and pSK61 which co-expresses SP-sfGFP-CTD$_{SprB1182}$ and SprF. Cartoons depicting the proteins expressed from the plasmids are indicated above the appropriate lanes.

77
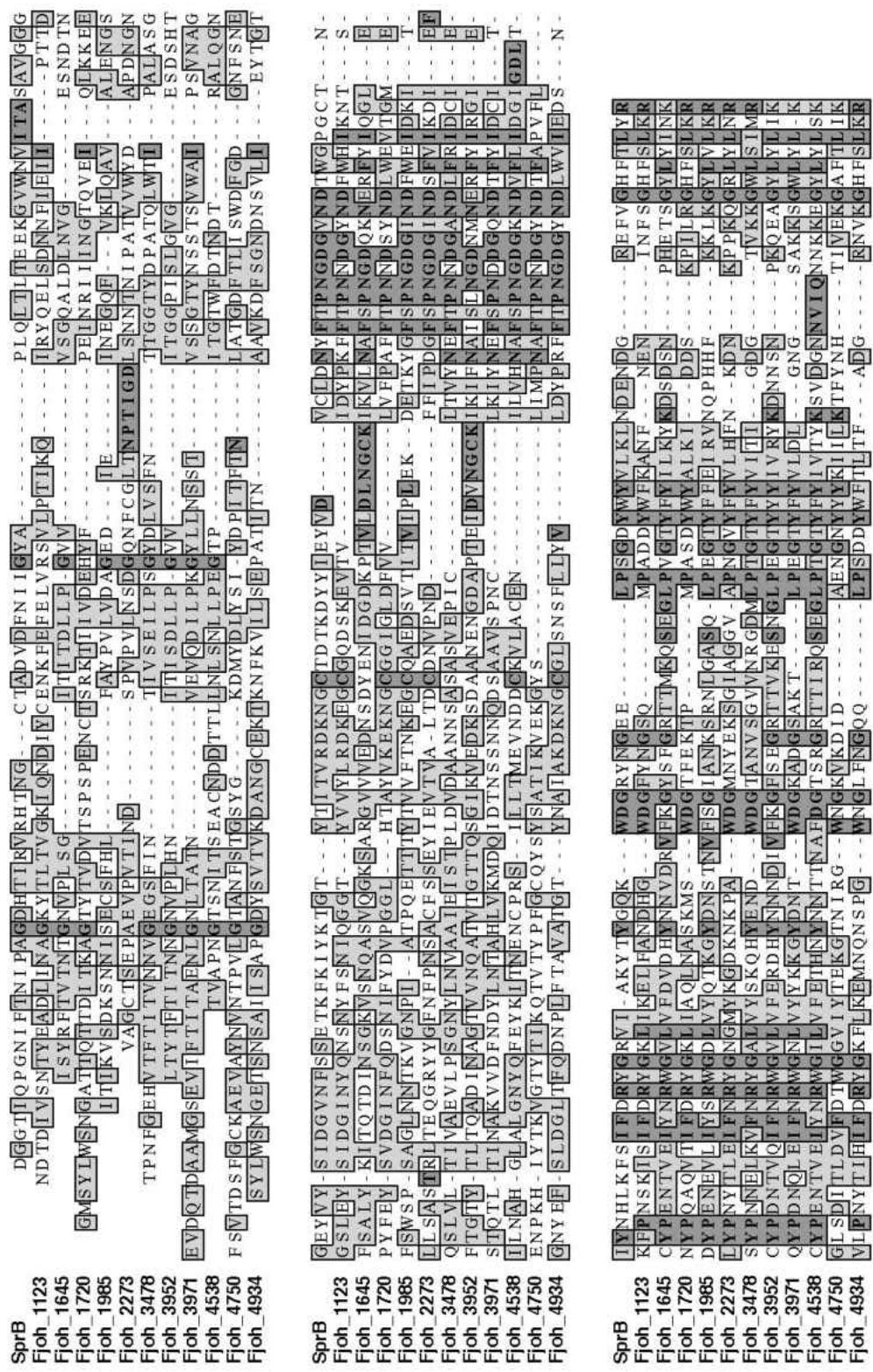
Figure 5. Alignment of the C-terminal 200 amino acids of *F. johnsoniae* proteins that belong to TIGRFAM family TIGR04131 (type-B CTD). Protein sequences were aligned using MUSCLE. Dark shading indicates identical amino acids and light shading indicates similar amino acids. Proteins that were examined experimentally in this study were SprB, Fjoh_3952, and Fjoh_1123.

Fusion of sfGFP to C-terminal regions of SprB resulted in its attachment to the cell surface and rapid movement. SprB attaches to the surface of cells after secretion by the T9SS (3, 9, 27). Cells that expressed SP-sfGFP-CTD$_{SprB}$ were examined for their ability to localize sfGFP to the cell surface by immunofluorescence microscopy using anti-GFP followed by secondary antibody conjugated to Alexa Fluor 594. Full length SprB with sfGFP inserted after the N-terminal signal peptide (SP-sfGFP-CTD$_{SprB(6421AA)}$) expressed from the chromosome localized to the cell surface (Fig. 6 and 7). Similarly, cells that expressed SP-sfGFP-CTD$_{SprB}$ with CTDs of 218 amino acids or longer had sfGFP on their surfaces. In contrast, cells expressing SP-sfGFP-CTD$_{SprB(149AA)}$ did not have sfGFP on the cell surface (Fig. 6 and 7). Surface associated sfGFP was not observed above background levels unless the fusion protein was coexpressed with SprF (Fig. 6 and 7). sfGFP did not interact with the cell surface unless it had the proper CTD. Fusion of SP-sfGFP to the CTDs of ChiA and AmyB, resulted in secretion of sfGFP but not cell surface attachment (12), as confirmed here by immunofluorescence microscopy (Fig. 8 and 9). SP-sfGFP-CTD$_{AmyB}$ and SP-sfGFP-CTD$_{SprB}$ had identical N-terminal signal peptides linked to sfGFP and only differed at their C-termini, suggesting that the 218-amino acid region of SprB was responsible for interaction with the cell surface. In all of the fluorescence microscopy experiments described above, cells were examined for red fluorescence. We also examined the same cells for green fluorescence, to demonstrate that the filters used allowed detection of green fluorescence and red fluorescence without overlap (Fig. 10). This also confirmed that sfGFP was present in cells that did not secrete it either because of a T9SS mutation ($\Delta gldK$) or because sfGFP was not fused to a C-terminal domain of SprB of 218 amino acids or longer.

Full length SprB with sfGFP inserted after the N-terminal signal peptide was propelled along the cell surface (Movie S1 in supplemental material of (31)), as has been reported previously for wild type SprB (9, 27). Similarly, sfGFP fused to CTDs of SprB of 218 amino acids or longer also moved rapidly along the cell surface, suggesting productive interaction of the C-terminal 218-amino acid region of SprB with the gliding motility apparatus (Fig. 7, 11 and Movie S2 in supplemental material of (31)). Deletion of the region spanning *sprC* and *sprD* from the chromosome resulted in decreased localization of SP-sfGFP-CTD$_{SprB(218\ AA)}$ on the cell surface, and no apparent movement (Fig. 7B) suggesting the possibility that SprC and/or SprD may be important for productive interaction with the rest of the motility machinery.

The motility protein GldJ is needed for gliding motility and for T9SS function (28). GldJ is required for stable accumulation of the T9SS protein GldK, explaining why GldJ is needed for secretion. Use of GldJ truncation mutants allows motility and secretion to be separated (28). *gldJ* mutant cells that express truncated GldJ$_{548}$, lacking the C-terminal 13 amino acids of GldJ, accumulate GldK and have a functional T9SS, but they are nonmotile. Such cells secrete SprB to the cell surface, but do not propel it along the cell surface. To demonstrate that the motility machinery was required for the observed movement of SP-sfGFP-CTD$_{SprB(218AA)}$ described above, we expressed this fusion protein in cells that produce truncated GldJ$_{548}$. These cells secreted sfGFP and localized it to the cell surface, but they failed to propel it along the cell surface (Fig. 7B and Movie S2 in supplemental material of (31)).
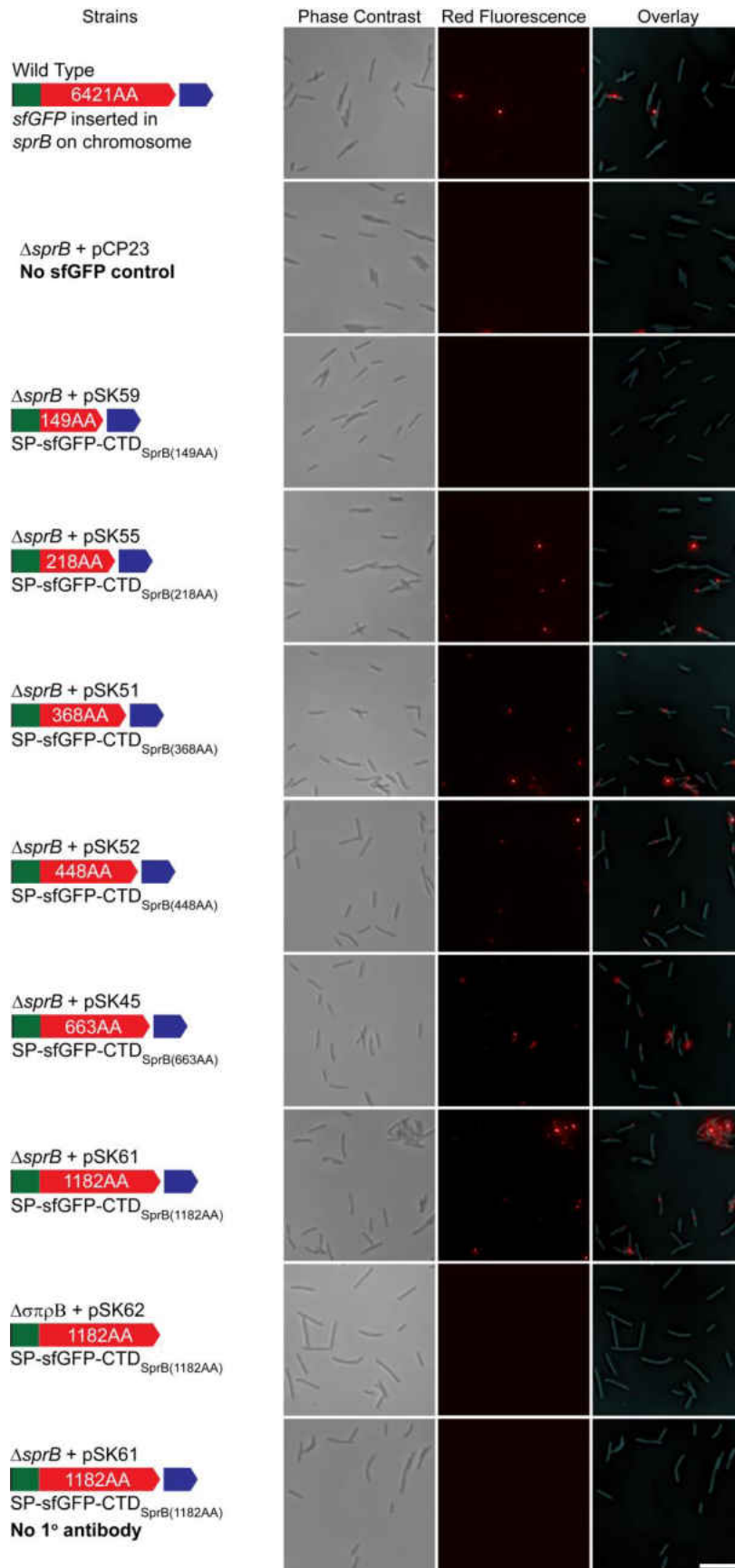
Figure 6. Surface-localization sfGFP by attachment to C-terminal regions of SprB. Cells expressing SP-sfGFP fused to C-terminal regions (CTDs) of SprB ranging from 149 to 6421 amino acids were exposed to anti-GFP and 2° antibody fused to Alexa Fluor 594 and observed by fluorescence microscopy to detect sfGFP exposed on the cell surface. Exposure times for fluorescence images were all 33 msec. Phase contrast images (left column) were superimposed with fluorescence images (middle column) to observe the relationship of the signals to cells (right column). Top left row of three images is wild type cells expressing full length SprB from the chromosome, with sfGFP fused after the signal peptide. All remaining rows of three images are $\Delta sprB$ mutant cells with, or without, plasmids expressing SP-sfGFP fused to CTD_{SprB} of the lengths indicated. All plasmids except the empty vector pCP23, and pSK62 (right, second row from bottom) also express SprF, to facilitate secretion. Anti-GFP was added to all cells except for those in the bottom right row. White scale bar in lower right panel = 10µm and applies to all panels.

81
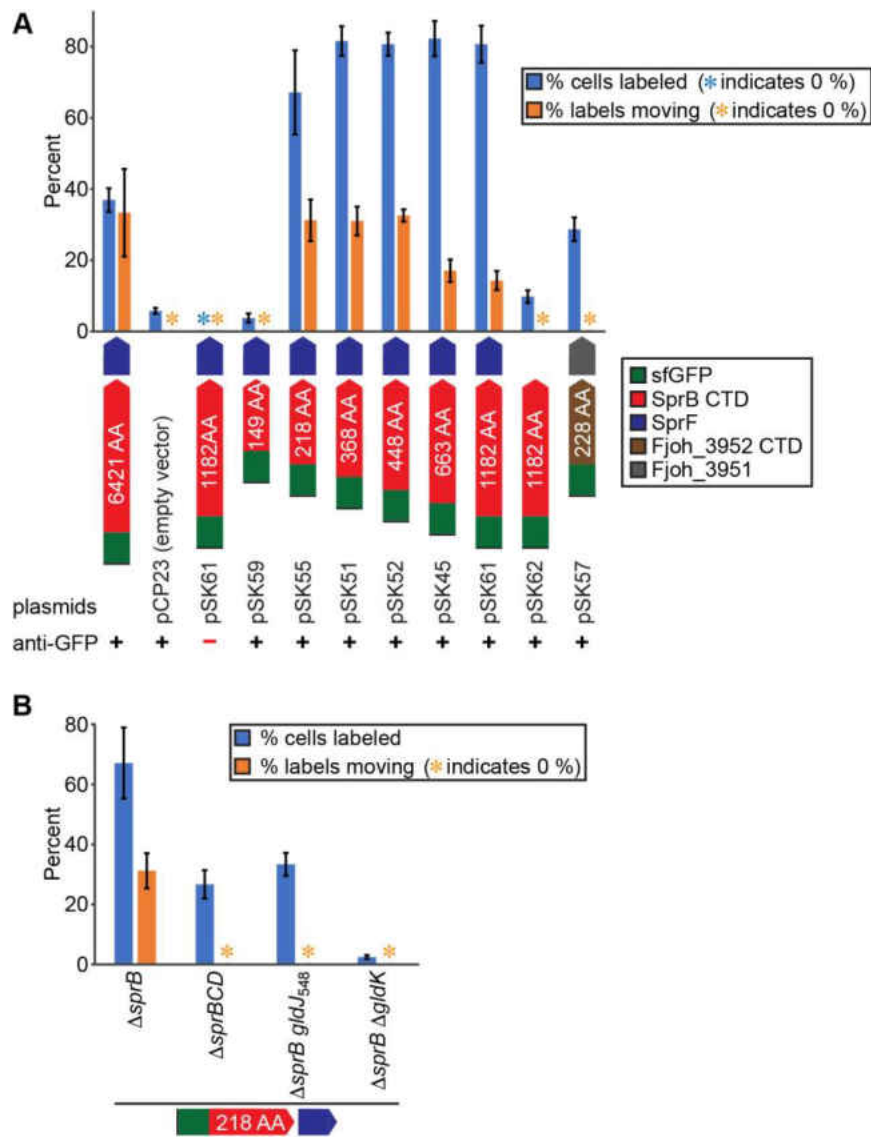
Figure 7. Labeling and movement of cell surface localized sfGFP. Cells expressing SP-sfGFP fused to C-terminal regions (CTDs) of SprB and Fjoh_3952 were exposed to anti-GFP and secondary antibody fused to Alexa Fluor 594 and observed by fluorescence microscopy to detect sfGFP exposed on the cell surface. In both panels, % of labeled cells and % of labels that moved were determined by examining three independent samples of 150 cells from each strain. For movement, cells were observed with simultaneous fluorescence excitation and low light phase-contrast and examined for fluorescent labeling and propulsion of the label along the cell surface. Labels counted as moving traveled ≥ 2.5 μm during the 20 s observation period. Examples of moving and nonmoving labels are shown in Movies S1-S3 in supplemental material of (31). Blue or orange asterisks indicate that 0 signals or 0 moving signals respectively, were observed for these samples. Error bars indicate standard deviations from three measurements. In panel A, '6421 AA' indicates full length SprB expressed from the chromosome, with sfGFP fused after the signal peptide. This strain also carried the empty vector, pCP23. All other sfGFP fusions were expressed from their respective plasmids in the $\Delta sprB$ mutant. In panel B, SP-sfGFP-CTD$_{SprB(218\ AA)}$ was expressed from pSK55 in $\Delta sprB$, $\Delta sprBCD$, $\Delta sprB\ gldJ_{548}$, and $\Delta sprB\ \Delta gldK$ mutants.
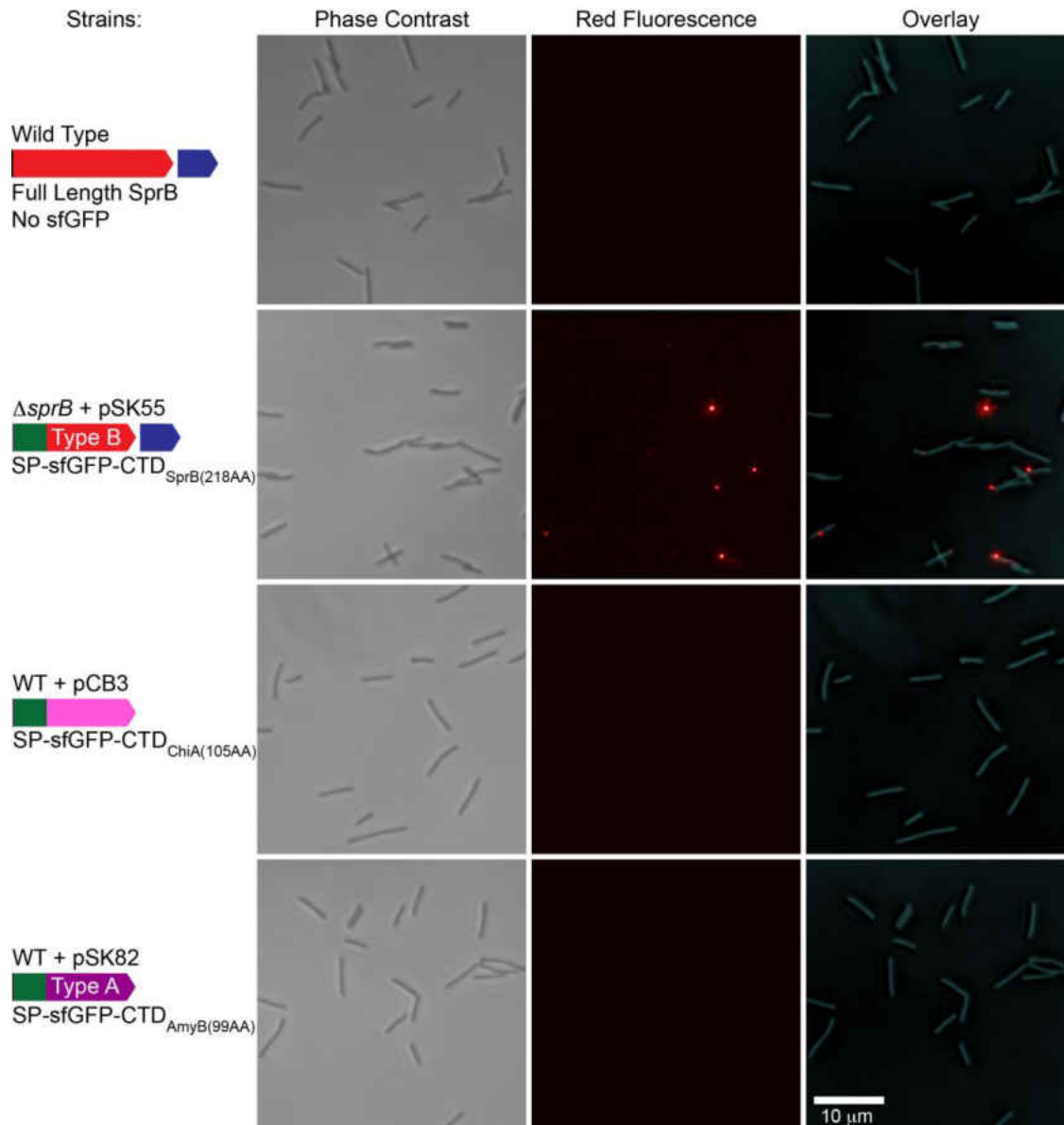
Figure 8. C-terminal regions of the soluble secreted proteins ChiA and AmyB fused to sfGFP do not result in attachment to the cell surface. Cells expressing SP-sfGFP fused to C-terminal regions (CTDs) of SprB, ChiA, and AmyB that are known to facilitate secretion were exposed to anti-GFP and 2° antibody fused to Alexa Fluor 594 and observed by fluorescence microscopy to detect sfGFP exposed on the cell surface. Exposure times for fluorescence images were all 33 msec. Phase contrast images were superimposed with fluorescence images to observe the relationship of the signals to cells. Top row is wild type (WT) cells with no sfGFP. The remaining rows are $\Delta sprB$ mutant cells or wild type cells with plasmids expressing SP-sfGFP fused to CTD_{SprB}, CTD_{ChiA}, or CTD_{AmyB} as indicated. Blue arrows indicate that SprF is expressed from the chromosome (top row) or from plasmid pSK55 (second row) to facilitate secretion. SprF is not needed to facilitate secretion of SP-sfGFP-CTD_{ChiA} or SP-sfGFP-CTD_{AmyB}, as previously indicated, and these are secreted as soluble proteins, as are full length ChiA and AmyB (1, 12, 19). 'Type B' indicates Type B CTD. 'Type A' indicates Type A CTD.

83
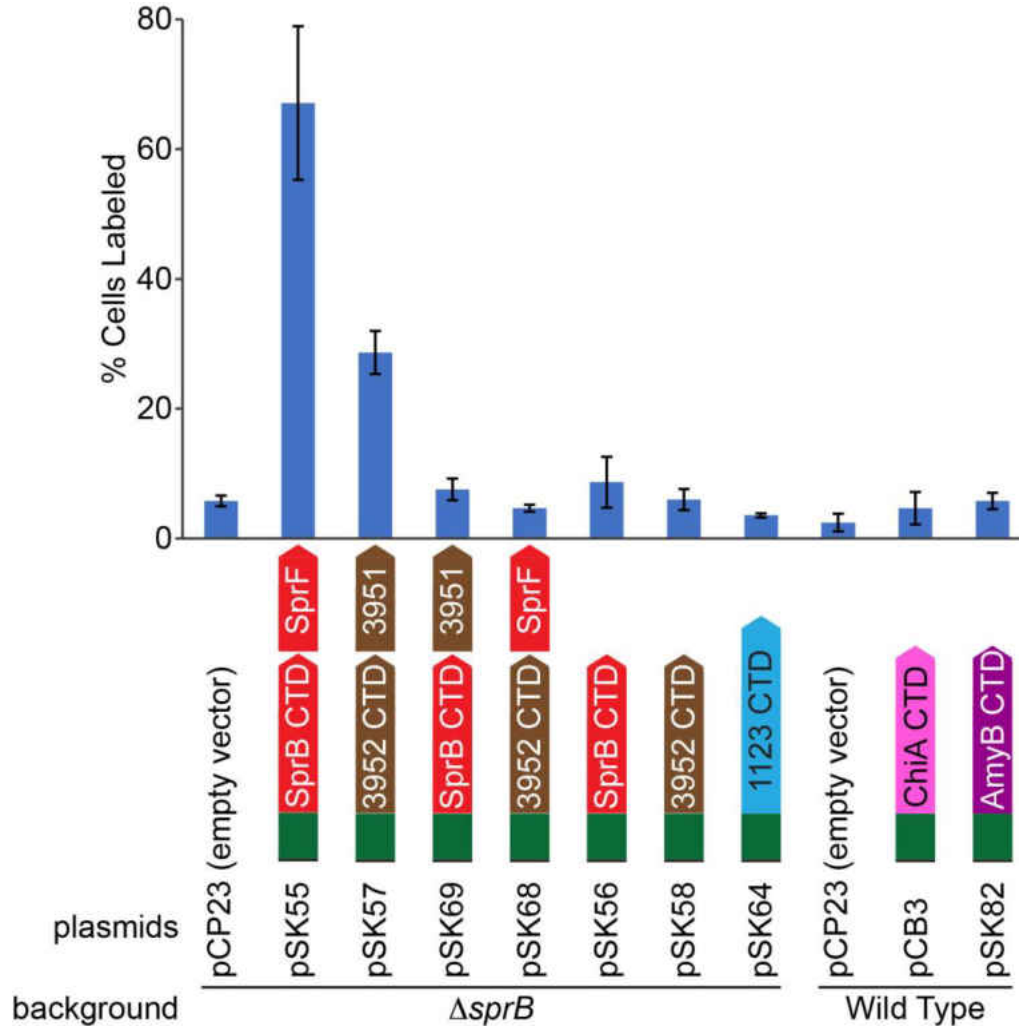
Figure 9. Labeling of cell surface localized sfGFP fused to T9SS CTDs. Cells expressing SP-sfGFP fused to C-terminal regions (CTDs) of SprB (218 AA), Fjoh_3952 (228 AA), Fjoh_1123 (238 AA), ChiA (105 AA) and AmyB (99 AA) were exposed to anti-GFP and secondary antibody fused to Alexa Fluor 594 and observed by fluorescence microscopy to detect sfGFP exposed on the cell surface. Percent of labeled cells was determined by examining three independent samples of 150 cells from each strain. Error bars indicate standard deviations from three measurements. All Type B CTD sfGFP fusions were expressed from their respective plasmids in the Δ*sprB* mutant. The ChiA and AmyB CTD sfGFP fusions were expressed from their respective plasmids in wild type cells.
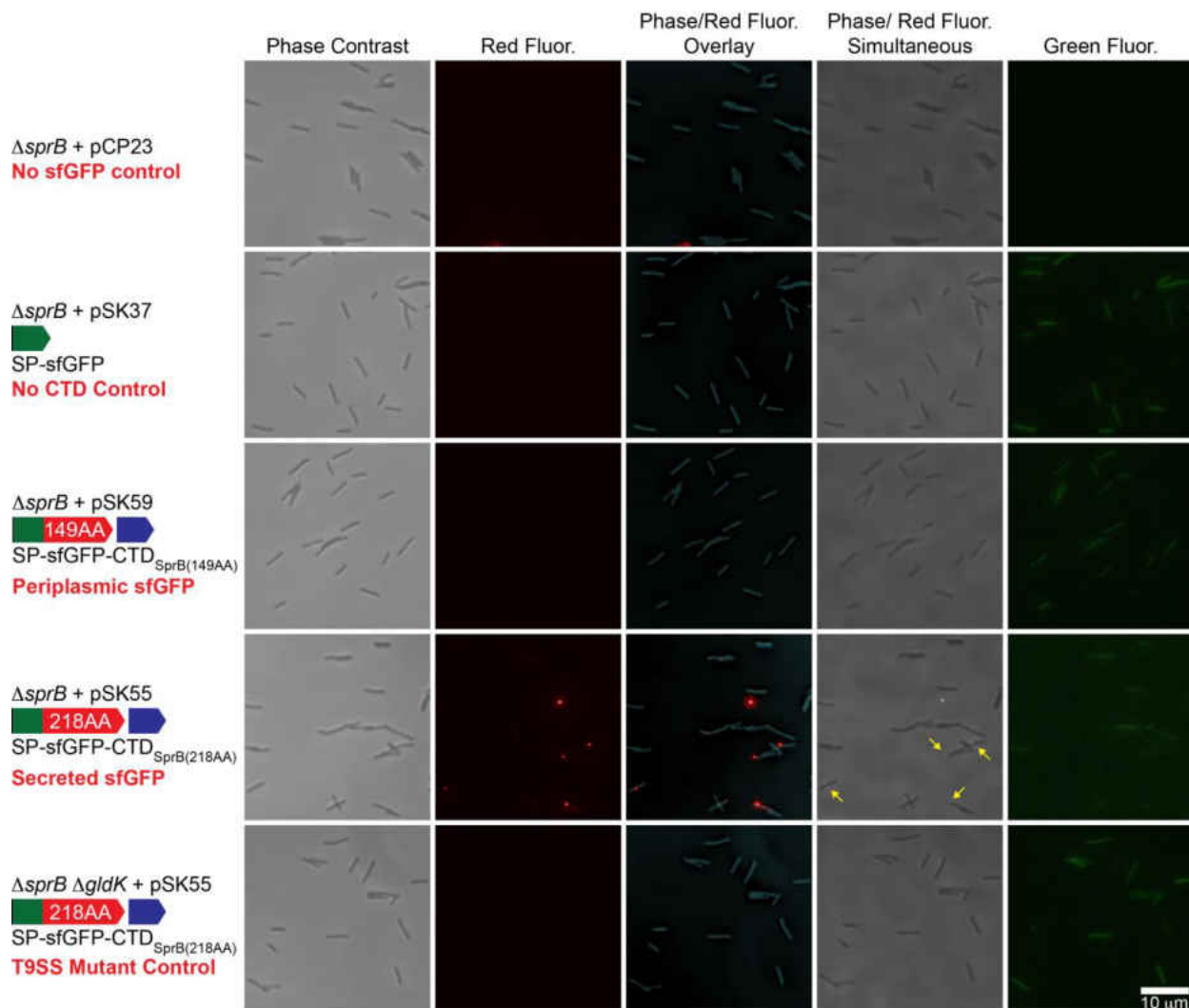
Figure 10. Detection of red and green fluorescence with no overlap, and demonstration of simultaneous phase contrast and fluorescence microscopy. Cells of the Δ*sprB* mutant CJ1922 expressing SP-sfGFP fused to C-terminal regions (CTDs) of SprB were exposed to anti-GFP and secondary antibody fused to Alexa Fluor 594 and observed by fluorescence microscopy to detect sfGFP exposed on the cell surface. Exposure times for fluorescence images were all 33 msec. Phase contrast images (left column) were superimposed with fluorescence images to generate overlay images (third column). The fourth column illustrates detection of cells and fluorescent signals by simultaneous phase contrast and fluorescence microscopy (yellow arrows point to signals). Green fluorescence (right column) demonstrated the presence of sfGFP in all cells except those of the 'No sfGFP' control, and demonstrated that surface localized sfGFP (red fluorescence) and total sfGFP (green fluorescence) could be separately detected. All plasmids except pCP23 (empty vector) expressed SP-sfGFP (green), in some cases fused to CTD$_{SprB}$ of different lengths (red), and with or without SprF (blue) as shown by the cartoons. The same region is shown in all five panels of a row.
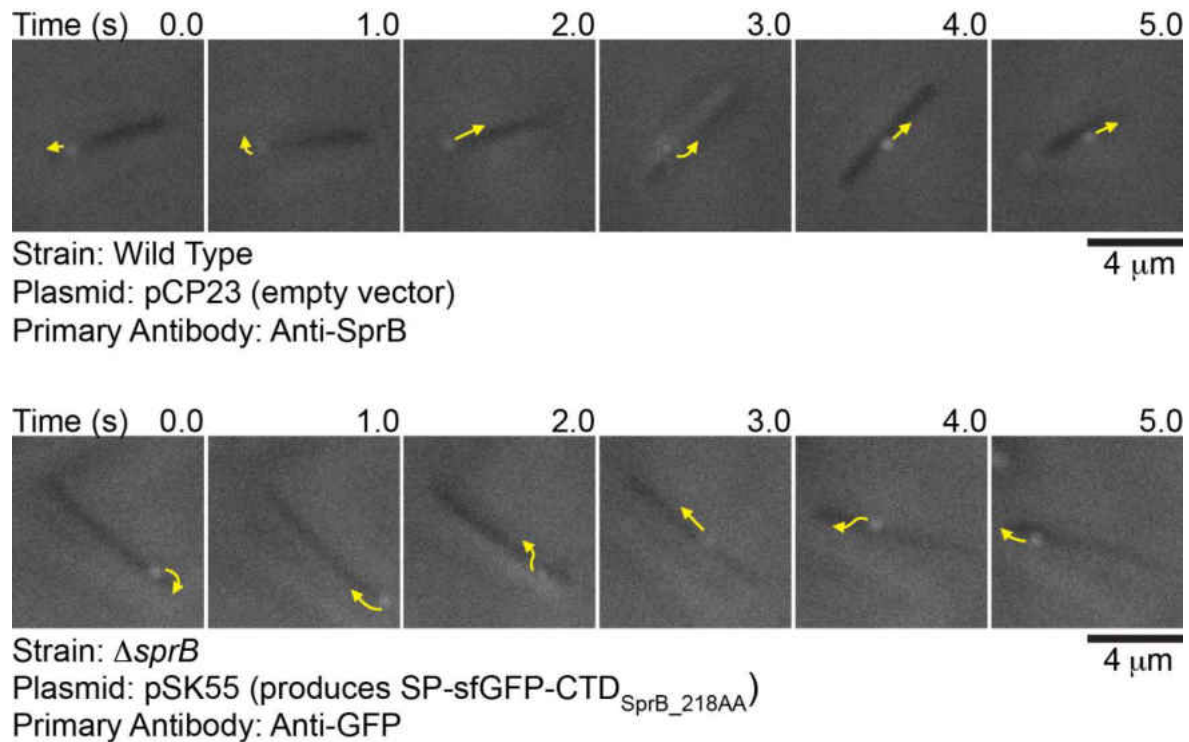
Figure 11. Movement of SprB and sfGFP on the cell surface. (A) Cells that expressed SprB, or that expressed SP-sfGFP fused to the C-terminal 218-amino acid region of SprB, were examined by simultaneous immunofluorescence and phase-contrast microscopy. Low-light phase contrast was used to detect the cells, and SprB and sfGFP were detected by exposure to appropriate antisera followed by exposure to goat anti-rabbit IgG conjugated to Alexa Fluor 594. Suspended cells were examined to avoid confusion resulting from the gliding movement of cells over surfaces. The sequences shown correspond to 5 second intervals from Movie S1 (top) and Movie S2 (bottom) in supplemental material of (31). Numbers in each panel indicate time in seconds. Arrows indicate the movements of fluorescent signals in the next second. Controls demonstrating specificity of anti-SprB are given in (27, 28) and controls demonstrating specificity of anti-GFP are given in Fig. 6, 7, 9 and 10.

Expression of SP-sfGFP-CTD$_{SprB}$ in a Δ*sprB* mutant did not restore wild type motility and colony spreading. *sprB* null mutants are partially defective in motility (13, 27, 32). They form nonspreading colonies on agar, and exhibit reduced but detectable motility on glass (Fig. 12 and 13). Whereas wild type cells move in long paths on agar or glass, Δ*sprB* mutant cells are less active, and also reverse direction frequently thus making little net progress. The residual motility of Δ*sprB* mutant cells is explained by the presence of alternative motility adhesins, such as RemA (7, 27). We examined the ability of cell-surface localized sfGFP-CTD$_{SprB}$ to restore motility to Δ*sprB* mutant cells. Δ*sprB* mutants expressing SP-sfGFP-CTD$_{SprB}$ with C-terminal regions of SprB of 218, 448, and 1182 amino acids failed to form spreading colonies on agar (Fig. 12) or to move effectively on glass (Fig. 13, and Movies S4 and S5 in supplemental material of (31)), although some cells of the Δ*sprB* mutant that expressed sfGFP-CTD$_{SprB(1182AA)}$ moved slightly longer distances on glass than did cells of the Δ*sprB* mutant. As described above, sfGFP-CTD$_{SprB}$ with C-terminal regions of SprB greater than 218 amino acids interacted with the motility machinery, as indicated by their rapid propulsion along the cell surface. Additional regions of SprB may be required for productive interaction with the substratum, to allow the gliding motors to propel the cells effectively over agar or glass. The longest C-terminal region of SprB added to plasmid encoded SP-sfGFP in this study (1182 amino acids) spanned approximately 18% of full length SprB. We failed to construct plasmids encoding SP-sfGFP fused to longer C-terminal regions of SprB, probably because of the extremely repetitive nature of the central region of *sprB* (27).

In addition to failing to restore full motility to a Δ*sprB* mutant as described above, expression of SP-sfGFP fused to C-terminal regions of SprB of 218, 448, and 1182 amino acids in wild type cells resulted in the formation of nonspreading colonies on agar (Fig. 12) and

decreased motility on glass (Fig. 13). Overexpression of fragments of SprB that allow interaction with the motility machinery may interfere with the ability of full length SprB to function properly. Expression of SP-sfGFP fused to the C-terminal 149 amino acids of SprB, which was not secreted from the cell, did not disrupt motility of wild type cells (Fig. 12 and 13). Cells in which the wild type chromosomal *sprB* was replaced with a modified and functional form of the gene that expresses full length SprB with sfGFP inserted after the signal peptide (SP-sfGFP-CTD$_{SprB(6421AA)}$) also moved similarly to the wild type on glass (Fig. 13).
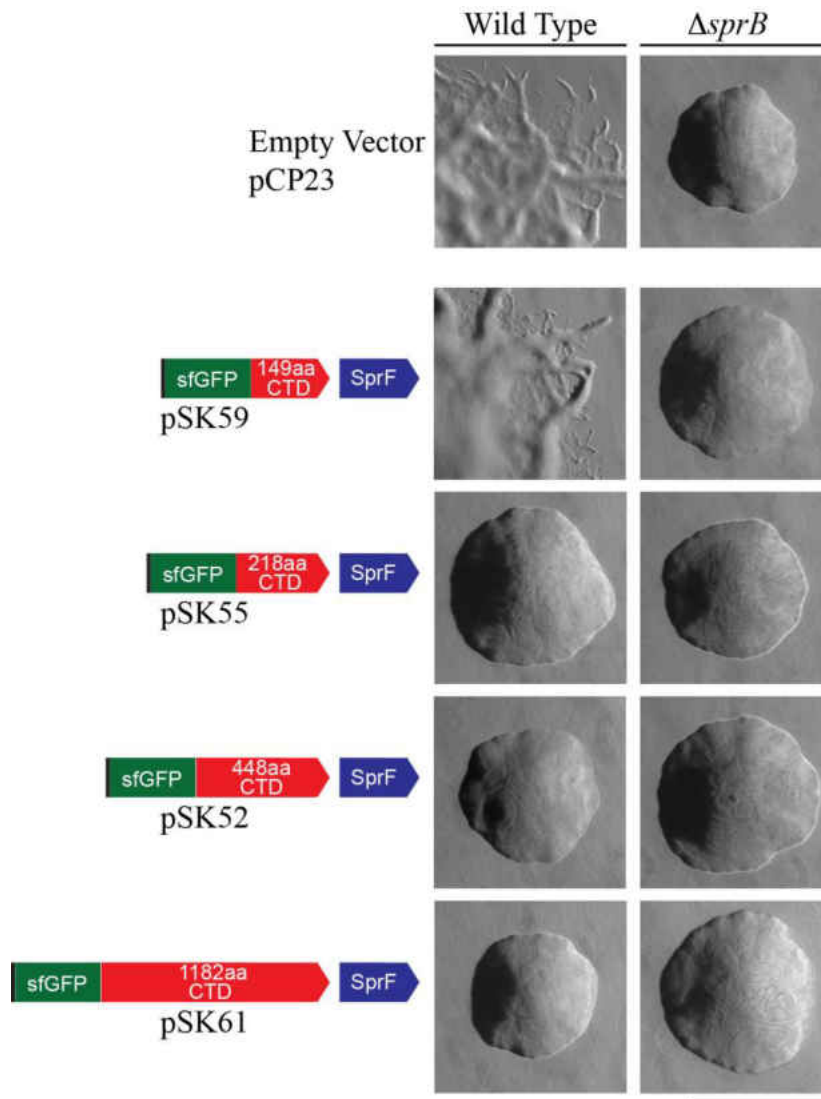
Figure 12. Colonies of wild type and Δ*sprB* mutant *F. johnsoniae* cells expressing SP-sfGFP fused to C-terminal regions of SprB. Colonies were incubated at 25°C on PY2 agar (33) for 40 h. Photomicrographs were taken with a Photometrics Cool-SNAP$_{cf}^2$ camera mounted on an Olympus IMT-2 phase contrast microscope. The left column is colonies of wild type cells, and the right column is colonies of Δ*sprB* mutant cells. Plasmids carried are indicated on the left, and the proteins encoded by the plasmids are shown by the cartoons. The scale bar indicates 1 mm and applies to all panels.
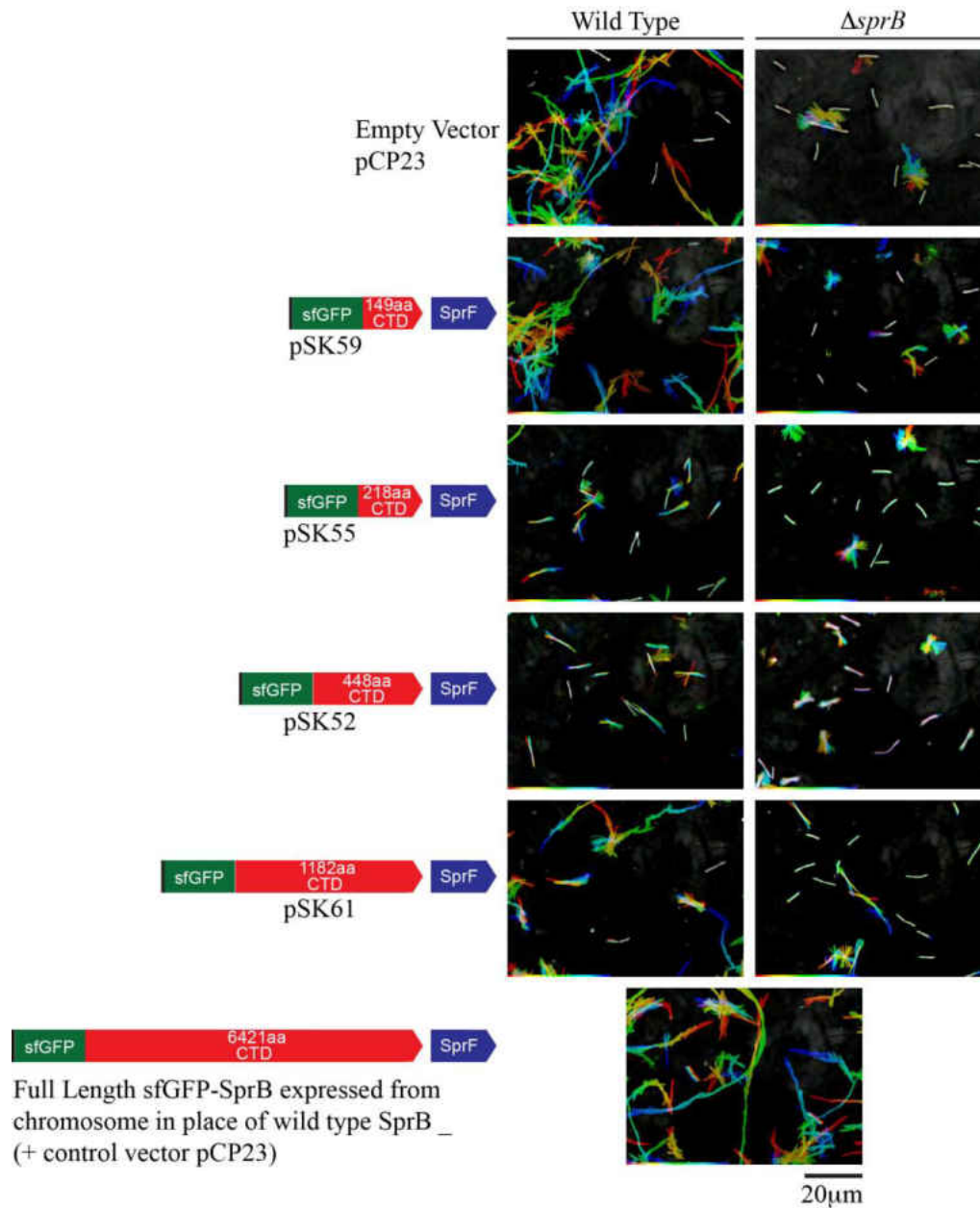
Figure 13. Gliding of wild type and Δ*sprB* mutant cells expressing SP-sfGFP fused to C-terminal regions of SprB. Cells carried either the empty vector pCP23, or the plasmids indicated that encode SP-sfGFP fused to C-terminal regions of SprB of various lengths. All plasmids except pCP23 also encode SprF. The bottom panel is wild type cells expressing full length SprB from the chromosome, with sfGFP fused after the signal peptide. Cells were grown in MM overnight without shaking at 25ºC, introduced into glass tunnel slides, and observed for motility at 25ºC using a phase-contrast microscope. A series of images were taken for 120 s. Individual frames were colored from red (time zero) to yellow, green, cyan, and finally blue (120 s), and integrated into one image, resulting in rainbow traces of gliding cells. White cells correspond to those that exhibited little or no net movement. Multicolored 'stars' indicate cells attached to the glass by one pole that rotated or flipped. The rainbow traces correspond to the sequences shown in Movies S4 and S5 in supplemental material of (31).

90

SprF and the PorP/SprF-like protein Fjoh_3951 appear to be specific for their cognate secreted proteins. *F. johnsoniae* is predicted to encode nine proteins that exhibit sequence similarity with and are similar in size to *F. johnsoniae* SprF, and to the *P. gingivalis* T9SS protein PorP (Fig. 14). Eight of the *F. johnsoniae* genes encoding these PorP/SprF-like proteins lie immediately downstream of genes encoding proteins with type B CTDs, similar to the relationship of *sprF* and *sprB* (Fig. 15). The type B CTD-containing protein Fjoh_3952 and the PorP/SprF-like protein Fjoh_3951 were studied to determine if they behaved like SprB and SprF. Fjoh_3952 is produced by and secreted from wild type cells in a process that requires the T9SS (1). The C-terminal 228-amino-acid region of Fjoh_3952 was fused to SP-sfGFP and secretion was analyzed with or without co-expression of the *porP/sprF*-like gene, Fjoh_3951. Coexpression of SP-sfGFP-CTD$_{Fjoh\_3952}$ and Fjoh_3951 from pSK57 in cells that were wild type for secretion (Δ*sprB* mutant used here) resulted in sfGFP accumulation in the spent medium (Fig. 16A). In contrast, sfGFP was not found in the spent medium of cells that carried pSK58, which expressed SP-sfGFP-CTD$_{Fjoh\_3952}$ without Fjoh_3951. Co-expression of SP-sfGFP-CTD$_{Fjoh\_3952}$ and Fjoh_3951 from pSK57 in cells of a Δ*gldK* (T9SS-deficient) mutant did not result in sfGFP secretion (Fig. 16A). The results indicate that an intact T9SS, and co-expression of the PorP/SprF-like protein Fjoh_3951 were required for secretion of SP-sfGFP-CTD$_{Fjoh\_3952}$. Wild type chromosomal Fjoh_3951 was present in all strains, but additional plasmid-encoded Fjoh_3951 protein was needed to foster secretion of SP-sfGFP-CTD$_{Fjoh\_3952}$, in the same way that additional plasmid-encoded SprF was needed for efficient secretion of SP-sfGFP- CTD$_{SprB}$ (Fig. 2). Some of the secreted sfGFP-CTD$_{Fjoh\_3952}$ attached to the cell surface (Fig. 7A, 9, and 17), as was observed for sfGFP-CTD$_{SprB}$. However, unlike sfGFP-CTD$_{SprB}$, sfGFP-CTD$_{Fjoh\_3952}$ did not

move along the cell surface (Fig. 7A and Movie S3 in supplemental material of (31)), suggesting

that Fjoh_3952 may not function as a motility adhesin as SprB does.

To determine if SprF and Fjoh_3951 are interchangeable we constructed pSK68, which

expresses SP-sfGFP-CTD$_{Fjoh\_3952}$ and SprF, and pSK69, which expresses SP-sfGFP-CTD$_{SprB}$ and

Fjoh_3951. Cells carrying either plasmid failed to efficiently secrete soluble or cell surface

localized sfGFP (Fig. 9, 16, and 17), suggesting that the cognate PorP/SprF-like proteins were

required for secretion of proteins carrying the CTDs of SprB and Fjoh_3952.

Figure 14. Alignment of *F. johnsoniae* SprF-like proteins and *P. gingivalis* W83 PorP.
Protein sequences were aligned using MUSCLE. Dark shading indicates identical amino acids and light shading indicates similar amino acids. Proteins examined experimentally in this study were SprF and Fjoh_3951. The entire protein sequences were used in the alignment, except for SprD for which only the N-terminal 320 amino acids of the 1588 amino acid protein were used.
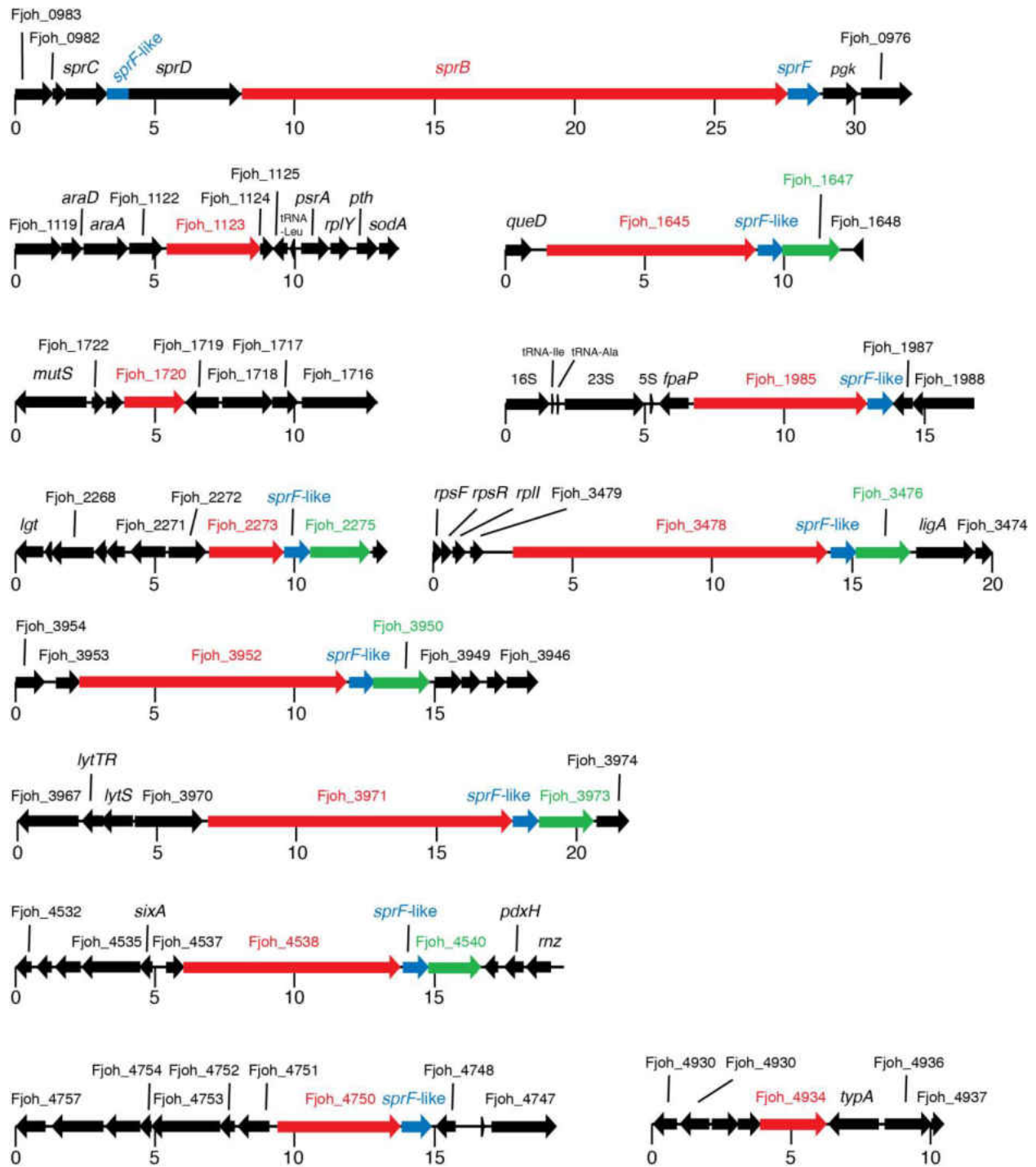
Figure 15. ***F. johnsoniae*** **genes encoding type B CTD-containing proteins (red).** *porP*/*sprF*-like genes are shown in blue, and PG1058-like genes are shown in green. One additional *porP*/*sprF*-like gene (Fjoh_1677) is present in the genome but is not shown here because it is not located adjacent to a gene encoding a type B CTD-containing protein.

94
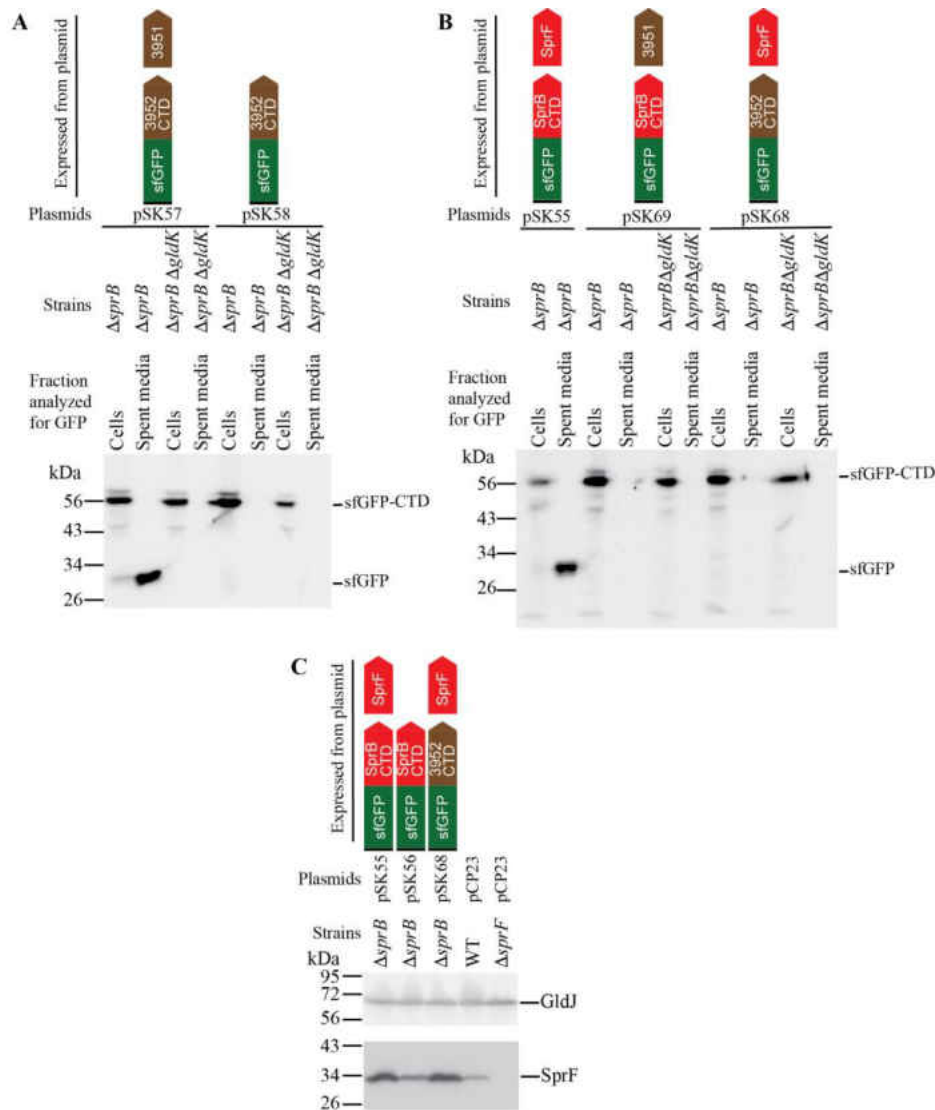
Figure 16. Efficient secretion of SP-sfGFP fused to CTD$_{SprB}$ or to CTD$_{Fjoh\_3952}$ requires coexpression with the appropriate PorP/SprF-like protein. Cultures of wild type (WT), Δ*sprB* mutant, Δ*sprB* Δ*gldK* (T9SS-defective) mutant, and Δ*sprF* mutant, carrying the plasmids indicated, were incubated in CYE at 25°C with shaking and harvested in the late exponential phase of growth. For panels A and B, cells and spent culture media were separated by centrifugation and analyzed by Western blot using antiserum against GFP. Whole cell samples corresponded to 10 μg protein per lane and samples from spent media corresponded to the volume of spent medium that contained 10 μg protein before the cells were removed. For panel C, cells (20 μg protein per lane) were examined by Western blot using antiserum against SprF and antiserum against GldJ (loading control). Plasmids used were pCP23 (Empty vector); pSK58, which expresses SP-sfGFP fused to the 228 amino acid CTD of Fjoh_3952 (SP-sfGFP-CTD$_{Fjoh\_3952}$); pSK57, which co-expresses SP-sfGFP-CTD$_{Fjoh\_3952}$ and Fjoh_3951; pSK56, which expresses SP-sfGFP- CTD$_{SprB218AA}$; pSK55, which co-expresses SP-sfGFP- CTD$_{SprB218AA}$ and SprF; pSK68, which coexpresses SP-sfGFP-CTD$_{Fjoh\_3952}$ and SprF; and pSK69, which coexpresses SP-sfGFP-CTD$_{SprB218AA}$ and Fjoh_3951. Cartoons depicting the proteins expressed from the plasmids are indicated above the appropriate lanes.
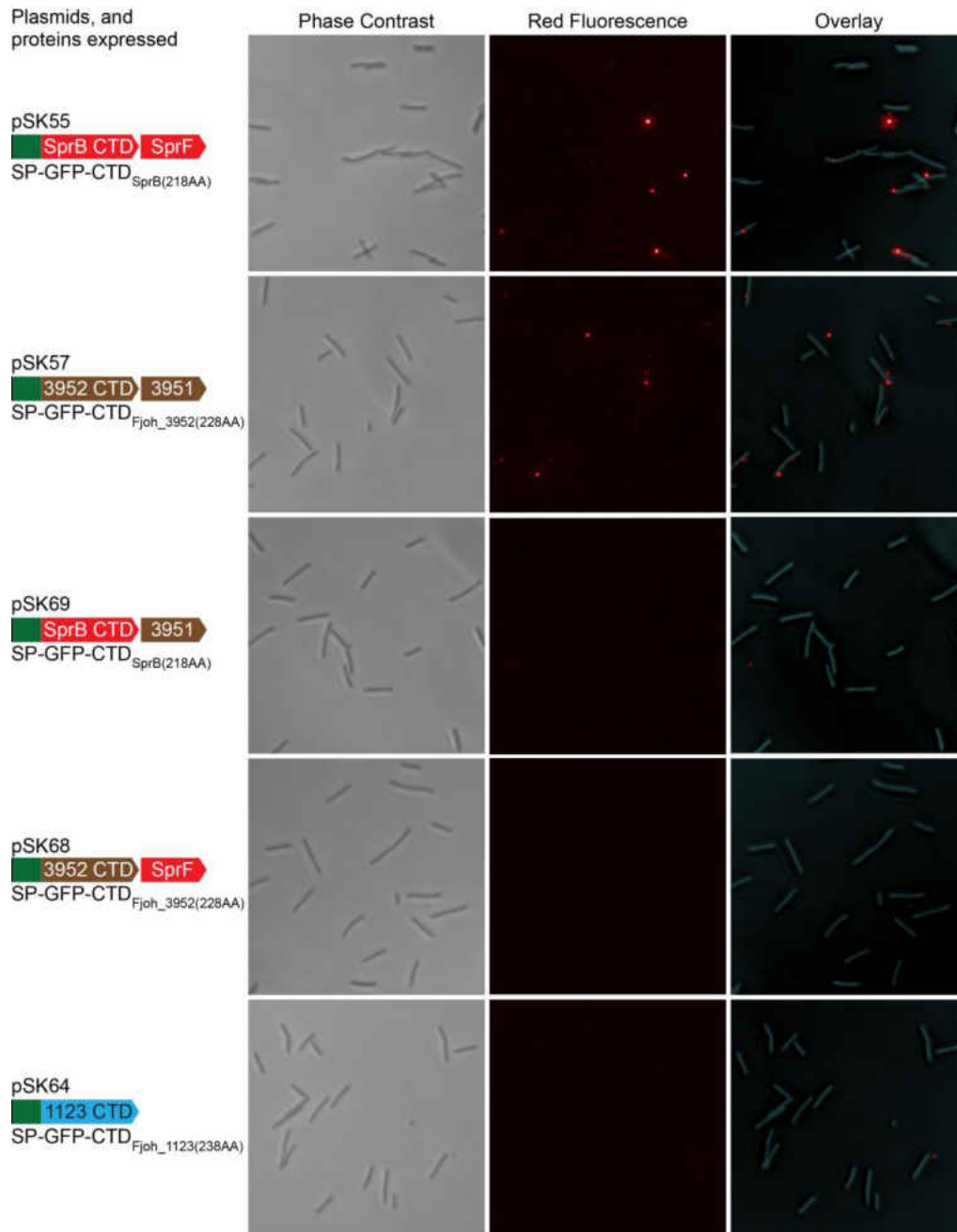
Figure 17. Fusion of the C-terminal region of Fjoh_3952 to sfGFP and co-expression with the cognate SprF-like protein Fjoh_3951 results in attachment of sfGFP to the cell surface. Cells expressing SP-sfGFP fused to C-terminal regions (CTDs) of SprB, Fjoh_3952, or Fjoh_1123 were exposed to anti-GFP and secondary antibody fused to Alexa Fluor 594 and observed by fluorescence microscopy to detect sfGFP exposed on the cell surface. Exposure times for fluorescence images were all 33 msec. Phase contrast images (left column) were superimposed with fluorescence images (middle column) to observe the relationship of the signals to cells (right column). All panels are $\Delta sprB$ mutant cells with plasmids indicated expressing SP-sfGFP fused to CTD$_{SprB(218AA)}$, CTD$_{Fjoh\_3952(228AA)}$, or CTD$_{Fjoh\_1123(238AA)}$ with or without a PorP/SprF-like protein (either SprF or Fjoh_3951) as shown. Bar indicates 10 μm and applies to all panels.

96
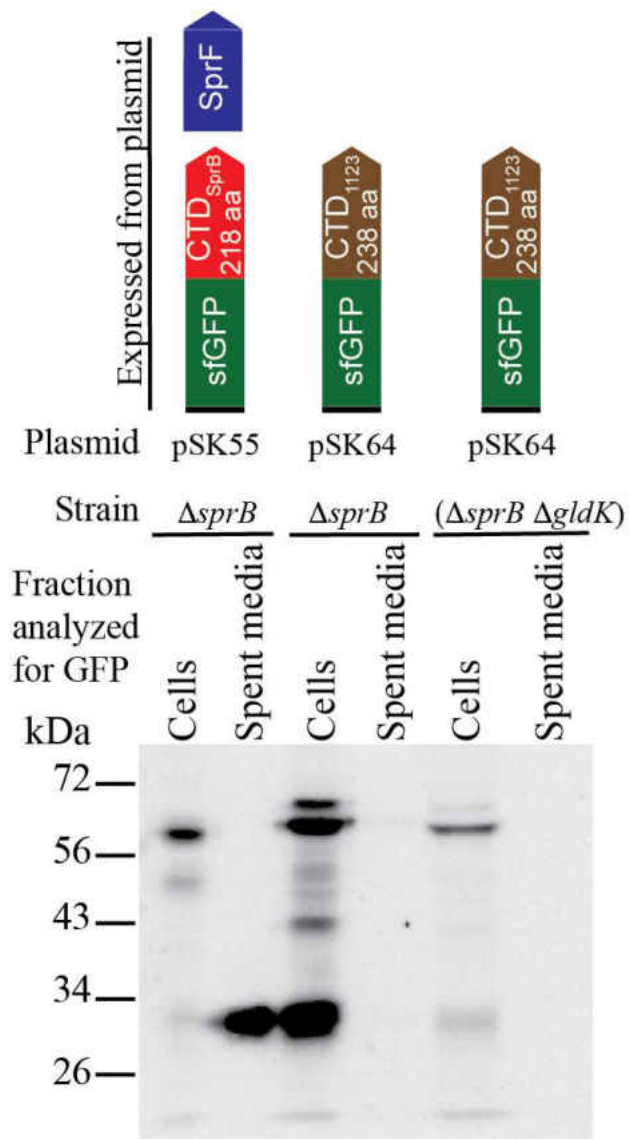
Figure 18. The type B CTD of Fjoh_1123 is not sufficient to target sfGFP for secretion. To determine if Fjoh_1123 CTD can target sfGFP for secretion, cells of Δ*sprB* and of T9SS mutant Δ*sprB* Δ*gldK*, carrying plasmids that expressed SP-sfGFP fused to 238 amino acids of Fjoh_1123 (pSK64) were analyzed. The culture supernatant (spent medium) and intact cells were analyzed for sfGFP by western blot using anti-GFP antiserum. Whole cell samples corresponded to 10 μg protein per lane and samples from spent media corresponded to the volume of spent medium that contained 10 μg protein before the cells were removed.

Analysis of the type B CTD of secreted protein Fjoh_1123. Fjoh_1123 has a type B CTD and was shown to be secreted by the T9SS (1). Unlike most other *F. johnsoniae* genes encoding proteins with type B CTDs, Fjoh_1123 is not located near a *porP/sprF*-like gene (Fig. 15). To determine if the Fjoh_1123 CTD would target sfGFP for secretion without coexpression with a *porP/sprF*-like gene we constructed a plasmid that expressed SP-sfGFP fused to the C-terminal 238 amino acids of Fjoh_1123 (SP-sfGFP-CTD$_{Fjoh\_1123}$). Western blot analysis and immunofluorescence microscopy demonstrated that sfGFP was not secreted by cells expressing this fusion protein (Fig. 9, 17 and 18). Co-expression with one of the 10 *F. johnsoniae* PorP/SprF-like proteins may be required to facilitate secretion of Fjoh_1123 and SP-sfGFP-CTD$_{Fjoh\_1123}$.

SprF outer membrane localization. SprF might be an adaptor or chaperone that aids secretion and surface localization of SprB. PSORTb and CELLO analyses predict that SprF is an outer membrane protein (13). Cell fractionation and western blot analyses using anti-SprF antibodies were performed to test this prediction. SprF was detected in the outer membrane fraction of wild type or Δ*sprB* mutant cells, whereas the known cytoplasmic membrane protein GldL localized to the cytoplasmic membrane (Fig. 19). SprF was not detected on the surface of intact wild type or Δ*sprB* mutant cells using fluorescently labeled anti-SprF antibodies (data not shown). SprF was not susceptible to proteinase K treatment of intact wild-type cells but SprF in Δ*sprB* cells was partially digested by proteinase K (Fig. 20). These results suggest that a limited portion of SprF is exposed on the external surface of the outer membrane, but is protected from added proteinase K by SprB.

Bioinformatic analysis of *F. johnsoniae* proteins predicted to be secreted by the T9SS. Many proteins secreted by T9SSs have type A or type B CTDs (12). *F. johnsoniae* has 41

genes encoding proteins with type A CTDs and 12 encoding proteins with type B CTDs (Table 1 and 2). Many of these are secreted by wild type cells, and they fail to be secreted by mutants that are deficient for the T9SS (1). Some proteins secreted by the T9SS, such as ChiA (19), lack regions of sequence similarity to either type A or type B CTDs. For this reason, the number of proteins secreted by the *F. johnsoniae* T9SS may be higher than the estimate given above. Of the 41 *F. johnsoniae* proteins with type A CTDs, 20 have predicted enzymatic activities (Table 1). In contrast, none of the 12 proteins with type B CTDs have predicted enzymatic activities but 8 of them have features associated with some adhesins (Table 2). The 12 proteins with type B CTDs are very large, ranging from 78.5 to 672.0 kDa before processing, with a median of 239.6 kDa (Table 2). In contrast, *F. johnsoniae* proteins with type A CTDs have a median size of 94.3 kDa (Table 1).
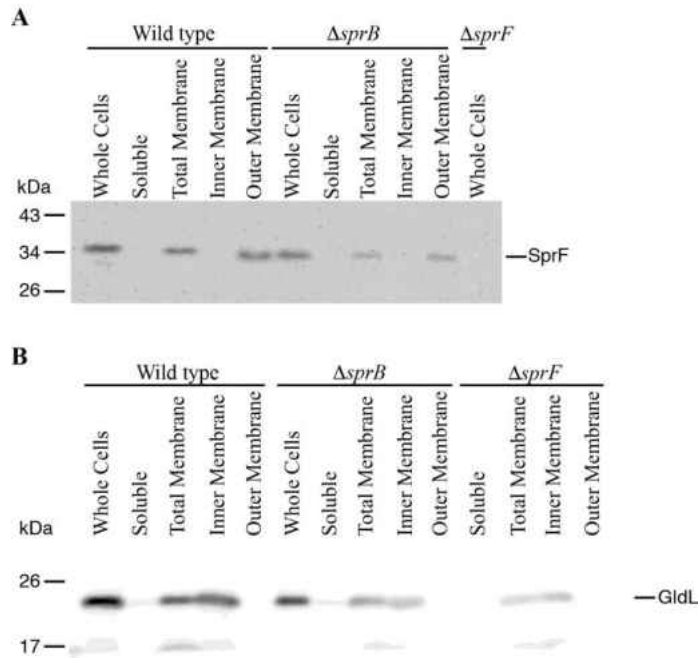
Figure 19. Localization of SprF. Wild type and mutant cells were disrupted and separated into soluble and membrane fractions. Membranes were fractionated further by differential solubilization in Sarkosyl. Equal amounts of each fraction based on 20 μg protein of the starting material (Whole Cells) were loaded in each lane and separated by SDS-PAGE. Antisera against SprF (A) and GldL (B) were used to detect the respective proteins by Western blot analyses.
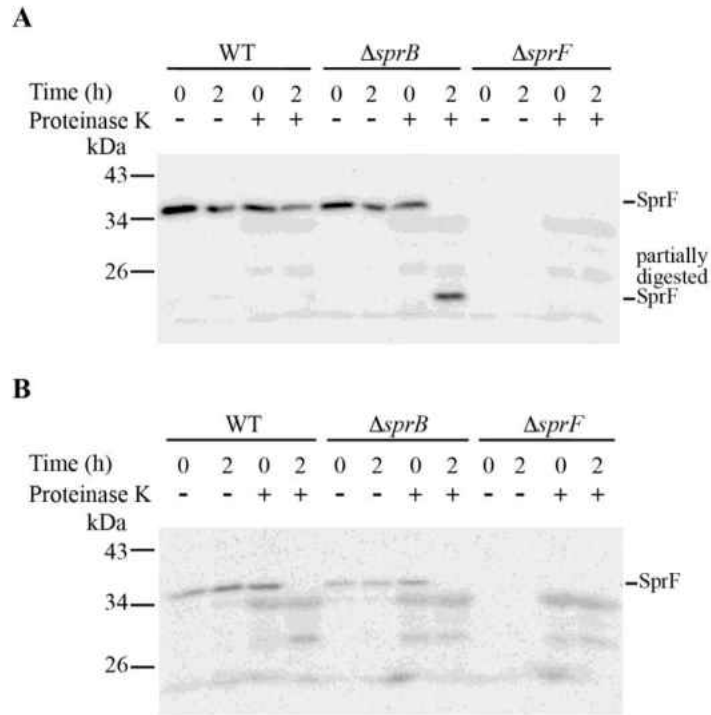
Figure 20. Proteinase K treatment to determine if SprF localizes to the cell surface. Wild-type, Δ*sprB* and Δ*sprF* strains were analyzed. Proteinase K was added at a final concentration of 1 mg/ml to intact cells (A) and to cell extracts prepared by French pressure cell treatment (B), and cells and extracts were incubated at 25ºC. Samples were removed at 0 h and 2 h for immunoblot analyses. Samples were separated by SDS-PAGE and SprF was detected using antiserum against SprF. Samples not exposed to proteinase K (-) were also included.

Table 1. *F. johnsoniae* **T9SS type A CTD-containing proteins[1].**

Locus tag	Molecular Mass (kDa)	Gene name	Domains	Known or predicted function
Fjoh_0074	123.1		endonuclease/exonuclease/phosphatase	nuclease/phosphatase
Fjoh_0547	12.6			
Fjoh_0549	59.3		CARDB, 2 copies	adhesin
Fjoh_0707	83.7			
Fjoh_0798	95.7		Metallo-peptidase M12B Proprotein convertase	peptidase
Fjoh_0808	154.0	*remA*	Gal_Lectin	galactose/rhamnose-binding lectin, gliding motility adhesin (7)
Fjoh_0848	54.2		TPR_2; TPR_8; TPR_16	
Fjoh_0886	99.1		Thermolysin, peptidase M4 fn3	peptidase
Fjoh_1022	51.1		GH8	glycoside hydrolase
Fjoh_1188	152.7		LRR_4	
Fjoh_1189	181.4		RCC1 (7 copies) SprB repeat (2 copies) Laminin_G_3	Lectin, Possible motility adhesin
Fjoh_1208	112.5	*amyB*	α amylase GH13 Big_2 (3 copies) CBM26	α amylase (1, 12)
Fjoh_1231	97.8		pectate lyase CBM77	pectate lyase
Fjoh_1269	94.3		SprB repeat (5 copies)	Possible motility adhesin
Fjoh_1408	106.0		α amylase GH13	α amylase
Fjoh_1905	75.1		GH30 RicinB_lectin_2 (2 copies) CBM13	glycoside hydrolase
Fjoh_2150	39.0			
Fjoh_2336	14.0			
Fjoh_2338	12.9		DUF3244	
Fjoh_2339	14.7			
Fjoh_2389	57.7		Peptidase_S8	peptidase
Fjoh_2456	100.1		PL1	polysaccharide lyase
Fjoh_2666	61.2			
Fjoh_3203	104.9		GH87 Big_2 (2 copies)	Glycoside hydrolase
Fjoh_3246	299.4		CARDB	adhesin
Fjoh_3296	65.1			
Fjoh_3324	105.3		Glucose-sorbosone dehydrogenase CBM6 PKD	Glucose-sorbosone dehydrogenase
Fjoh_3421	17.8			
Fjoh_3731	60.5			

Fjoh_3777	128.1		DUF676	Possible lipase/esterase
Fjoh_3855	31.4			
Fjoh_4051	226.7		SprB repeat (13 copies)	Possible motility adhesin
Fjoh_4174	102.5		RicinB_lectin_2 CBM6	carbohydrate binding
Fjoh_4175	57.7		GH18 CBM6	glycoside hydrolase
Fjoh_4176	95.4		GH64 beta gamma crystallin RicinB_lectin_2 CBM13 CBM6	glycoside hydrolase
Fjoh_4177	144.9		GH16 Discoidin	Possible glycoside hydrolase
Fjoh_4242	100.5		Peptidase_S8	peptidase
Fjoh_4436	131.8		GH27 CBM13 RicinB_lectin_2 SusF SusE starch binding (3 copies)	glycoside hydrolase
Fjoh_4721	67.1		endonuclease fn3 LTD	endonuclease
Fjoh_4723	66.0		endonuclease fn3 LTD	endonuclease
Fjoh_4948	34.5			
Average	78.8			
Median	94.3			

[1]The T9SS type A CTD (TIGR04183) is a C-terminal domain that targets a protein for secretion by the T9SS. TIGR04183 is described as 'Por secretion system C-terminal sorting domain' on the J. Craig Venter Institute TIGR website (http://www.jcvi.org/cgi-bin/tigrfams/index.cgi). Each of these proteins contains an N-terminal signal peptide for export across the cytoplasmic membrane, and a T9SS type A C-terminal domain (CTD) for secretion across the outer membrane by the T9SS. In addition, they contain the conserved domains shown:
Carbohydrate active enzymes/proteins as assigned by CAZY: Glycoside hydrolase (GH); polysaccharide lyase (PL); carbohydrate binding (CBM) domains as assigned by CAZY (34). α amylase also assigned based on (pfam00128); pectate lyase also assigned based on (pfam00544).
Other potential carbohydrate active/binding proteins: Fjoh_4177 assigned as GH16 based on relationship to (pfam00722); Galactose/rhamnose-binding lectin (Gal_Lectin, pfam02140); RicinB_lectin_2 (pfam14200); SusF SusE starch binding (pfam16411); Glucose-sorbosone dehydrogenase (pfam07995).
Peptidases: Metallo-peptidase M12B (pfam13583); Proprotein convertase (pfam01483); Thermolysin, peptidase M4 (pfam07504, pfam01447, pfam02868); Peptidase_S8 (pfam00082).
Other Enzymes: Endonuclease/exonuclease/phosphatase family (IPR005135); endonuclease (pfam04231).

Other: Cell adhesion related domain (CARDB, pfam07705); tetratricopeptide repeat domains: TPR_2 (pfam07719), TPR_8 (pfam13181), and TPR_16 (pfam13432); Fibronectin type III domain (fn3; pfam00041); leucine rich repeat 4 (LRR_4, pfam12799); Laminin_G_3 (pfam13385); SprB repeat (pfam13573); Regulator of chromosome condensation (RCC1, pfam00415); bacterial Ig-like domain (Big_2, pfam02368); PKD (pfam00801); beta gamma crystallin (pfam00030)**;** Discoidin (pfam00754); Lamin Tail Domain (LTD, pfam00932); DUF3244 (pfam11589); DUF676 (pfam05057).

.

Table 2. *F. johnsoniae* T9SS Type B CTD-containing proteins[1]

Locus tag	Molecular Mass (kDa)	Gene name	Domains	Function or predicted function
Fjoh_0979	672.0	*sprB*	SprB repeat (20 copies)	Gliding motility adhesin (27)
Fjoh_1123	121.9		PKD domain	Possible adhesin
Fjoh_1645	258.1		Hyalin repeat (3 copies) DUF11 (2 copies)	Possible adhesin
Fjoh_1720	78.5		C-type lectin	Predicted carbohydrate-binding adhesin
Fjoh_1985	221.0		Hyalin repeat (8 copies) FG-GAP repeat of integrins (2 copies)	Possible adhesin
Fjoh_2273	93.3			
Fjoh_3478	386.0		DUF11	
Fjoh_3952	330.6		VCBS repeat DUF11 (3 copies)	Possible adhesin
Fjoh_3971	375.3		DUF11 (16 copies)	
Fjoh_4538	271.0		LRR_adjacent (8 copies) VWA_2 Collagen binding protein, Cna	Possible adhesin
Fjoh_4750	158.1		PKD domain (3 copies) SprB repeat (3 copies)	Possible gliding motility adhesin
Fjoh_4934	84.7			
Average	378.4			
Median	239.6			

[1]The T9SS type B CTD (TIGR04131) is a C-terminal domain that targets a protein for secretion by the T9SS. TIGR04131 is described as 'gliding motility-associated C-terminal domain' on the J. Craig Venter Institute TIGR website (http://www.jcvi.org/cgi-bin/tigrfams/index.cgi). Each of these proteins contains an N-terminal signal peptide for export across the cytoplasmic membrane, and a T9SS type B C-terminal domain (CTD) for secretion across the outer membrane by the T9SS. In addition, individual proteins contain the conserved domains shown: SprB repeat (pfam13573); PKD domain (IPR000601); Hyalin repeat (pfam02494); C-type lectin (IPR016186, IPR016187, IPR001304); FG-GAP repeat of integrins (pfam01839); VCBS repeat (TIGR01965); LRR_adjacent (pfam08191); DUF11 (pfam01345); von Willebrand factor type A domain, VWA_2 (pfam13519); Collagen binding protein Cna (IPR008970).

Genomic context of *F. johnsoniae porP/sprF-like* genes. *F. johnsoniae* is predicted to encode 10 PorP/SprF-like proteins (including SprF) that are similar in size (Fig. 14 and 15). The N-terminal 299 amino acid region of the much larger protein SprD (1588 amino acids) also exhibits limited similarity to SprF. Each of the 10 PorP/SprF-like proteins has an N-terminal signal peptide, and each is predicted to be an outer membrane protein by CELLO analysis (35). Nine of the genes encoding these proteins lie immediately downstream of genes encoding proteins with type B CTDs (Fig. 15). The PorP/SprF-like proteins encoded by these genes presumably aid the secretion of the product of the upstream gene. Of these nine *porP/sprF*-like genes, six are located immediately upstream of, and transcribed in the same direction as, genes encoding predicted outer membrane proteins that are similar in sequence to PG1058 (Fig. 15 and 21), which is required for *P. gingivalis* T9SS function (36). The C-terminal regions of each of these PG1058-like proteins are similar in sequence to the C-terminal peptidoglycan-interacting domain of *E. coli* OmpA (37, 38). Unlike *P. gingivalis* PG1058, which was predicted to be a lipoprotein (36), each of the *F. johnsoniae* PG1058-like proteins lack the conserved cysteine adjacent to the amino terminal signal peptide that is required of bacterial lipoproteins. The synteny of *porP/sprF*-like genes and PG1058-like genes suggests possible functional links between the encoded proteins in T9SS-mediated secretion.

Predicted secreted proteins and *porP/sprF*-like genes in other members of the *Bacteroidetes*. Examination of the completed genome sequences of 104 members of the phylum *Bacteroidetes* revealed the presence of core genes of the T9SS in 90 of these (12). Each of these has proteins with type A CTDs, and 88 also have proteins with type B CTDs. In most cases they encode multiple proteins with type A CTDs and multiple proteins with type B CTDs (Table 3). Of those examined, *Fluviicola taffensis* DSM 16823 had the most predicted secreted proteins:

180 proteins with type A CTDs and 50 with type B CTDs. Members of the class *Bacteroidia* are unusual among the *Bacteroidetes* in encoding few proteins with type B CTDs. Among 17 genomes from members of the class *Bacteroidia* with T9SS genes, 14 encode only a single type B CTD-containing protein, and another has none.

Each of the organisms that have genes encoding type B CTDs also have one or more *porP/sprF*-like genes (Table 3). The number of predicted proteins with type B CTDs often reflects the number of predicted PorP/SprF-like proteins. For example, *F. johnsoniae* has 12 type B CTD-containing proteins and 11 PorP/SprF-like proteins, whereas *P. gingivalis* has a single type B CTD-containing protein, PG1035, and a single PorP/SprF-like protein, PorP (Table 3). Type B CTD-encoding genes and *porP/sprF*-like genes are absent in all but one of the organisms that lack core T9SS genes.

Similar to the situation for *F. johnsoniae*, *porP/sprF*-like genes in other *Bacteroidetes* are often located immediately downstream of genes encoding proteins with type B CTDs. Of 527 *porP/sprF*-like genes identified, 314 (60%) lie immediately downstream of and transcribed in the same direction as genes encoding type B CTD-containing proteins (Table 3). In some cases, multiple type B CTD-encoding genes are found immediately upstream of individual *porP/sprF*-like genes. In the most extreme case (*Cytophaga hutchinsonii* CHU_3434) five type B CTD-encoding genes are immediately upstream. Our analysis underestimates the association of *porP/sprF*-like genes with type B CTD-encoding genes for two reasons. First, some *porP/sprF*-like genes are immediately upstream (instead of downstream) of genes encoding type B CTDs, and these were excluded. Some of these are transcribed in the same direction as the genes encoding type B CTDs, whereas others are oriented in the opposite direction. Second, some

porP/sprF-like genes are not immediately adjacent to genes encoding type B CTD-containing

proteins but instead are separated by one gene and were thus not counted in our analysis.

In addition to the genes described above that are located near genes encoding predicted

T9SS-secreted proteins, other *porP/sprF*-like genes are adjacent to genes encoding components

of the T9SS secretion machine. Of the 527 *porP/sprF*-like genes in Table 3, forty-two are

immediately upstream and oriented in the same direction as *gldK*, *gldL*, *gldM*, and *gldN*, which

encode core components of the T9SS. These include *P. gingivalis porP* (3) and *Cytophaga*

hutchinsonii sprP (39). *gldK*, *gldL*, *gldM*, and *gldN* form an operon (8) and are arranged in this

order in each organism that has these genes, whether or not they have a *porP/sprF*-like gene

upstream. In addition to the *porP/sprF*-like genes associated with *gldK*, twelve *porP/sprF*-like

genes lie immediately upstream of *gldJ*, which is similar in sequence to *gldK* and has been linked

to both gliding motility and T9SS function (28). The association of *porP/sprF*-like genes with

gldJ and *gldK* suggests that the gliding motility and T9SS proteins GldJ and GldK may have a

functional relationship with PorP/SprF-like proteins.

Figure 21. Alignment of *F. johnsoniae* proteins related to *P. gingivalis* W83 PG1058. Protein sequences were aligned using MUSCLE. Dark shading indicates identical amino acids and light shading indicates similar amino acids. The entire protein sequences were used in the alignments.

Table 3. Prevalence of T9SS genes, CTD-encoding genes and *porP/sprF*-like genes in 104 members of the phylum *Bacteroidetes*[a]

Genome	T9SS components					CTDs		porP/sprF-like genes	porP/sprF-like genes that have type B CTD-encoding genes immediately upstream
	GldK TIGR03525	GldL TIGR03513	GldM TIGR03517	GldN TIGR03523	SprA TIGR04189	Type A CTD TIGR04183	Type B CTD TIGR04131	TIGR03519	
Class Flavobacteriia									
Aequorivita sublithincola DSM 14238	1	1	1	1	1	112	5	4	3
Algibacter alginicilyticus HZ22	1	1	1	1	1	55	10	7	6
Capnocytophaga canimorsus Cc5	1	1	1	1	1	1	10	6	5
Capnocytophaga haemolytica CCUG 32990	1	1	1	1	1	2	6	5	3
Capnocytophaga ochracea DSM 7271	1	1	1	1	1	2	8	5	3
Capnocytophaga sp. F0383	1	1	1	1	1	2	7	5	3
Cellulophaga algicola DSM 14237	1	1	1	1	1	13	16	12	8
Cellulophaga lytica DSM 7489	1	1	1	1	1	14	13	10	6
Chryseobacterium sp. IHB B 17019	1	1	1	1	1	83	18	1	0
Chryseobacterium sp. StRB126	1	1	1	1	1	101	10	1	0
Croceibacter atlanticus HTCC2559	1	1	1	1	1	45	8	4	4
Dokdonia sp. 4H-3-7-5	1	1	1	1	1	15	10	7	5
Dokdonia sp. PRO95	1	1	1	1	1	17	10	7	5
Elizabethkingia meningoseptica FMS-007	0	0	0	0	0	0	0	0	0
Elizabethkingia miricola BM10	0	0	0	0	0	0	0	0	0
Flavobacteriaceae bacterium 3519-10	1	1	1	1	1	55	6	1	0
Flavobacterium branchiophilum FL-15	1	1	1	1	1	37	10	3	3
Flavobacterium columnare ATCC 49512	1	1	1	1	1	35	7	6	4
Flavobacterium indicum GPTSA100-9	1	1	1	1	1	43	16	5	5
Flavobacterium johnsoniae ATCC 17061	1	1	1	2	1	40	12	11	9
Flavobacterium psychrophilum JIP02/86	1	1	1	1	1	38	10	7	5
Fluviicola taffensis DSM 16823	1	1	2	2	1	180	50	15	9
Gramella forsetii KT0803	1	1	1	1	1	11	7	5	4
Lacinutrix sp. 5H-3-7-4	1	1	1	1	1	31	16	8	7
Lutibacter profundi LP1	1	1	1	1	1	19	3	2	1
Maribacter sp. HTCC2170	1	1	1	1	1	10	13	8	3
Muricauda lutaonensis CC-HSB-11	1	1	1	1	1	7	13	9	6
Muricauda ruestringensis DSM 13258	1	1	1	1	1	7	13	13	7
Myroides profundi D25	1	1	1	1	1	7	12	11	10
Myroides sp. A21	1	1	1	1	1	4	7	8	5
Nonlabens dokdonensis DSW-6	1	1	1	1	1	85	17	5	2
Ornithobacterium rhinotracheale DSM 15997	1	1	1	1	1	6	2	1	0
Owenweeksia hongkongensis DSM 17368	1	1	1	1	1	159	26	4	1
Polaribacter sp. MED152	1	1	1	1	1	27	8	5	4
Riemerella anatipestifer DSM 15868	1	1	1	1	1	15	1	1	0
Robiginitalea biformata HTCC2501	1	1	1	1	1	7	12	8	4
Siansivirga zeaxanthinifaciens CC-SAMT-1	1	1	1	1	1	51	10	6	5
Weeksella virosa DSM 16922	1	1	1	1	1	36	3	1	1
Winogradskyella sp. PG-2	1	1	1	1	1	66	17	8	6
Zobellia galactanivorans DsijT	1	1	1	1	1	29	17	14	9
Zunongwangia profunda SM-A87	1	1	1	1	1	7	5	3	2
Class Cytophagia									
Belliella baltica DSM 15883	1	1	1	1	1	11	4	6	3
Bernardetia litoralis DSM 6794	1	1	1	3	1	52	11	5	1
Cyclobacterium amurskyense KCTC 12363	1	1	1	1	1	20	5	7	3
Cyclobacterium marinum DSM 745	1	1	1	1	1	18	7	7	5
Cytophaga hutchinsonii ATCC 33406	1	1	2	2	1	118	27	16	8
Dyadobacter fermentans DSM 18053	1	1	1	1	1	88	11	3	0
Echinicola vietnamensis DSM 17526	1	1	1	1	1	17	9	9	6
Emticicia oligotrophica DSM 17448	1	1	1	1	1	31	10	4	1
Hymenobacter sp. APR13	1	1	1	1	1	83	9	2	0
Hymenobacter sp. DG25A	1	1	1	1	1	54	6	3	1
Hymenobacter sp. PAMC26554	1	1	1	1	1	51	8	3	1
Hymenobacter swuensis DY53	1	1	1	1	1	100	8	3	1
Leadbetterella byssophila DSM 17132	1	1	1	1	1	17	4	4	0
Marivirga tractuosa DSM 4126	1	1	1	1	1	39	11	12	7
Persicobacter sp. JZB09	1	1	1	1	1	32	3	4	1
Pontibacter akesuensis AKS 1T	1	1	1	1	1	47	11	8	5
Pontibacter korlensis X14-1T	1	1	1	1	1	47	11	9	7
Rufibacter sp. DG15C	1	1	1	1	1	49	13	10	7
Rufibacter tibetensis 1351	1	1	1	1	1	56	11	9	6

	GldK TIGR03525	GldL TIGR03513	GldM TIGR03517	GldN TIGR03523	SprA TIGR04189	Type A CTD TIGR04183	Type B CTD TIGR04131	porP/sprF-like genes TIGR03519	porP/sprF-like genes that have type B CTD-encoding genes immediately upstream
Runella slithyformis DSM 19594	1	1	1	1	1	33	18	5	1
Spirosoma linguale DSM 74	1	1	1	1	1	53	14	4	1
Spirosoma radiotolerans DG5A	1	1	1	1	1	50	15	5	2
Class Sphingobacteriia									
Algoriphagus sp. M8-2	1	1	1	1	1	16	6	8	5
Arachidicoccus sp. BS20	2	1	1	2	1	11	0	0	0
Chitinophaga pinensis DSM 2588	1	1	1	1	1	51	36	17	13
Haliscomenobacter hydrossis DSM 1100	1	1	1	1	1	144	36	14	4
Mucilaginibacter PAMC26640	1	1	1	2	1	7	9	4	3
Niabella soli DSM 19437	0	0	0	0	0	0	0	0	0
Niastella koreensis DSM 17620	1	1	1	1	1	111	31	17	12
Pedobacter cryoconitis PAMC 27485	1	1	1	1	1	3	5	6	4
Pedobacter heparinus DSM 2366	1	1	1	1	1	8	13	10	7
Pedobacter sp. PACM 27299	1	1	1	1	1	1	9	7	6
Pseudopedobacter saltans DSM 12145	1	1	1	1	1	29	10	11	10
Saprospira grandis Lewin	1	1	1	3	2	67	16	10	2
Solitalea canadensis DSM 3403	1	1	1	1	1	6	18	11	8
Sphingobacterium sp. 21	2	1	1	2	1	1	2	1	1
Sphingobacterium sp. ML3W	1	1	1	1	0	1	0	0	0
Class Bacteroidia									
Alistipes finegoldii DSM 17242	0	0	0	0	0	0	0	0	0
Bacteroides cellulosilyticus WH2	1	1	1	1	1	19	1	1	0
Bacteroides dorei CL03T12C01	0	0	0	0	0	0	0	0	0
Bacteroides fragilis NCTC 9343	0	1	1	0	0	0	0	0	0
Bacteroides helcogenes DSM 20613	0	0	0	0	0	0	0	0	0
Bacteroides ovatus ATCC 8483	0	0	0	0	0	0	0	0	0
Bacteroides thetaiotaomicron VPI-5482	0	0	0	0	0	0	0	0	0
Bacteroides vulgatus ATCC 8482	0	0	0	0	0	0	0	0	0
Bacteroides xylanisolvens XB1A	0	0	0	0	0	0	0	0	0
Barnesiella viscericola DSM 18177	1	1	1	1	1	41	1	1	0
Draconibacterium orientale FH5	2	1	1	1	1	23	7	9	4
Odoribacter splanchnicus DSM 20712	0	0	0	0	2	2	1	2	0
Paludibacter propionicigenes DSM 17365	1	1	1	1	1	10	6	6	5
Parabacteroides distasonis ATCC 8503	1	1	1	1	1	7	1	1	0
Porphyromonas asaccharolytica DSM 20707	1	1	1	1	1	29	1	1	0
Porphyromonas gingivalis ATCC 33277	1	1	1	1	1	17	1	1	0
Prevotella dentalis EDSM 3688	1	1	1	1	1	9	1	1	0
Prevotella denticola F0289	1	1	1	1	1	8	1	1	0
Prevotella enoeca F0113	1	1	1	1	1	4	1	1	0
Prevotella fusca W1435	1	1	1	1	1	6	1	1	0
Prevotella intermedia 17-2	1	1	1	1	1	19	1	1	0
Prevotella melaninogenica ATCC 25845	1	1	1	1	1	14	1	1	0
Prevotella ruminicola 23	1	1	1	1	1	1	1	1	0
Prevotella sp. F0039	1	1	1	1	1	13	1	1	0
Rikenellaceae bacterium M3	0	0	0	0	0	0	0	0	0
Tannerella forsythia ATCC 43037	1	1	1	1	1	28	0	1	0
total								527	314

	T9SS components					CTDs		porP/sprF-like genes	porP/sprF-like genes that have type B CTD-encoding genes immediately upstream
	GldK	GldL	GldM	GldN	SprA	Type A CTD	Type B CTD		
	TIGR03525	TIGR03513	TIGR03517	TIGR03523	TIGR04189	TIGR04183	TIGR04131	TIGR03519	

[a]Only members of the *Bacteroidetes* with completed genome sequences were examined and only one member of each species was used. Occurrence of genes encoding T9SS components or of genes encoding proteins with T9SS-associated CTDs are shown. Tan shading indicates the presence of a gene and the number indicates the number of such genes in the genome. Genes were identified using the Integrated Microbial Genomes (IMG version 4.0.1) Function Profile Tool and using the TIGRFAM and pfam terms listed. For TIGRFAM terms the trusted cutoffs set by The Institute for Genomic Research were used as indicated in the Methods section of the main text. These may underrepresent the actual number of proteins secreted by T9SSs. For example, more than 30 proteins are thought to be secreted by the *P. gingivalis* T9SS (29), but only 18 were identified above.

Discussion

T9SSs are prevalent in members of the phylum *Bacteroidetes* and secrete tens to hundreds of different proteins from a single strain. These proteins have type A or type B CTDs that target them to the secretion system (1, 8, 27, 29, 40). The features of type A CTDs have been functionally studied in *F. johnsonia*e and *P. gingivalis* (12, 21, 22) but type B CTDs have received little attention. The results presented here demonstrate that type B CTDs are common in the phylum *Bacteroidetes*, and suggest that they target proteins for secretion by the T9SS.

Type B CTDs differ in sequence from type A CTDs (12, 19) and they also appear to differ functionally. Regions longer than 149 amino acids of the SprB type B CTD were required to target sfGFP for secretion. An additional protein, SprF, was also required for secretion. Wild type levels of SprF were not sufficient to facilitate secretion of SP-sfGFP-CTD$_{SprB}$ expressed from a plasmid. However, efficient secretion occurred when SP-sfGFP-CTD$_{SprB}$ and SprF were expressed together from the same plasmid. *F. johnsoniae* encodes nine PorP/SprF-like proteins in addition to SprF. Many of the *porP/sprF*-like genes are arranged like *sprF*, immediately downstream of genes encoding proteins with type B CTDs. Expression of one of these, Fjoh_3951, was required for efficient secretion of sfGFP linked to the type B CTD of Fjoh_3952. SprF and Fjoh_3951 were not interchangeable. Expression of SprF did not facilitate secretion of SP-sfGFP-CTD$_{Fjoh\_3952}$, and expression of Fjoh_3951 did not facilitate secretion of SP-sfGFP-CTD$_{SprB}$. It appears that proteins carrying each of these CTDs required co-expression with the appropriate cognate PorP/SprF-like protein for secretion.

P. gingivalis has only a single protein, PorP, that is similar to *F. johnsoniae* SprF. *P. gingivalis* PorP is essential for T9SS-mediated secretion, including secretion of proteins with

type A CTDs (3). In contrast, the individual *F. johnsoniae* PorP/SprF proteins that have been examined have more limited roles in secretion. SprF, for example, is only known to be required for secretion of SprB (7, 13). Further studies are needed to determine if any of the *F. johnsoniae* PorP/SprF-like proteins are critical for T9SS function, or if collectively they perform a critical role that is masked by redundancy.

The exact functions of PorP, SprF, or any of the PorP/SprF-like proteins in secretion are not known. They are all predicted outer membrane β-barrel proteins, and outer membrane localization was confirmed for PorP (3) and SprF (Fig. 19 and 20). Recent results indicate that *P. gingivalis* PorP interacts directly or indirectly with the T9SS components PorK and PorM, both of which have large periplasmic domains (15). PorK, PorL, PorM, and PorN are each essential components of the T9SS and they appear to form a complex (3, 15). The interactions of *P. gingivalis* PorP with PorK and PorM, and the genetic arrangement of *porP* immediately upstream of the *porK*, *porL*, *porM*, *porN* operon (15) suggest that PorP may interact with this T9SS complex to perform its role in secretion.

After secretion by the T9SS, SprB is attached on the cell surface (3, 9, 27). The C-terminal 218 amino acid region of SprB was sufficient to allow this attachment. We do not know how SprB interacts with the cell surface but SprF and other outer membrane motility proteins such as SprC and SprD may be involved. Wild type cells have large amounts of SprB on the cell surface, and only a small amount appears to be released from the cells (27). In contrast, we observed that cells expressing SP-sfGFP-CTD$_{SprB}$ not only had sfGFP on the cell surface, but they also released substantial amounts of soluble sfGFP into the spent medium (Fig. 2 and Fig. 4). *F. johnsoniae* produces many secreted proteases that could explain the release of sfGFP from the cell surface, although other explanations are possible.

SprB is a motility adhesin that moves rapidly along the cell surface, propelled by other components of the motility machinery (9, 27). The C-terminal 218 amino acid region of SprB was sufficient to allow productive interaction with the motility machinery, resulting in movement. Identification of proteins that interact with this C-terminal region of SprB may help determine how it is linked to the gliding machinery. Since SprF is required for secretion of proteins carrying the C-terminal region of SprB, it may interact with this region. It may also remain attached to SprB after its secretion, and perform additional roles in motility, although this has not been demonstrated. *sprC*, *sprD*, *sprB* and *sprF* are part of an operon, and nonpolar mutations in each gene cause similar motility defects (13). The N-terminal region of the large motility protein SprD is similar in sequence to SprF (Fig. 14 and 15), suggesting the possibility that SprD may also interact with SprB. Deletion of *sprC* and *sprD* resulted in decreased localization of SP-sfGFP-CTD$_{SprB}$ to the cell surface and lack of movement along the cell surface (Fig. 7), further suggesting that SprC or SprD may be involved in these processes. In addition to interacting with the motility machinery, SprB is thought to interact with the substratum to provide the traction needed for cell movement. Expression of sfGFP fused to C-terminal regions of SprB ranging from 218 to 1182 amino acids failed to substantially enhance cell movement beyond the limited movement already exhibited by the ΔsprB mutant cells. Additional studies are needed to dissect the 6497 amino acid SprB protein and determine the regions required for productive interaction with the substratum.

The importance of T9SSs in the nutrition, physiology, motility, and virulence of members of the phylum *Bacteroidetes* has been demonstrated (1, 3, 19, 39, 41-43). Most of the proteins with easily predicted functions that are secreted by T9SSs have type A CTDs. In contrast, with the exception of the motility protein SprB, the functions of the many proteins with type B CTDs

are not known. Many of these are large and have features that are found in some adhesins (Table 2). They may allow cells to interact with each other and with surfaces. The results presented demonstrate that these proteins are common among members of the phylum *Bacteroidetes*, and highlight the roles of type B CTDs and their associated outer membrane PorP/SprF-like proteins in T9SS-mediated secretion across the outer membrane.

Materials and Methods

Bacterial strains, plasmids and growth conditions. *F. johnsoniae* ATCC 17061 (UW101) and its *rpsL2* streptomycin resistant derivative CJ1827 were the wild-type strains used in this study (30, 32, 44, 45). Unless indicated otherwise, *F. johnsoniae* strains were grown in Casitone-Yeast Extract (CYE) medium at 30°C, as previously described (46). *Escherichia coli* strains were grown in Lysogeny Broth (LB) at 37°C (47). Strains and plasmids used in this study are listed in Table 4, and primers are listed in Table 5. Antibiotics were used at the following concentrations when needed: ampicillin, 100 µg/ml; erythromycin 100 µg/ml; kanamycin, 30 µg/ml; streptomycin, 100 µg/ml; and tetracycline, 20 µg/ml.

Construction of deletion mutants. The *sprF* deletion mutant CJ2518 was generated using pYT316 as described (48) except that the deletion was introduced into *F. johnsoniae* CJ1827. The Δ*sprB* Δ*gldK* double mutant CJ2737 was constructed using pJJ01 to delete *gldK* as described (8) except that the deletion was introduced into the Δ*sprB* mutant CJ1922 (32). The Δ*sprB gldJ_{548}* double mutant was constructed using pRR67 to delete *sprB* as described (32) except that the deletion was introduced into the *gldJ548* truncation mutant CJ2386 (28).

Insertion of *sfGFP* into chromosomal *sprB*. The sfGFP-encoding gene was inserted into chromosomal *sprB* essentially as previously described for myc tag insertions (7). A 2.3-kbp

fragment starting upstream of *sprB* and extending through base 228, numbered from the 'A' of the start codon, was amplified by PCR using Phusion DNA polymerase (New England BioLabs, Ipswich, MA) and primers 1356 (engineered XbaI site) and 1302 (engineered BamHI site). This fragment and pRR51 were digested with XbaI and BamHI and ligated together to form pYT108. A second fragment starting at base 229 of *sprB* and extending 1.9-kbp downstream was amplified using primers 1358 (engineered SalI site) and 1305 (engineered SphI site), digested with SalI and SphI, and ligated into pYT108 that had been digested with the same enzymes to generate pYT112. A 756 bp region encoding sfGFP with upstream linker (peptide sequence LEGPAGL) and downstream linker (peptide sequence GGSGGGSG) was amplified from pTB263 using primer 1749 (engineered XbaI site) and primer 1366 (engineered SalI site). This fragment and pYT112 were digested with XbaI and SalI and ligated together resulting in insertion of the sfGFP-encoding fragment between the *sprB* fragments as pYT296. Plasmid pYT296 was introduced into *F. johnsoniae* strain CJ1827 by triparental conjugation and a mutant that encoded full length SprB with sfGFP inserted after the signal peptide was isolated as previously described (7) and confirmed by PCR amplification and DNA sequencing.

Generation of plasmids that express fluorescent proteins with signal peptides at the N-termini and with regions of SprB CTDs at the C-termini. Regions of DNA encoding the C-terminus of SprB (CTD$_{SprB}$) were introduced into plasmid pYT179 that expressed the N-terminal signal peptide of RemA fused to sfGFP (SP-sfGFP) (12), resulting in plasmids that produce SP-sfGFP-CTD$_{SprB}$. These include pSK56 (expresses SP-sfGFP-CTD$_{SprB(218AA)}$) and pSK62 (expresses SP-sfGFP-CTD$_{SprB(1182AA)}$) that have been previously described (12). Additional plasmids expressing SP-sfGFP-CTD$_{SprB(149AA)}$ (pSK60), SP-sfGFP-CTD$_{SprB(368AA)}$ (pSK53), SP-sfGFP-CTD$_{SprB(448AA)}$ (pSK54), and SP-sfGFP-CTD$_{SprB(663AA)}$ (pSK50), were constructed in a

similar way using the primers listed in Table 5. In each case a region encoding the C-terminus of SprB was amplified and inserted into the XbaI and SphI sites of pYT179, to generate a construct encoding SP-sfGFP-CTD$_{SprB}$. Plasmids that also included *sprF* downstream from each of the SP-sfGFP-CTD$_{SprB}$-encoding constructs were also prepared. For example, a 657-bp fragment encoding 218 amino acids of CTD$_{SprB}$, 17-bp intergenic region and 1294-bp fragment encoding *sprF* gene was amplified by PCR primers 1843 (engineered XbaI site) and 955 (engineered SphI site). This fragment was introduced into XbaI and SphI digested pYT179 to generate pSK55. Plasmids encoding SP-sfGFP-CTD$_{SprB}$ with 149, 368, 448, 663, and 1182 amino acids from the C-terminus of SprB followed by and coexpressed with *sprF* (pSK59, pSK51, pSK52, pSK45, and pSK61 respectively) were constructed similarly using the primers listed in Table 5. A plasmid encoding mCherry as a periplasmic marker was generated by cloning the *chiA* promoter and N-terminal signal peptide region fused to the *mCherry* gene from pSSK54 (19) into pCP11. A 1254-bp fragment was amplified from pSSK54 with primers 2429 (engineered XbaI site) and 2430 (engineered SalI site). This fragment and pCP11 were digested using XbaI and SalI, and ligated together to form pJJ21.

Generation of plasmids that express SP-sfGFP fused to regions of the CTDs of Fjoh_3952 and Fjoh_1123. A 687-bp fragment encoding the C-terminal 228 amino acids of the type B CTD-containing protein Fjoh_3952 and the entire *porP/sprF*-like gene Fjoh_3951 was amplified and cloned into pYT179 using primers 1868 (engineered XbaI site) and 1869 (engineered SphI site) to generate plasmid pSK57.

The plasmid pSK69, which encodes both SP-sfGFP-CTD$_{SprB}$ and Fjoh_3951, was also constructed, as was plasmid pSK68, which encodes both SP-sfGFP-CTD$_{Fjoh\_3952}$ and SprF. Fjoh_3951 was amplified using primers 1892 (engineered SphI site) and 1969 (engineered SphI

site) and cloned into the SphI site of pSK56, generating pSK69. Similarly, *sprF* was amplified using primers 1883 (engineered SphI site) and 955 (engineered SphI site), and cloned into the SphI site of pSK58 (12) to generate pSK68. Plasmids were confirmed by sequencing. A region spanning 762-bp of CTD_{Fjoh_1123} was also cloned into pYT179 using primers 1881 (engineered XbaI site) and 1182 (engineered SphI site), generating plasmid pSK64 which encodes SP-sfGFP-CTD_{Fjoh_1123}.

Western blot analyses. *F. johnsoniae* cells were grown to early stationary phase in CYE at 25°C with shaking as previously described (12). Cells were pelleted by centrifugation at 22,000 x g for 15 min, and the culture supernatant (spent medium) was separated. For whole-cell samples, the cells were suspended in the original culture volume of phosphate-buffered saline consisting of 137 mM NaCl, 2.7 mM KCl, 10 mM Na_2PO_4, and 2 mM KH_2PO_4 (pH 7.4). Equal amounts of spent media and whole cells were boiled in SDS-PAGE loading buffer for 10 min. Proteins were separated by SDS-PAGE, and Western blot analyses were performed as previously described (49) except that polyvinylidene difluoride (PVDF) membranes were used instead of nitrocellulose membranes. Equal amounts of each sample based on the starting material were loaded in each lane. For cell extracts this corresponded to 10 μg protein, whereas for spent medium this corresponded to the equivalent volume of spent medium that contained 10 μg cell protein before the cells were removed. Anti-GFP (0.5 mg per ml; GenScript, Piscataway, NJ) was used at a dilution of 1:3,000 to detect sfGFP in Western blots, and anti-mCherry (BioVision Incorporated, Milpitas, CA) was used at a dilution of 1:5,000 to detect mCherry. Affinity purified polyclonal antibodies against the SprF peptide QSISNCPCTQSPVHD were produced by Biomatik Corporation (Cambridge, Ontario, Canada) and were used at a dilution of 1:3,000. Polyclonal antisera against GldL and GldJ were previously described (8, 50).

Localization of SprF. Wild-type and mutant cells of *F. johnsoniae* were grown to early stationary phase in MM medium (51) at 25°C with shaking. Cells were harvested and washed once in PBS by centrifugation for 10 min at 4,000 × g, suspended in PBS, adjusted to OD_{600}=1.5 and EDTA-free Halt protease inhibitor cocktail was added (Thermo Fisher Scientific, Rockford, IL). The cells were disrupted by using a French pressure cell and fractionated into soluble, inner membrane (Sarkosyl-soluble), and outer membrane (Sarkosyl-insoluble) fractions essentially as described previously (52). Equal amounts of each fraction based on 20 µg protein of the starting material (whole cells) were separated by SDS-PAGE, and Western blotting was performed as described above.

Proteinase K treatment of cells to determine the localization of SprF. Cells of *F. johnsoniae* were grown in CYE at 25°C with shaking. Cells were collected, washed and suspended in 20 mM sodium phosphate-10 mM $MgCl_2$ (pH 7.5) and diluted to an OD_{600} reading of 1.5. To examine SprF, proteinase K was added to the intact cells to a final concentration of 1 mg/ml and incubated at 25°C with gentle mixing. In each case an identical sample was lysed using a French pressure cell, unbroken cells and debris were removed by centrifugation and then proteinase K was added as above. At 0 and 2 h, 150 µl of cells or lysed cells were sampled, 10 mM phenylmethylsulfonyl fluoride was added and the samples were boiled for 1 min to stop digestion. SDS-PAGE loading buffer was added and the samples were boiled for another 7 min. Control samples that were not exposed to proteinase K were also included. Equal volumes were separated by SDS-PAGE and transferred to PVDF membranes, and proteins were detected with anti-serum against SprF.

Microscopic observation of cell movement. The movement of *F. johnsoniae* cells on glass was examined by phase-contrast microscopy at 25˚C. Cells were grown in MM at 25˚C

119

without shaking until late exponential phase. Motility on glass was analyzed using liquid filled tunnel slides prepared as described previously (7), using Nichiban NW-5 double sided tape (Nichiban Co, Tokyo, Japan) to hold a glass coverslip over a glass slide. Cells suspended in MM medium were introduced into tunnel slides, incubated for 5 min, and observed for motility using an Olympus BH-2 phase-contrast microscope. Images were recorded using a Photometrics Cool-SNAP$_{cf}{}^{2}$ camera and analyzed using MetaMorph software (Molecular Devices, Downingtown, PA) and ImageJ version 1.52i (http://rsb.info.nih.gov/ij/). Rainbow traces of cell movements were made using ImageJ and the macro Color FootPrint (9).

Analysis of wild-type and mutant cells for surface localization and movement of sfGFP. Cell-surface localization of sfGFP was examined by immunofluorescence microscopy. Cells were grown in MM at 25°C without shaking until late exponential phase. One ml of cell culture was centrifuged at $1000 \times$ g for 10 min and the cell pellet was suspended and washed 2 times in 500 µl of TC buffer (46). The cells were pelleted by centrifugation, suspended in 50 µl of TC + 2% BSA. Cells were exposed to 1 µl of polyclonal anti-GFP rabbit IgG (0.5 mg/ml; GenScript, Piscataway, NJ) for 30 minutes at room temperature and cells were pelleted ($1000 \times$ g for 10 min), washed 1 time with 500 µl TC buffer, suspended in 50 µl TC + 2% BSA, and exposed to 1 µl of F(ab') fragment of goat anti-rabbit IgG conjugated to Alexa-594 (2 mg/ml; Invitrogen, Carlsbad, CA). Cells were incubated 30 min in the dark and collected by centrifugation ($1000 \times$ g for 10 min). Cells were washed once with 500 µl of TC, suspended in 200 µl of TC, and kept in the dark until analysis (no more than 1 hour after labeling). Samples were spotted on glass slides previously coated with a thin layer of 1.0% agarose dissolved in TC and allowed to sit 30 seconds before applying coverslips. Samples were observed using a Nikon Eclipse 50i microscope (Nikon Instruments, Inc., Melville, NY) with an ExFo XL120 mercury

120

lamp, a Y-2E/C TR filter to detect red fluorescence, and an Endow 41017 GFP filter to detect green fluorescence (Chroma Technology Corp., Bellows Falls, VT). Epifluorescence and phase contrast images were recorded separately with a Hamamatsu ORCA-Flash4.0 LT+ camera through a Nikon CFI60 Plan Fluor Phase Contrast DLL 100x/1.3 objective using NIS-Elements Advanced Research software (Nikon Instruments, Inc., Melville, NY) and ImageJ. Exposure times for all fluorescence images were 33 msec.

GIMP (https://www.gimp.org/) was used to generate overlay images showing red fluorescence over phase contrast. Briefly, the phase contrast images were inverted and the contrast adjusted so the cells were light grey on a black background. These were then colorized to dark turquoise (RGB 12, 28, 28) using the "Colorize" command. Red fluorescence was similarly processed without inversion and colorized red (RGB 204, 0, 0). The black background of red fluorescence images were then made transparent and overlaid on the corresponding colorized phase contrast images. Surface localization statistics were based on examination of overlay images of 150 cells in three replicate experiments (450 cells total).

To examine cells for movement of cell-surface localized sfGFP, cells labeled with antibodies as above were introduced into a tunnel slide and incubated for 3 min before imaging. Cells were imaged by simultaneous low-light phase-contrast microscopy and fluorescence microscopy and images were recorded as above. Suspended cells were examined to avoid confusion resulting from the gliding movement of cells over surfaces. A total of 450 cells for each strain were observed for 20 s each in three replicate experiments (150 cells per experiment). Cells were counted as labeled if a fluorescent signal remained associated with the cell for the entire 20 s observation period. Signals were considered to have moved if they were displaced by 2.5 µm or more with respect to a cell pole at any time during observation.

Bioinformatic analyses. Genome sequences were analyzed for T9SS genes that encode proteins that belong to appropriate TIGRFAM multiple-sequence alignment families (53). This was accomplished using the Integrated Microbial Genomes (IMG version 4.0.1 [https://img.jgi.doe.gov/]) Function Profile Tool to examine the genomes for sequences predicted to encode orthologs of GldK (TIGR03525), GldL (TIGR03513), GldM (TIGR03517), GldN (TIGR03523), and SprA (TIGR04189). The genomes were also examined for genes encoding proteins with type A CTDs (TIGR04183), type B CTDs (TIGR04131), and for genes encoding PorP/SprF-like proteins (TIGR03519) in the same way. In each case, the trusted cutoffs assigned by The J. Craig Venter Institute (JCVI) were used to identify family members. These cutoffs allow identification of the vast majority of family members with vanishingly few false positives (53). *F. johnsoniae* proteins related to *P. gingivalis* W83 PG1058 were identified by BLASTP analysis (54).

Table 4. Strains and plasmids used in this study.

Strain	Genotype and Description[a]	Reference
E. coli strains		
DH5αmcr	Strain used for general cloning	Life Technologies (Grand Island, NY, USA)
HB101	Strain used with pRK2013 for triparental conjugation	(55, 56)
F. johnsoniae strains		
UW101	Wild type *F. johnsoniae* ATCC 17061^T	(30, 45)
CJ1584	Δ(*sprC sprD sprB*)	(13)
CJ1827	*rpsL2*; Sm^r 'wild-type' *F. johnsoniae* strain used in construction of deletion mutants	(32)
CJ1922	Δ*sprB rpsL2*; (Sm^r)	(32)
CJ2122	Δ*gldK rpsL2*; (Sm^r)	(8)
CJ2518	Δ*sprF rpsL2*; (Sm^r)	This study
CJ2386	*gldJ$_{548}$ rpsL2*; (Sm^r)	(28)
CJ2491	*sfGFP*::*sprB rpsL2*; (Sm^r)	This study
CJ2737	Δ*sprB* Δ*gldK rpsL2*; (Sm^r)	This study
CJ2839	Δ*sprB gldJ$_{548}$ rpsL2*; (Sm^r)	This study
Plasmid	**Description**	**Reference**
pCB3	Encodes SP-sfGFP-CTD$_{ChiA(105AA)}$; Ap^r (Tc^r)	(12)
pCP11	*E. coli-F. johnsoniae* shuttle plasmid; Ap^r (Em^r)	(46)
pCP23	*E. coli-F. johnsoniae* shuttle plasmid; Ap^r (Tc^r)	(33)
pJJ01	Construct used to delete *gldK*; Ap^r (Em^r)	(8)
pJJ21	Expresses periplasmic mCherry from pCP11; Ap^r (Em^r)	This study
pRK2013	Helper plasmid for triparental conjugation; IncP Tra$^+$ Km^r	(56)
pRR51	*rpsL*-containing suicide vector used for constructing deletion mutants; Ap^r (Em^r)	(32)
pRR67	Construct used to delete *sprB*; Ap^r (Em^r)	(32)
pSK37	sfGFP with stop codon cloned into pYT40; Ap^r (Tc^r)	(12)
pSK45	1992-bp region encoding 663 amino acids of CTD$_{SprB}$, 16-bp intergenic region and 1178-bp region encoding SprF inserted into pYT179; Encodes SP-sfGFP-CTD$_{SprB(663AA)}$ and SprF; Ap^r (Tc^r)	This study

pSK50	1992-bp region encoding 663 amino acids of CTD$_{SprB}$ inserted into pYT179; Encodes SP-sfGFP-CTD$_{SprB(663AA)}$ Ap^r (Tc^r)	This study
pSK51	1107-bp region encoding 368 amino acids of CTD$_{SprB}$, 16-bp intergenic region and 1178-bp region encoding SprF inserted into pYT179; Encodes SP-sfGFP-CTD$_{SprB(368AA)}$ and SprF; Ap^r (Tc^r)	This study
pSK52	1347-bp region encoding 448 amino acids of CTD$_{SprB}$, 16-bp intergenic region and 1178-bp region encoding SprF inserted into pYT179; Encodes SP-sfGFP-CTD$_{SprB(448AA)}$ and SprF; Ap^r (Tc^r)	This study
pSK53	1107-bp region encoding 368 amino acids of CTD$_{SprB}$ inserted into pYT179; Encodes SP-sfGFP-CTD$_{SprB(368AA)}$; Ap^r (Tc^r)	This study
pSK54	1347-bp region encoding 448 amino acids of CTD$_{SprB}$ inserted into pYT179; Encodes SP-sfGFP-CTD$_{SprB(448AA)}$; Ap^r (Tc^r)	This study
pSK55	657-bp region encoding 218 amino acids of CTD$_{SprB}$, 16-bp intergenic region and 1178-bp region encoding SprF inserted into pYT179; Encodes SP-sfGFP-CTD$_{SprB(218AA)}$ and SprF; Ap^r (Tc^r)	This study
pSK56	Encodes SP-sfGFP-CTD$_{SprB(218AA)}$; Ap^r (Tc^r)	(12)
pSK57	687-bp region encoding 228 amino acids of CTD$_{Fjoh\_3952}$, 16-bp intergenic region and 1032-bp region encoding Fjoh_3951 inserted into pYT179; Encodes SP-sfGFP-CTD$_{Fjoh\_3952(228AA)}$ and Fjoh_3951;Ap^r (Tc^r)	This study
pSK58	687-bp region encoding 228 amino acids of CTD$_{Fjoh\_3952}$ inserted into pYT179; Encodes SP-sfGFP-CTD$_{Fjoh\_3952(228AA)}$; Ap^r (Tc^r)	(12)
pSK59	450-bp region encoding 149 amino acids of CTD$_{SprB}$, 16-bp intergenic region and 1178-bp region encoding SprF inserted into pYT179; Encodes SP-sfGFP-CTD$_{SprB(149AA)}$ and SprF; Ap^r (Tc^r)	This study
pSK60	450-bp region encoding 149 amino acids of CTD$_{SprB}$ inserted into pYT179; Encodes SP-sfGFP-CTD$_{SprB(149AA)}$; Ap^r (Tc^r)	This study
pSK61	3549-bp region encoding 1182 amino acids of CTD$_{SprB}$, 16-bp intergenic region and 1178-bp region encoding SprF inserted into pYT179; Encodes SP-sfGFP-CTD$_{SprB(1182AA)}$ and SprF; Ap^r (Tc^r)	This study
pSK62	3549-bp region encoding 1182 amino acids of CTD$_{SprB}$ inserted into pYT179; Encodes SP-sfGFP-CTD$_{SprB(1182AA)}$; Ap^r (Tc^r)	(12)
pSK64	762-bp region encoding 238 amino acids of Fjoh_1123 inserted into pYT179; Encodes SP-sfGFP-CTD$_{Fjoh\_1123(238AA)}$; Ap^r (Tc^r)	This study

pSK68	1294-bp region encoding SprF inserted into pSK58; Encodes SP-sfGFP- CTD$_{Fjoh\_3952(228AA)}$ and SprF; Ap^r (Tc^r)	This study
pSK69	1032-bp region encoding Fjoh_3951 inserted into pSK56; Encodes SP-sfGFP-CTD$_{SprB(218AA)}$ and Fjoh_3951; Ap^r (Tc^r)	This study
pSK82	Encodes SP-sfGFP-CTD$_{AmyB(99AA)}$; Ap^r (Tc^r)	(12)
pTB263	Expresses sfGFP; Ap^r	(57)
pYT40	*remA* promoter, start codon, and the N-terminal signal peptide-encoding region inserted into pCP23; Ap^r (Tc^r)	(12)
pYT108	Plasmid used to construct pYT296; Ap^r (Em^r)	This study
pYT112	Plasmid used to construct pYT296; Ap^r (Em^r)	This study
pYT179	sfGFP amplified without stop codon and cloned into pYT40; Encodes SP-sfGFP; Ap^r (Tc^r)	(12)
pYT296	Plasmid used to insert the gene encoding sfGFP into chromosomal *sprB* to construct CJ2491, which produces full length SprB with sfGFP inserted after the signal peptide; Ap^r (Em^r)	This study
pYT316	Construct used to delete *F. johnsoniae sprF*; Ap^r (Em^r)	(48)

^{a}Antibiotic resistance phenotypes are as follows: ampicillin, Ap^r; erythromycin, Em^r; kanamycin, Km^r; streptomycin, Sm^r; tetracycline, Tc^r. The antibiotic resistance phenotypes given in parentheses are those expressed in *F. johnsoniae* but not in *E. coli*. The antibiotic resistance phenotypes without parentheses are those expressed in *E. coli* but not in *F. johnsoniae*.

Table 5. Primers used in this study

Primer	Sequence and Description
954	5' GCTAG<u>TCTAGA</u>TGGCGAGGAATTACCTTCTGGTGA 3'; forward primer used in construction of pSK45, pSK51, pSK52 and pSK55; XbaI site underlined
955	5' GCTAG<u>GCATGC</u>GGACATTTCGGCTTGTGTTAAATTCG 3'; reverse primer used in construction of pSK59, pSK61 and pSK68; SphI site underlined
1302	5' GCTAG<u>GGATCC</u>CAGAAGCTACAGCGAAAGCAAAAG 3'; forward primer used in construction of pYT108 and pYT296; BamHI site underlined
1305	5' GCTAG<u>GCATGC</u>GAGGGTGTACACCTGACTGATTCTC 3'; reverse primer used in construction of pYT112 and pYT296; SphI site underlined
1356	5' GCTAG<u>TCTAGA</u>TACAGGGTTGGGAATGGTAGGTACT 3'; reverse primer used in construction of pYT108 and pYT296; XbaI site underlined
1358	5' GCTAG<u>GTCGAC</u>CTTAAGTACGCACAAGGAGAGTATGC 3'; forward primer used in construction of pYT112 and pYT296; SalI site underlined
1366	5' GCTAG<u>GTCGAC</u>ACCAGAACCACCACCAGAACCACCTTTGTAGAGCT CATCCATGCCGTG 3'; reverse primer used in the construction of pYT296; SalI site underlined; 24 nucleotide linker sequence immediately after Sal site
1400	5' GCTAG<u>GCATGC</u>TTATCTGTATAAAGTGAAATGTCCAAC 3'; reverse primer used in construction of pSK50, pSK53, pSK54 and pSK60; SphI site underlined
1694	5' GCTAG<u>TCTAGA</u>CCGGATCCAATTACATTTACAGCAG 3'; forward primer used in construction of pSK45 and pSK50; XbaI site underlined
1749	5' GCTAG<u>TCTAGA</u>CTCGAGGGTCCGGCTGGTCTGT 3'; forward primer used in construction of pYT296; XbaI site underlined
1828	5' GCTAG<u>TCTAGA</u> ACAGCTTACGAAGTACCAGGATCTATG 3'; forward primer used in construction of pSK51 and pSK53; XbaI site underlined
1829	5' GCTAG<u>TCTAGA</u>GCAGGTACAGAAATTAGACCGGCA 3'; forward primer used in construction of pSK52 and pSK54; XbaI site underlined
1843	5' GCTAG<u>TCTAGA</u>GTGGTGATTACAATTGATCCAAGC 3'; forward primer used in construction of pSK55; XbaI site underlined
1868	5' GCTAG<u>TCTAGA</u>GTCGAAGTGCCATCGATTACAGTA 3'; forward primer used in construction of pSK57; XbaI site underlined
1869	5' GCTAG<u>GCATGC</u>AACTGCTTTTTGTGCTATTGCGTT 3'; reverse primer used in construction of pSK69; SphI site underlined
1879	5' GCTAG<u>TCTAGA</u>GGTGTTTGGAACGTAATTACAGCT 3'; forward primer used in construction of pSK59 and pSK60; XbaI site underlined
1880	5' GCTAG<u>TCTAGA</u>CGTTCTGAAATTACGCTTACTCCG 3'; forward primer used in construction of pSK61; XbaI site underlined
1881	5' GCTAG<u>TCTAGA</u>TTCGTAAATGATCTGCCAACAGTA 3'; forward primer used in construction of pSK64; XbaI site underlined
1882	5' GCTAG<u>GCATGC</u>ATAAATGTTTGAATGCCATCTCCT 3'; reverse primer used in construction of pSK64; SphI site underlined
1883	5' GCTAG<u>GCATGC</u>TGGCGAGGAATTACCTTCTGGTGA 3'; reverse primer used in construction of pSK68; SphI site underlined

1892	5' GCTAG<u>GCATGC</u>AGTCCAAATCAATAAAATGGCTTA 3'; reverse primer used in construction of pSK57 and pSK69; SphI site underlined
2429	5' GCTAG<u>TCTAGA</u>TTCCCCGGTAGAGATAGTTATGGCTAT 3'; forward primer used in construction of pJJ21; XbaI site underlined
2430	5' GCTAG<u>GTCGAC</u>TTACTTGTACAGCTCGTCCATGCCG 3'; reverse primer used in construction of pJJ21; SalI site underlined

References

1. Kharade SS, McBride MJ. 2015. *Flavobacterium johnsoniae* PorV is required for secretion of a subset of proteins targeted to the type IX secretion system. J Bacteriol 197:147-158.
2. McBride MJ, Zhu Y. 2013. Gliding motility and Por secretion system genes are widespread among members of the phylum *Bacteroidetes*. J Bacteriol 195:270-278.
3. Sato K, Naito M, Yukitake H, Hirakawa H, Shoji M, McBride MJ, Rhodes RG, Nakayama K. 2010. A protein secretion system linked to bacteroidete gliding motility and pathogenesis. Proc Natl Acad Sci USA 107:276-281.
4. Sato K, Sakai E, Veith PD, Shoji M, Kikuchi Y, Yukitake H, Ohara N, Naito M, Okamoto K, Reynolds EC, Nakayama K. 2005. Identification of a new membrane-associated protein that influences transport/maturation of gingipains and adhesins of *Porphyromonas gingivalis* J Biol Chem 280:8668-8677.
5. Braun TF, Khubbar MK, Saffarini DA, McBride MJ. 2005. *Flavobacterium johnsoniae* gliding motility genes identified by *mariner* mutagenesis. J Bacteriol 187:6943-6952.
6. Nelson SS, Glocka PP, Agarwal S, Grimm DP, McBride MJ. 2007. *Flavobacterium johnsoniae* SprA is a cell-surface protein involved in gliding motility. J Bacteriol 189:7145-7150.
7. Shrivastava A, Rhodes RG, Pochiraju S, Nakane D, McBride MJ. 2012. *Flavobacterium johnsoniae* RemA is a mobile cell-surface lectin involved in gliding. J Bacteriol 194:3678-3688.
8. Shrivastava A, Johnston JJ, van Baaren JM, McBride MJ. 2013. *Flavobacterium johnsoniae* GldK, GldL, GldM, and SprA are required for secretion of the cell-surface gliding motility adhesins SprB and RemA. J Bacteriol 195:3201-3212.
9. Nakane D, Sato K, Wada H, McBride MJ, Nakayama K. 2013. Helical flow of surface protein required for bacterial gliding motility. Proc Natl Acad Sci USA 110:11145-11150.
10. Shrivastava A, Roland T, Berg HC. 2016. The screw-like movement of a gliding bacterium is powered by spiral motion of cell-surface adhesins. Biophys J 111:1008-1013.
11. Rhodes RG, Samarasam MN, Van Groll EJ, McBride MJ. 2011. Mutations in *Flavobacterium johnsoniae sprE* result in defects in gliding motility and protein secretion. Journal of Bacteriology 193:5322-7.
12. Kulkarni SS, Zhu Y, Brendel CJ, McBride MJ. 2017. Diverse C-terminal sequences involved in *Flavobacterium johnsoniae* protein secretion. J Bacteriol 199:e00884-16.
13. Rhodes RG, Nelson SS, Pochiraju S, McBride MJ. 2011. *Flavobacterium johnsoniae sprB* is part of an operon spanning the additional gliding motility genes *sprC*, *sprD*, and *sprF*. J Bacteriol 193:599-610.
14. Gorasia DG, Veith PD, Hanssen EG, Glew MD, Sato K, Yukitake H, Nakayama K, Reynolds EC. 2016. Structural Insights into the PorK and PorN Components of the *Porphyromonas gingivalis* Type IX Secretion System. PLoS Pathog 12:e1005820.
15. Vincent MS, Canestrari MJ, Leone P, Stathopulos J, Ize B, Zoued A, Cambillau C, Kellenberger C, Roussel A, Cascales E. 2017. Characterization of the *Porphyromonas gingivalis* Type IX Secretion Trans-envelope PorKLMNP Core Complex. J Biol Chem 292:3252-3261.
16. Leone P, Roche J, Vincent MS, Tran QH, Desmyter A, Cascales E, Kellenberger C, Cambillau C, Roussel A. 2018. Type IX secretion system PorM and gliding machinery GldM form arches spanning the periplasmic space. Nature Communications 9:ARTN 429.

17.   Shrivastava A, Lele PP, Berg HC. 2015. A rotary motor drives *Flavobacterium* gliding. Curr Biol 25:338-341.
18.   Lauber F, Deme JC, Lea SM, Berks BC. 2018. Type 9 secretion system structures reveal a new protein transport mechanism. Nature 564:77-82.
19.   Kharade SS, McBride MJ. 2014. The *Flavobacterium johnsoniae* chitinase ChiA is required for chitin utilization and is secreted by the type IX secretion system. J Bacteriol 196:961-970.
20.   Nguyen KA, Travis J, Potempa J. 2007. Does the importance of the C-terminal residues in the maturation of RgpB from *Porphyromonas gingivalis* reveal a novel mechanism for protein export in a subgroup of Gram-Negative bacteria? J Bacteriol 189:833-843.
21.   Seers CA, Slakeski N, Veith PD, Nikolof T, Chen YY, Dashper SG, Reynolds EC. 2006. The RgpB C-terminal domain has a role in attachment of RgpB to the outer membrane and belongs to a novel C-terminal-domain family found in *Porphyromonas gingivalis*. J Bacteriol 188:6376-6386.
22.   Shoji M, Sato K, Yukitake H, Kondo Y, Narita Y, Kadowaki T, Naito M, Nakayama K. 2011. Por secretion system-dependent secretion and glycosylation of *Porphyromonas gingivalis* hemin-binding protein 35. PLOS One 6:e21372.
23.   Slakeski N, Seers CA, Ng K, Moore C, Cleal SM, Veith PD, Lo AW, Reynolds EC. 2011. C-terminal domain residues important for secretion and attachment of RgpB in *Porphyromonas gingivalis*. J Bacteriol 193:132-142.
24.   Glew MD, Veith PD, Peng B, Chen YY, Gorasia DG, Yang Q, Slakeski N, Chen D, Moore C, Crawford S, Reynolds E. 2012. PG0026 is the C-terminal signal peptidase of a novel secretion system of *Porphyromonas gingivalis*. J Biol Chem 287:24605-24617.
25.   de Diego I, Ksiazek M, Mizgalska D, Koneru L, Golik P, Szmigielski B, Nowak M, Nowakowska Z, Potempa B, Houston JA, Enghild JJ, Thogersen IB, Gao J, Kwan AH, Trewhella J, Dubin G, Gomis-Ruth FX, Nguyen KA, Potempa J. 2016. The outer-membrane export signal of *Porphyromonas gingivalis* type IX secretion system (T9SS) is a conserved C-terminal beta-sandwich domain. Sci Rep 6:23123.
26.   Lasica AM, Goulas T, Mizgalska D, Zhou X, de Diego I, Ksiazek M, Madej M, Guo Y, Guevara T, Nowak M, Potempa B, Goel A, Sztukowska M, Prabhakar AT, Bzowska M, Widziolek M, Thogersen IB, Enghild JJ, Simonian M, Kulczyk AW, Nguyen KA, Potempa J, Gomis-Ruth FX. 2016. Structural and functional probing of PorZ, an essential bacterial surface component of the type-IX secretion system of human oral-microbiomic *Porphyromonas gingivalis*. Sci Rep 6:37708.
27.   Nelson SS, Bollampalli S, McBride MJ. 2008. SprB is a cell surface component of the *Flavobacterium johnsoniae* gliding motility machinery. J Bacteriol 190:2851-2857.
28.   Johnston JJ, Shrivastava A, McBride MJ. 2018. Untangling *Flavobacterium johnsoniae* gliding motility and protein secretion. J Bacteriol 200:e00362-17.
29.   Veith PD, Nor Muhammad NA, Dashper SG, Likic VA, Gorasia DG, Chen D, Byrne SJ, Catmull DV, Reynolds EC. 2013. Protein substrates of a novel secretion system are numerous in the *Bacteroidetes* phylum and have in common a cleavable C-terminal secretion signal, extensive post-translational modification and cell surface attachment. J Proteome Res 12:4449-4461.
30.   McBride MJ, Xie G, Martens EC, Lapidus A, Henrissat B, Rhodes RG, Goltsman E, Wang W, Xu J, Hunnicutt DW, Staroscik AM, Hoover TR, Cheng YQ, Stein JL. 2009. Novel

features of the polysaccharide-digesting gliding bacterium *Flavobacterium johnsoniae* as revealed by genome sequence analysis. Appl Environ Microbiol 75:6864-6875.

31.   Kulkarni SS, Johnston JJ, Zhu Y, Hying ZT, McBride MJ. 2019. The carboxy-terminal region of *Flavobacterium johnsoniae* SprB facilitates its secretion by the type IX secretion system and propulsion by the gliding motility machinery. J Bacteriol doi:10.1128/JB.00218-19.

32.   Rhodes RG, Pucker HG, McBride MJ. 2011. Development and use of a gene deletion strategy for *Flavobacterium johnsoniae* to identify the redundant motility genes *remF*, *remG*, *remH*, and *remI*. J Bacteriol 193:2418-2428.

33.   Agarwal S, Hunnicutt DW, McBride MJ. 1997. Cloning and characterization of the *Flavobacterium johnsoniae* (*Cytophaga johnsonae*) gliding motility gene, *gldA*. Proc Natl Acad Sci USA 94:12139-12144.

34.   Lombard V, Golaconda Ramulu H, Drula E, Coutinho PM, Henrissat B. 2014. The carbohydrate-active enzymes database (CAZy) in 2013. Nucleic Acids Res 42:D490-5.

35.   Yu CS, Chen YC, Lu CH, Hwang JK. 2006. Prediction of protein subcellular localization. Proteins 64:643-651.

36.   Heath JE, Seers CA, Veith PD, Butler CA, Nor Muhammad NA, Chen YY, Slakeski N, Peng B, Zhang L, Dashper SG, Cross KJ, Cleal SM, Moore C, Reynolds EC. 2016. PG1058 is a novel multidomain protein component of the bacterial type IX secretion system. PLoS One 11:e0164313.

37.   Ortiz-Suarez ML, Samsudin F, Piggot TJ, Bond PJ, Khalid S. 2016. Full-length OmpA: structure, function, and membrane interactions predicted by molecular dynamics simulations. Biophys J 111:1692-1702.

38.   Samsudin F, Ortiz-Suarez ML, Piggot TJ, Bond PJ, Khalid S. 2016. OmpA: a flexible clamp for bacterial cell wall attachment. Structure 24:2227-2235.

39.   Zhu Y, McBride MJ. 2014. Deletion of the *Cytophaga hutchinsonii* type IX secretion system gene *sprP* results in defects in gliding motility and cellulose utilization. Appl Microbiol Biotechnol 98:763-775.

40.   Sato K, Yukitake H, Narita Y, Shoji M, Naito M, Nakayama K. 2013. Identification of *Porphyromonas gingivalis* proteins secreted by the Por secretion system. FEMS Microbiol Lett 338:68-76.

41.   Li N, Zhu Y, LaFrentz BR, Evenhuis JP, Hunnicutt DW, Conrad RA, Barbier P, Gullstrand CW, Roets JE, Powers JL, Kulkarni SS, Erbes DH, Garcia JC, Nie P, McBride MJ. 2017. The type IX secretion system is required for virulence of the fish pathogen *Flavobacterium columnare*. Appl Environ Microbiol 83:e01769-17.

42.   Guo YQ, Hu D, Guo J, Wang T, Xiao YC, Wang XL, Li SW, Liu M, Li ZL, Bi DR, Zhou ZT. 2017. *Riemerella anatipestifer* type IX secretion system is required for virulence and gelatinase secretion. Frontiers in Microbiology 8:ARTN 2553.

43.   Kita D, Shibata S, Kikuchi Y, Kokubu E, Nakayama K, Saito A, Ishihara K. 2016. Involvement of the type IX secretion system in *Capnocytophaga ochracea* gliding motility and biofilm formation. Appl Environ Microbiol 82:1756-66.

44.   Chang LYE, Pate JL, Betzig RJ. 1984. Isolation and characterization of nonspreading mutants of the gliding bacterium *Cytophaga johnsonae*. J Bacteriol 159:26-35.

45.   McBride MJ, Braun TF. 2004. GldI is a lipoprotein that is required for *Flavobacterium johnsoniae* gliding motility and chitin utilization. J Bacteriol 186:2295-2302.

46.	McBride MJ, Kempf MJ. 1996. Development of techniques for the genetic manipulation of the gliding bacterium *Cytophaga johnsonae*. J Bacteriol 178:583-590.

47.	Sambrook J, Fritsch EF, Maniatis T. 1989. Molecular cloning: a laboratory manual. Cold Spring Harbor Laboratory, Cold Spring Harbor, N. Y.

48.	Zhu Y, Thomas F, Larocque R, Li N, Duffieux D, Cladiere L, Souchaud F, Michel G, McBride MJ. 2017. Genetic analyses unravel the crucial role of a horizontally acquired alginate lyase for brown algal biomass degradation by *Zobellia galactanivorans* Environ Microbiol 19:2164-2181.

49.	Rhodes RG, Samarasam MN, Shrivastava A, van Baaren JM, Pochiraju S, Bollampalli S, McBride MJ. 2010. *Flavobacterium johnsoniae gldN* and *gldO* are partially redundant genes required for gliding motility and surface localization of SprB. J Bacteriol 192:1201-1211.

50.	Braun TF, McBride MJ. 2005. *Flavobacterium johnsoniae* GldJ is a lipoprotein that is required for gliding motility. J Bacteriol 187:2628-2637.

51.	Liu J, McBride MJ, Subramaniam S. 2007. Cell-surface filaments of the gliding bacterium *Flavobacterium johnsoniae* revealed by cryo-electron tomography. J Bacteriol 189:7503-7506.

52.	Hunnicutt DW, McBride MJ. 2000. Cloning and characterization of the *Flavobacterium johnsoniae* gliding motility genes, *gldB* and *gldC*. J Bacteriol 182:911-918.

53.	Haft DH, Selengut JD, Richter RA, Harkins D, Basu MK, Beck E. 2013. TIGRFAMs and genome properties in 2013. Nucleic Acids Res 41:D387-95.

54.	Altschul SF, Madden TL, Schaffer AA, Zhang J, Zhang Z, Miller W, Lipman DJ. 1997. Gapped BLAST and PSI-BLAST: a new generation of protein database search programs. Nucleic Acids Res 25:3389-402.

55.	Bolivar F, Backman K. 1979. Plasmids of *Escherichia coli* as cloning vectors. Methods Enzymol 68:245-267.

56.	Figurski DH, Helinski DR. 1979. Replication of an origin-containing derivative of plasmid RK2 dependent on a plasmid function provided in trans. Proc Natl Acad Sci USA 76:1648-1652.

57.	Uehara T, Dinh T, Bernhardt TG. 2009. LytM-domain factors are required for daughter cell separation and rapid ampicillin-induced lysis in *Escherichia coli*. J Bacteriol 191:5094-5107.

Chapter 4. Summary

The bacterium *Flavobacterium johnsoniae* is a member of the phylum *Bacteroidetes* that utilizes the type IX secretion system (T9SS) and exhibits gliding motility. The T9SS and the *Bacteroidetes* form of gliding motility are apparently confined to the phylum, and they appear to be interconnected. The T9SS is required for secretion of extracellular enzymes, such as the chitinase ChiA, as well as the secretion and localization of the cell surface motility adhesins SprB and RemA. These adhesins are propelled by the gliding motility machinery to provide cell motility. The proteins GldK, GldL, GldM, GldN, SprA, SprE, and SprT comprise the core of the T9SS. Orthologs of these are found in members of the *Bacteroidetes* that have functional T9SSs. In addition to these proteins, *F. johnsoniae* also makes the gliding motility proteins GldA, GldB, GldD, GldF, GldH, GldI, and GldJ. Chapter 2 demonstrates that *F. johnsoniae* cells with mutations in the genes encoding these gliding motility proteins show defects in motility and secretion. The presence of functional GldA, B, D, F, H, I, and J are thus essential for T9SS-mediated secretion. Cells with mutations in the genes encoding any of these seven proteins had normal levels of *gldK* mRNA but dramatically reduced levels of GldK protein, which is required for a functional T9SS. GldJ is needed for the accumulation of GldK and mutants lacking GldA, B, D, F, H, or I failed to accumulate GldJ (Fig 1). *F. johnsoniae* cells that produce truncated GldJ, lacking eight to thirteen amino acids from the C-terminus, accumulated truncated GldJ, GldK, and secreted SprB to the cell surface (Fig 2). This cell surface localized SprB was not propelled by the gliding motility machinery and the cells were deficient in motility on agar and glass. Thus, the C-terminal region of GldJ is required for gliding motility but not for secretion. Chapter 3 explores the role of the Type B carboxy-terminal domain (CTD) in secretion and localization of SprB and other Type B CTD containing proteins. *F. johnsoniae* cells secrete the foreign protein sfGFP when it is fused to regions spanning the SprB type B CTD of 218 amino

acids or longer. This secretion is enhanced when the protein is co-expressed with SprF from the same plasmid. *sprF* and genes encoding similar proteins are frequently found downstream of genes encoding Type B CTD containing proteins. The SprF-like proteins appear to only enhance secretion of their cognate Type B CTD proteins. Regions of the SprB Type B CTD that allowed secretion of sfGFP also facilitated the localization of sfGFP to the cell surface and interaction with the gliding motility machinery (Fig 3). This thesis begins to untangle the *F. johnsoniae* motility machinery from the T9SS and describes the requirements of the major cell surface adhesin SprB for secretion by the T9SS and propulsion by the motility machinery.
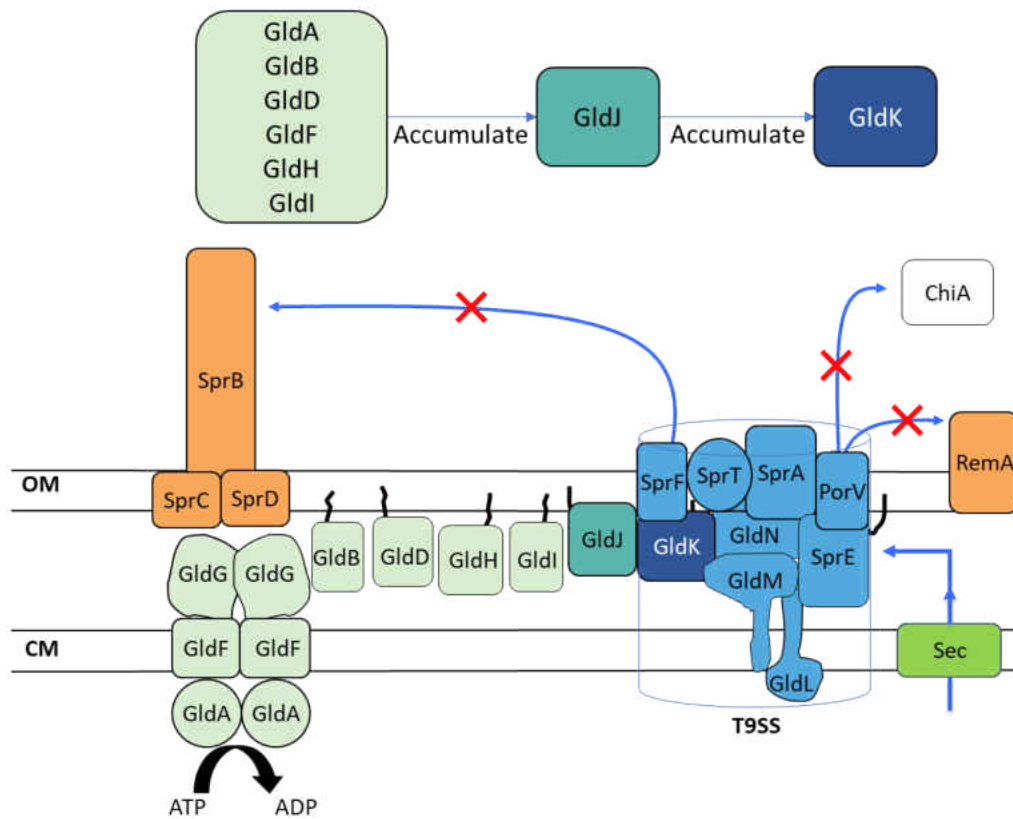
Figure 1. GldA-I are required for accumulation of GldJ and subsequently GldK. *F. johnsoniae* strains with mutations in *gldA*, *gldB*, *gldD*, *gldF*, *gldH*, or *gldI* (light green) fail to accumulate GldJ (turquoise). Strains lacking GldJ fail to accumulate GldK (dark blue). *F. johnsoniae* strains that lack GldK are defective in secretion of the surface motility adhesins SprB and RemA (orange), the extracellular enzyme ChiA (white), and many other proteins secreted by the T9SS.
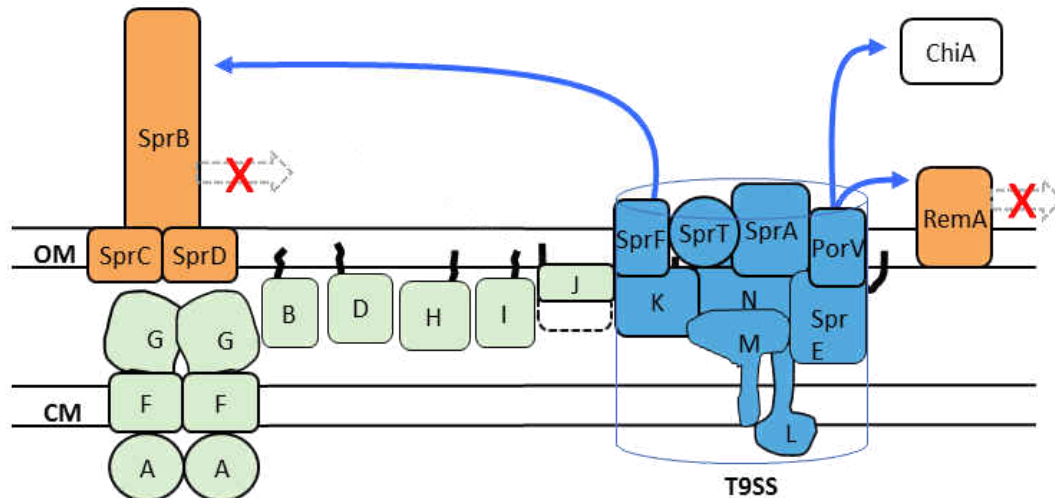
Figure 2. *F. johnsoniae* **cells expressing truncated forms of GldJ exhibit T9SS-mediated secretion but not gliding motility.** Cells expressing forms of GldJ lacking the carboxy-terminal eight to thirteen amino acids of GldJ accumulate GldK. These cells secrete and localize the cell surface adhesins SprB and RemA, and secrete the extracellular chitinase ChiA. However, the surface adhesins are not propelled by the gliding machinery and the cells exhibit motility defects on agar and glass.
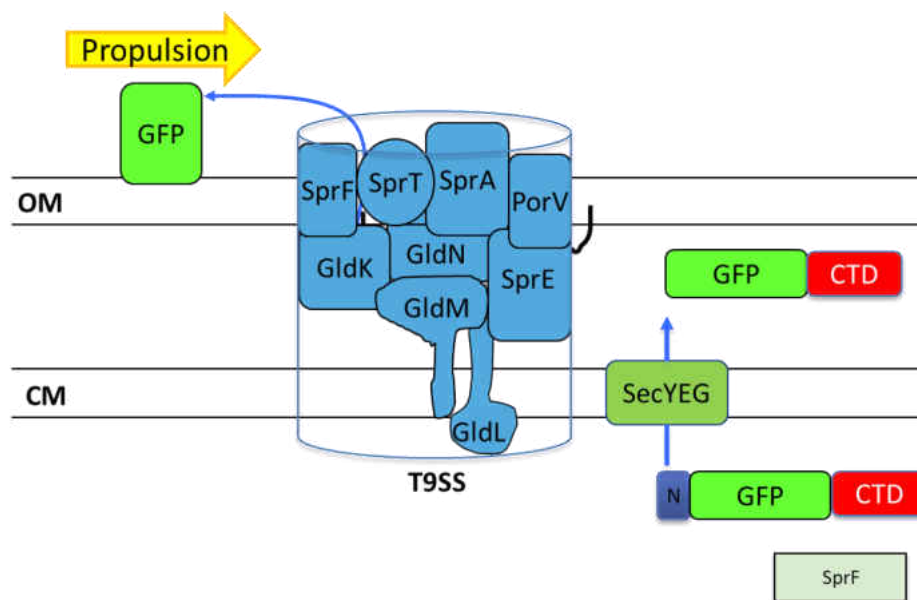
Figure 3. Fusion of sfGFP to CTD$_{SprB}$ is sufficient for secretion by the T9SS, localization to the cell surface, and interaction with the motility machinery. When co-expressed with SprF sfGFP is detectable on the cell surface by fluorescent immunolabeling. Additionally, this cell surface localize sfGFP is propelled along the cell, presumably by the motility machinery that would normally interact with SprB.

134

Appendix. Investigation of *Flavobacterium johnsoniae* proteins Fjoh_0891 and Fjoh_3155 for roles in the type IX secretion system (T9SS) and gliding motility.

The *mariner* based transposon *HimarEm1* is a genetic tool that is used to identify genes involved in *F. johnsoniae* gliding motility and protein secretion. Following transfer of the plasmid pHimarEm1 into wild-type cells, colonies are screened for resistance to erythromycin conferred by *HimarEm1* integration into the chromosome (1). Colonies of interest are further identified for study based on spreading and/or secretion phenotypes. Utilizing this method to isolate mutants that formed totally non-spreading colonies resulted in identification of gliding motility machinery and T9SS components (1). Kulkarni attempted to identify genes related to chemotaxis and other means of regulating motility by screening for colonies with partial, rather than full, motility defects (2). Of the eleven 'poor-spreading' mutants identified by this screen, two were selected for follow up in this study. The strain CJ2303 was shown to contain a single *HimarEm1* insertion in *fjoh_0891* and was noted as poor spreading with slightly improved spreading of colonies in close proximity to each other (2). The other strain, CJ2160, contains an insertion in *fjoh_3155* and is noted as poor spreading with the inability to digest chitin, suggesting a T9SS defect (2, 3). Strains and plasmids used in this study are shown in Table 1.

The protein Fjoh_0891 is annotated as a PSP1 domain containing protein and currently has no known role in *F. johnsoniae* gliding motility or T9SS mediated secretion. It has been shown that the PSP1 protein in *Saccharomyces cerevisiae* suppressed temperature sensitivity of mutations in DNA polymerase alpha and partially suppressed mutations of DNA polymerase delta (4). Of greater interest in this case is the location of *fjoh_0891* immediately upstream of the gliding motility gene *gldH*. Since GldH is required for motility (5), it is likely that polar effects of the *HimarEm1* insertion in *fjoh_0891* disrupt the expression of *gldH* and result in the observed

poor-spreading phenotype. To test this hypothesis, transfer of pMM293 carrying wild-type *gldH* into CJ2303 was performed to complement the potential defect of expression of chromosomal *gldH*.

Following conjugative transfer of pMM293 from *Escherichia coli* S17-1 to CJ2303 as previously described (6), colony spreading was observed on PY2 agar as comparable to wild-type (data not shown). This indicates the phenotype observed is due to polar effects of the insertion on *gldH*, not the disruption of *fjoh_0891*. As such, it is not likely that Fjoh_0891 has a direct function in gliding motility.

The *HimarEm1* insertion in CJ2160 has been identified to disrupt *fjoh_3155*, which is annotated as an *Rhs* element Vgr-like protein. Vgr proteins are components of the type VI secretion system (T6SS) which resembles the contractile tail of T4 bacteriophage (7). VgrG/TssI and PAAR proteins form the cell-puncturing tip of the T6SS and are often carriers of effector molecules or function as effectors themselves (8-10). The related species *Flavobacterium columnare* is predicted to possess the genes necessary to express a functional T6SS (11, 12). However, no studies have been published showing the expression or utilization of this secretion system in *F. columnare* or *F. johnsoniae*.

To ensure that motility and chitin digestion defects observed in CJ2160 resulted from only the disruption of *fjoh_3155*, the disruption was repeated using the suicide vector pLYL03. The procedure is essentially as previously described (13). Primers 2306 and 2307 were used to amplify a 1011bp region of *fjoh_3155* and provide engineered BamHI and SalI sites at each respective end of the fragment (Table 2). This fragment and pLYL03 were digested with BamHI and SalI then ligated together to form pRZ01. This plasmid was then introduced into wild-type *F. johnsoniae* strain UW101 by triparental conjugation and plated on casitone yeast extract

(CYE) agar with 100 µg/ml erythromycin (Em). Erythromycin resistant colonies arose following integration of pRZ01 into the chromosome by homologous recombination with the region of *fjoh_3155*. Insertion was verified by PCR.

The resultant strain CJ2835 was assayed for colony spreading on PY2+Em agar and digestion of a chitin overlay on MYA+Em agar as previously described (14). Resulting colonies were compared to CJ2160 and to wild-type cells carrying pCP11 to provide Em-resistance. The colony spreading and chitin digestion phenotypes of CJ2835 were indistinguishable to those observed for the wild-type (Fig. 1 and data not shown). CJ2160 failed to form spreading colonies or to digest chitin.

The discrepancy between the phenotypes of the newly constructed *fjoh_3155* disruption mutant, and the previously isolated *HimarEm1* mutant suggest that CJ2160 (the *HimarEm1* mutant) may contain a second mutation. This unknown mutation could be a second insertion of *HimarEm1* or a spontaneous point mutation, both of which have been observed to occur at low frequency following *HimarEm1* mutagenesis (McBride, MJ, unpublished data). Attempts were made to isolate a second *Himar* insertion by digesting isolated CJ2160 chromosomal DNA with a different restriction enzyme, though this only resulted in identifying the previously known insertion. Locating a point mutation was beyond the scope of this study. Such a mutations may have occurred in a known *gld* or *spr* gene. The results indicate that *fjoh_3155* does not have a function in gliding motility or T9SS mediated protein secretion, in contrast what was suggested by Kulkarni (2).
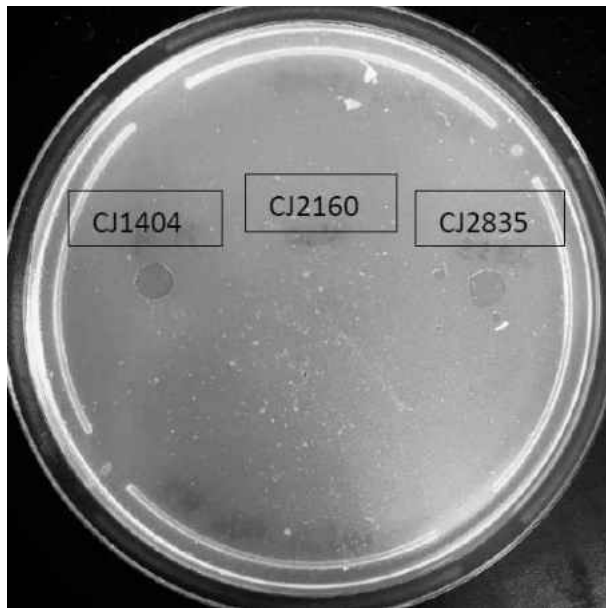
Figure 1. Digestion of chitin is unaffected by disruption of *fjoh_3155*. Approximatesly 10^6 cells of wild-type *F. johnsoniae* UW101 carrying pCP11 (CJ1404), *HimarEm1* disrupted *fjoh_3155* (CJ2160), and pLYL03 disrupted *fjoh_3155* (CJ2835) were spotted on MYA-chitin containing 100 µg/ml erythromycin and incubated for 48 hours at 25°C. CJ1404 and CJ2835 produced similar clearing of the chitin overlay whereas CJ2160 caused no visible clearing.

Table 1. Strains and plasmids used in this study.

Strain	Genotype and Description[a]	Reference
E. coli strains		
DH5αmcr	Strain used for general cloning	Life Technologies (Grand Island, NY, USA)
S17-1 λ *pir*	Strain used for diparental conjugation	(15)
HB101	Strain used with pRK2013 for triparental conjugation	(16, 17)
F. johnsoniae strains		
ATCC 17061[T] (UW101)	Wild type	(1, 14)
CJ2160	*fjoh_3155 HimarEm2* mutant; (Em[r])	(2)
CJ2303	*fjoh_0891 HimarEm2* mutant; (Em[r])	(2)
CJ2835	*fjoh_3155* pLYL03 insertion mutant; (Em[r])	This study
Plasmid	**Description**	
pLYL03	*E. coli* plasmid carrying erythromycin resistance; Ap[r] (Em[r])	(18)
pCP11	*E. coli*-*F. johnsoniae* shuttle plasmid; Ap[r] (Em[r])	(6)
pCP23	*E. coli*-*F. johnsoniae* shuttle plasmid; Ap[r] (Tc[r])	(13)
pMM293	pCP23 carrying *gldH*; Ap[r] (Tc[r])	(5)
pRZ01	Construct used to disrupt *fjoh_3155*; 1011-bp region of *fjoh_3155* amplified with primers 2306 and 2307, cloned into BamHI and SalI sites of pLYL03; Ap[r] (Em[r])	This study

[a]Antibiotic resistance phenotypes are as follows: ampicillin, Ap[r]; cefoxitin, Cf[r]; erythromycin, Em[r]; streptomycin, Sm[r]; tetracycline, Tc[r]. The antibiotic resistance phenotypes given in parentheses are those expressed in *F. johnsoniae* but not in *E. coli*. The antibiotic resistance phenotypes without parentheses are those expressed in *E. coli* but not in *F. johnsoniae*.

Table 2. **Primers used in this study.**

Primer	Sequence and Description
21	5' GCTAG<u>GGATCC</u>ACCAGTAAAAGTGCAGATTTA 3'; used to construct pRZ01; BamHI site underlined
22	5' GCTAG<u>GTCGAC</u>GTTTACGGTCCAGTTTCC 3'; used to construct pRZ01; SalI site underlined

References

1. Braun TF, Khubbar MK, Saffarini DA, McBride MJ. 2005. *Flavobacterium johnsoniae* gliding motility genes identified by mariner mutagenesis. J Bacteriol 187:6943-52.
2. Kulkarni SS. 2017. Targeting of *Flavobacterium Johnsoniae* Proteins for Secretion by the Type IX Secretion System. Dissertation. University of Wisconsin - Milwaukee.
3. Kharade SS, McBride MJ. 2014. *Flavobacterium johnsoniae* chitinase ChiA is required for chitin utilization and is secreted by the type IX secretion system. J Bacteriol 196:961-70.
4. Formosa T, Nittis T. 1998. Suppressors of the temperature sensitivity of DNA polymerase alpha mutations in *Saccharomyces cerevisiae*. Mol Gen Genet 257:461-8.
5. McBride MJ, Braun TF, Brust JL. 2003. *Flavobacterium johnsoniae* GldH is a lipoprotein that is required for gliding motility and chitin utilization. J Bacteriol 185:6648-57.
6. McBride MJ, Kempf MJ. 1996. Development of techniques for the genetic manipulation of the gliding bacterium *Cytophaga johnsonae*. J Bacteriol 178:583-590.
7. Liang X, Moore R, Wilton M, Wong MJ, Lam L, Dong TG. 2015. Identification of divergent type VI secretion effectors using a conserved chaperone domain. Proc Natl Acad Sci U S A 112:9106-11.
8. Bondage DD, Lin JS, Ma LS, Kuo CH, Lai EM. 2016. VgrG C terminus confers the type VI effector transport specificity and is required for binding with PAAR and adaptor-effector complex. Proc Natl Acad Sci U S A 113:E3931-40.
9. Brunet YR, Zoued A, Boyer F, Douzi B, Cascales E. 2015. The Type VI Secretion TssEFGK-VgrG Phage-Like Baseplate Is Recruited to the TssJLM Membrane Complex via Multiple Contacts and Serves As Assembly Platform for Tail Tube/Sheath Polymerization. PLoS Genet 11:e1005545.
10. Durand E, Cambillau C, Cascales E, Journet L. 2014. VgrG, Tae, Tle, and beyond: the versatile arsenal of Type VI secretion effectors. Trends Microbiol 22:498-507.
11. Kumru S, Tekedar HC, Gulsoy N, Waldbieser GC, Lawrence ML, Karsi A. 2017. Comparative Analysis of the *Flavobacterium columnare* Genomovar I and II Genomes. Front Microbiol 8:1375.
12. Tekedar HC, Karsi A, Reddy JS, Nho SW, Kalindamar S, Lawrence ML. 2017. Comparative Genomics and Transcriptional Analysis of *Flavobacterium columnare* Strain ATCC 49512. Front Microbiol 8:588.
13. Agarwal S, Hunnicutt DW, McBride MJ. 1997. Cloning and characterization of the *Flavobacterium johnsoniae* (*Cytophaga johnsonae*) gliding motility gene, gldA. Proc Natl Acad Sci U S A 94:12139-44.
14. McBride MJ, Braun TF. 2004. GldI is a lipoprotein that is required for *Flavobacterium johnsoniae* gliding motility and chitin utilization. J Bacteriol 186:2295-302.
15. de Lorenzo V, Timmis KN. 1994. Analysis and construction of stable phenotypes in gram-negative bacteria with Tn5- and Tn10-derived minitransposons. Methods Enzymol 235:386-405.
16. Bolivar F, Backman K. 1979. Plasmids of *Escherichia coli* as cloning vectors. Methods Enzymol 68:245-267.

17.   Figurski DH, Helinski DR. 1979. Replication of an origin-containing derivative of plasmid RK2 dependent on a plasmid function provided in trans. Proc Natl Acad Sci USA 76:1648-1652.

18.   Li L-Y, Shoemaker NB, Salyers AA. 1995. Location and characterization of the transfer region of a *Bacteroides* conjugative transposon and regulation of the transfer genes. J Bacteriol 177:4992-4999.

Joseph Johnston
University of Wisconsin-Milwaukee
3209 N Maryland Ave
Milwaukee, WI 53201

Education

University of Wisconsin – Milwaukee, Milwaukee, WI
Ph. D. Molecular Biology and Biochemistry
Expected Graduation: August 2019

University of Wisconsin – Milwaukee, Milwaukee, WI
B.S. Chemistry and Microbiology (2012)

Community College of the Air Force, Maxwell-Gunter AFB, AL
A.A.S. Electronic Systems Technology (2008)

Teaching Experience

2017 – 2019   University of Wisconsin – Milwaukee
              Undergraduate Research Mentor

- Advised and guided undergraduate student laboratory research activities, taught advanced techniques in molecular biology and genetic manipulation, assisted with experiment design, and coached presentation skills and scientific writing. These activities culminated with my undergraduate receiving Best Undergraduate Microbiology poster at the UWM Biological Sciences symposium and inclusion on a manuscript in preparation for publication.

2012 – 2018   University of Wisconsin – Milwaukee
              Teaching Assistant, General Microbiology Laboratory (Bio Sci 383)

- Delivered lectures detailing principles and techniques, demonstrated correct and safe use of laboratory equipment, generated short answer quiz questions, graded quizzes and lab reports, provided individual coaching to improve laboratory skills and scientific writing, and administered end of semester practical examinations. Experiments included isolation, cultivation, and identification of microorganisms, microscopy and staining procedures, and genetic and molecular analyses of microorganisms.

2016 – 2017   University of Wisconsin – Milwaukee
Teaching Assistant, Genetics Discussion (Bio Sci 325)

- Led and moderated interactive discussions focused on difficult topics and problem solving in classical and molecular genetics of animals, plants and microorganisms, generated and graded online assignments and in-class quizzes, organized and led exam review sessions, and offered individual and small group tutoring.

Research Experience

2012 – 2019   University of Wisconsin – Milwaukee
Graduate Student Researcher
Advisor: Dr. Mark J. McBride

2011 – 2012   University of Wisconsin – Milwaukee
Undergraduate Student Researcher
Advisor: Dr. Mark J. McBride

- Performed molecular and genetic research on *Flavobacterium johnsoniae* and *Flavobacterium columnare* exploring functions and relationships of proteins comprising the type IX protein secretion system and the gliding motility machinery

2012   University of Wisconsin – Milwaukee
Milwaukee School of Engineering
Advisor: Dr. Steven Forst

- Developed 3D printed models and online lecture material used in upper division biological sciences courses to explain the functional arrangement and movement of DNA polymerase amino acids during replication of bacterial DNA.

Awards and Funding

2013 – 2018   UW-Milwaukee Chancellor's Graduate Student Award
University of Wisconsin – Milwaukee

2008 – 2012   Undergraduate Dean's honors list [All Semesters]
University of Wisconsin – Milwaukee

2012   Connecting Researchers, Educators, and Students (CREST) Internship
Milwaukee School of Engineering
University of Wisconsin – Milwaukee

2011   Emeritus chemistry faculty scholarship to the outstanding junior chemistry
            major
            University of Wisconsin – Milwaukee

2007   Academic Award
            Airman Leadership School, Barksdale AFB, LA

Publications
(* indicates authors who contributed equally to the publication, ᵘ indicates undergraduate researchers mentored by JJ Johnston)

Zhu Y*, **Johnston JJ***, Hying ZT*, Zdero R^u, and McBride MJ. Dissecting the *Flavobacterium* gliding motility adhesin SprB. [Manuscript in preparation].

Kulkarni S*, **Johnston JJ***, Zhu Y, Hying ZT, and McBride MJ. The carboxy-terminal region of *Flavobacterium johnsoniae* SprB facilitates its secretion by the type IX secretion system and interaction with the gliding motility machinery. J. Bacteriol. 2019 Jul 1. pii: JB.00218-19. doi: 10.1128/JB.00218-19. [Epub ahead of print]

Johnston JJ*, Shrivastava A*, and McBride MJ. Untangling *Flavobacterium johnsoniae* gliding motility and protein secretion. J. Bacteriol. 2017; 200(2). pii: e00362-17. doi: 10.1128/JB.00362-17.

Shrivastava A, **Johnston JJ**, van Baaren JM, and McBride MJ. *Flavobacterium johnsoniae* GldK, GldL, GldM, and SprA are required for secretion of the cell surface gliding motility adhesins SprB and RemA. J. Bacteriol. 2013 Jul;195(14):3201-12. doi: 10.1128/JB.00333-13.

Poster and Podium Presentations
(ᵘ indicates undergraduate researchers mentored by JJ Johnston)

Zdero R^u, **Johnston JJ**, McBride MJ. Bacteriophage recognition of *Flavobacterium johnsoniae sprB* mutants. Department of Biological Sciences Symposium, University of Wisconsin – Milwaukee (2019).
[Won best undergraduate microbiology poster]

Johnston JJ, McBride MJ. *Flavobacterium* gliding motility: from protein secretion to cell surface adhesin movements. Milwaukee Microbiology Seminar Series, School of Freshwater Sciences, University of Wisconsin – Milwaukee (2019).

Johnston JJ, McBride MJ. *Flavobacterium* gliding motility: from protein secretion to cell surface adhesin movements. Department of Biological Sciences Colloquium, University of Wisconsin – Milwaukee (2019).

McBride MJ, Zhu Y, Kulkarni S, **Johnston JJ**, Li N, Hunicutt D, The roles of *Flavobacterium* Type IX Secretion Systems in motility, virulence and polysaccharide digestion. Flavobacterium 2015 (International Conference), Auburn University, AL (2015).

Johnston JJ, Shrivastava A, McBride MJ. Untangling *Flavobacterium* gliding motility and secretion. Department of Biological Sciences Symposium, University of Wisconsin – Milwaukee (2015).

Johnston JJ, Shrivastava A, McBride MJ. Untangling *Flavobacterium* gliding motility and secretion. International BLAST XIII Conference, Tucson, AZ (2015).

Johnston JJ, Landrie BD, Wannamaker AM, and Forst S. Structural and functional analysis through molecular modeling of DNA polymerase III α-subunit. CREST Teaching and Research Symposium, Milwaukee School of Engineering (2012)

Technical Proficiencies

Genetic Manipulation
- DNA isolation, RNA isolation, bacterial gene cloning, site-directed mutagenesis, PCR, DNA sequence analysis, random/transposon mutagenesis, phage transduction

Assays and Analysis
- Gel electrophoresis, SDS-PAGE, western blotting, southern blotting, recombinant protein expression and purification, flow cytometry, Coomassie staining, silver staining, affinity purification, fluorescence microscopy, light microscopy

Software and Miscellaneous
- Microsoft Windows/Office, Adobe Illustrator, Adobe Photoshop, GNU Image Manipulation Program (GIMP), ImageJ/FIJI, Nikon NIS-Elements AR, MetaMorph Research Imaging, Jmol

Professional Development Organizations

2018 – 2019   Vice President, Graduate Organization of Biological Sciences

- Organized social, mentorship, and research events to benefit graduate students in the Department of Biological Sciences.

2013 – 2019   Member, Graduate Organization of Biological Sciences